NASA/CR—2013-217812

Aero-Thermal Calibration of the NASA Glenn Icing Research Tunnel (2012 Tests)

Christine Pastor-Barsi and E. Allen Arrington
Sierra-Lobo, Inc., Cleveland, Ohio

March 2013

NASA STI Program . . . in Profile

Since its founding, NASA has been dedicated to the advancement of aeronautics and space science. The NASA Scientific and Technical Information (STI) program plays a key part in helping NASA maintain this important role.

The NASA STI Program operates under the auspices of the Agency Chief Information Officer. It collects, organizes, provides for archiving, and disseminates NASA's STI. The NASA STI program provides access to the NASA Aeronautics and Space Database and its public interface, the NASA Technical Reports Server, thus providing one of the largest collections of aeronautical and space science STI in the world. Results are published in both non-NASA channels and by NASA in the NASA STI Report Series, which includes the following report types:

- TECHNICAL PUBLICATION. Reports of completed research or a major significant phase of research that present the results of NASA programs and include extensive data or theoretical analysis. Includes compilations of significant scientific and technical data and information deemed to be of continuing reference value. NASA counterpart of peer-reviewed formal professional papers but has less stringent limitations on manuscript length and extent of graphic presentations.

- TECHNICAL MEMORANDUM. Scientific and technical findings that are preliminary or of specialized interest, e.g., quick release reports, working papers, and bibliographies that contain minimal annotation. Does not contain extensive analysis.

- CONTRACTOR REPORT. Scientific and technical findings by NASA-sponsored contractors and grantees.

- CONFERENCE PUBLICATION. Collected papers from scientific and technical conferences, symposia, seminars, or other meetings sponsored or cosponsored by NASA.

- SPECIAL PUBLICATION. Scientific, technical, or historical information from NASA programs, projects, and missions, often concerned with subjects having substantial public interest.

- TECHNICAL TRANSLATION. English-language translations of foreign scientific and technical material pertinent to NASA's mission.

Specialized services also include creating custom thesauri, building customized databases, organizing and publishing research results.

For more information about the NASA STI program, see the following:

- Access the NASA STI program home page at *http://www.sti.nasa.gov*

- E-mail your question to *help@sti.nasa.gov*

- Fax your question to the NASA STI Information Desk at 443–757–5803

- Phone the NASA STI Information Desk at 443–757–5802

- Write to:
  STI Information Desk
  NASA Center for AeroSpace Information
  7115 Standard Drive
  Hanover, MD 21076–1320

NASA/CR—2013-217812

Aero-Thermal Calibration of the NASA Glenn Icing Research Tunnel (2012 Tests)

Christine Pastor-Barsi and E. Allen Arrington
Sierra-Lobo, Inc., Cleveland, Ohio

Prepared under Contract NNC05CA95C

National Aeronautics and
Space Administration

Glenn Research Center
Cleveland, Ohio 44135

March 2013

Level of Review: This material has been technically reviewed by NASA technical management OR expert reviewer(s).

Available from

NASA Center for Aerospace Information
7115 Standard Drive
Hanover, MD 21076–1320

National Technical Information Service
5301 Shawnee Road
Alexandria, VA 22312

Available electronically at http://www.sti.nasa.gov

Contents

List of Figures

List of Tables

Aero-Thermal Calibration of the NASA Glenn Icing Research Tunnel (2012 Tests)

Christine Pastor-Barsi and E. Allen Arrington
Sierra Lobo, Inc.
Fremont, Ohio 44135

Summary

A full aero-thermal calibration of the NASA Glenn Icing Research Tunnel (IRT) was completed in 2012 following the major modifications to the facility that included replacement of the refrigeration plant and heat exchanger. The calibration test provided data used to fully document the aero-thermal flow quality in the IRT test section and to construct calibration curves for the operation of the IRT.

Introduction

Updating and maintaining the icing cloud calibration, aero-thermal calibration and flow quality data are critical tasks in the NASA Glenn Icing Research Tunnel (IRT). Establishing and maintaining the calibrations is the only way to ensure that correct test section operating conditions are being set for a given set of facility control inputs. Without knowledge of the calibration and flow quality data, it is impossible to provide high-quality test data for customers and researchers. To ensure that the data quality from the IRT is always at the highest standards, IRT staff and wind tunnel calibration personnel have developed and continue to refine the calibration methodologies used.

The aero-thermal calibration test program provides the calibration relationships needed to accurately determine the test section operating conditions for total pressure, airspeed (comparable Mach number) and total temperature. Once these calibrated conditions are determined, all other aero-thermal operating conditions can be calculated. In addition to the calibration information, detailed flow quality data (spatial uniformity) is also collected. The collected calibration and flow quality data provide a complete description of the aero-thermal operation of the IRT.

The current aero-thermal calibration methodology and instrumentation has evolved based on lessons learned by the calibration team over the past 20 years, input from IRT customers, in-house research staff, IRT facility personnel, and recommendations from references [1] and [2]. The SAE Standard "Calibration and Acceptance of Icing Wind Tunnels" (reference [1]) defines a time table and level of calibration that should be conducted following modifications to an icing tunnel. Correspondingly, the AIAA Recommended Practice "Calibration of Subsonic and Transonic Wind Tunnels" (reference [2]) states that short, check calibrations should be conducted multiple times each year to ensure repeatable operation of the wind tunnel. Based on these recommendations, the following aero-thermal calibration tests have been defined:

- Full calibration: Includes collection of aero-thermal calibration data over the entire operating range of the IRT as well as a complete mapping of the IRT flow quality at

one cross section of the test section, typically at the centerline of the turntable. A full calibration should be conducted every 5 years or following a major facility modification. The full calibration provides all of the information needed to develop the aero-thermal calibration relationships, or calibration curves, for the facility and provides extensive detailed information on the aero-thermal flow quality characteristics of the test section.

- Interim calibration: Includes collection of aero-thermal calibration data over the entire operating range of the IRT, however, data is only required from the test section centerline. An interim calibration is conducted one year following a full calibration. The interim calibration is used to validate the data collected during the full calibration, therefore, if the full calibration and interim calibration data match then the facility is operating properly, however if not, then an investigation must commence immediately to rectify the discrepancies.

- Check calibration: A one-day test using a very simple rake. Check calibration testing covers the entire operating range and typically lasts one day, the test matrix is not as extensive as a full or interim calibration. This calibration should be conducted 2 to 3 times per year. The check calibration data is used in a statistical process control analysis to monitor the stability and repeatability of the facility operation.

This paper provides a detailed description of the full aero-thermal calibration conducted in the IRT in 2012. This calibration was required due to the major modifications to the IRT, consisting of the replacement of the refrigeration plant and heat exchanger. The 2012 full calibration was also needed to update the calibration curves that are used to set operating conditions in the test section of the IRT. Previous to the 2012 calibration, the most recent full calibration was completed in 2009 following removal of ramps in the bellmouth of the facility (reference [3]). Additionally, an Interim calibration was completed in 2010. The goals for the 2012 aero-thermal full calibration are listed below:

- Complete data collection and construct aero-thermal calibration curves for the IRT. The three calibration relationships used are total pressure, Mach number and total temperature.

- Complete detailed flow quality surveys using the 9-foot survey rake, 2-D RTD array, hot-wire rake, and the quick-check rake.

Nomenclature

Symbols	
A	Conductive heat transfer, hot-wire/film
B	Convective heat transfer, hot-wire/film
C_0, C_1, C_2	RTD probe total temperature flow recovery curve-fit coefficients
C_α	Pitch angle pressure coefficient
C_β	Yaw angle pressure coefficient
C_o	Total pressure coefficient (9-foot rake pressure probes)
C_q	Static pressure coefficient (9-foot rake pressure probes)
E	hot-wire anemometer output voltage, volts
K_0 *to* K_2	Flow-angle prediction coefficients, degrees
l	characteristic length, ft
M	Mach number
N	Number of data points
n	coefficient, hot-wire/film
P	Pressure, psia
P_1 *to* P_9	Flow-angle probe pressures, psia
P_{air}	Spray bar air pressure, psig
P_{avg}	Average of P_1, P_2, P_3, and P_4, psia
P_{rat}	Ratio of static to total pressure
P_S	Static pressure, psia (psf)
$P_{S,rake}$	Average of P_6, P_7, P_8, and P_9 (probe static pressure), psia
P_T	Total pressure, psia (psf)
$P_{T,rake}$	Equal to P_5 (probe total pressure), psia
Q	Measured velocity, hot-wire/film
q	Dynamic pressure, psi
R	Specific gas constant for air, $1716 \frac{ft^2}{(sec^2 \circ R)}$
Re	Reynolds number
T	Temperature, °C(°F)
T_s	Static temperature, °C(°F)
T_T	Total temperature, °C(°F)
$T_{T,davg}$	Average of the 24 D-corner total temperature measurements, °C(°F)
$T_{T,d,i}$	D-corner total temperature measurement, °C(°F)
U	Velocity, knots (ft/sec, mph)
X	Axial coordinate, with axis origin at bellmouth/test section weld seam, inches
Y	Spanwise coordinate, with axis origin at the test section inner wall, inches
Z	Vertical coordinate, with axis origin at the test section floor, inches
α	Pitch flow-angle, degrees
β	Yaw flow-angle, degrees
γ	Ratio of specific heats, 1.4
Δ	Measured pitch or yaw angle offset, degrees
Subscripts	
arm	6-degree-of-freedom inspection arm

array	2D RTD array
avg	Average
bm	Tunnel bellmouth
i	Data point index
j	Data point index
level	Digital level, inclinometer
local	Test section parameters after all calibration coefficients have been included
north	North bellmouth rake
rake	9-ft survey rake
ruler	Ruler or tape measure
south	South bellmouth rake
ts	Tunnel test section

Description of Facility

A schematic of the NASA Glenn Icing Research Tunnel (IRT) is shown in Figure 1. The IRT is a closed loop atmospheric tunnel. The test section is a 6-feet high by 9-feet wide and 20-feet in length with no divergence along any surface. The spraybars which inject atomized water into the flow stream to create the icing conditions are located in the settling chamber between the D-corner turning vanes and the bellmouth inlet.

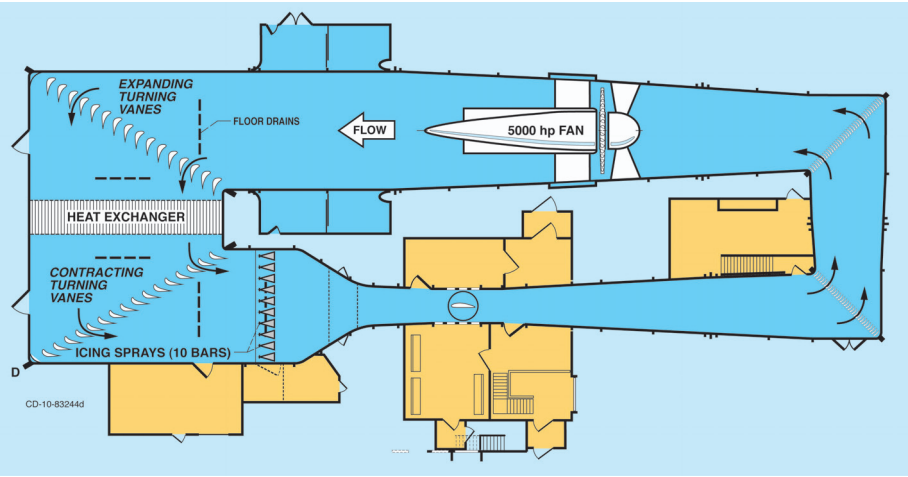

Figure 1: Schematic of the NASA Glenn Icing Research Tunnel

Operational velocities of the IRT range from 25 knots to 350 knots and tunnel temperature is controllable from +20 °C total temperature to −40 °C test section static temperature. The recently upgraded heat exchanger, from a flat-panel to a chevron-design (Figure 2), which enables this range of temperatures is located between C and D corners on the left in Figure 1. Additionally, the upgraded refrigeration plant is located adjacent to the tunnel near the C-corner. Pushing airflow around the circuit is a 5000-horsepower electric motor driving a 25-foot diameter, 12-blade wooden fan [3].

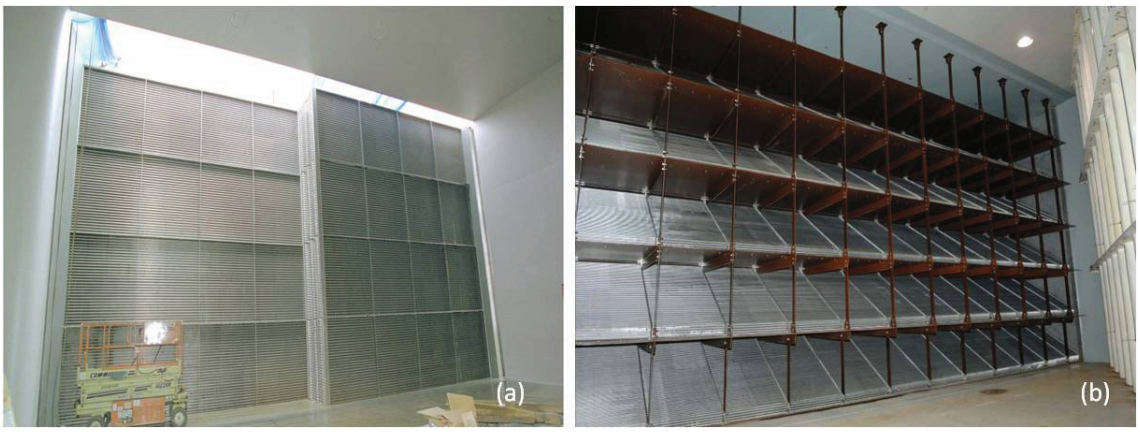

Figure 2: (a)previous flat-panel heat exchanger, (b)current chevron-design heat exchanger

Test Hardware, Instrumentation and Data Systems

Several pieces of hardware are utilized to collect data during a full aero-thermal calibration of the IRT: the 9-foot survey rake, 2D Resistive Temperature Detector (RTD) survey array, the hot-wire survey rake, and the quick-check rake. The test hardware, instrumentation and data systems will be described in detail in the subsequent sections.

9-Foot Survey Rake

The 9-foot survey rake (Figure 3) is used to measure total pressure, static pressure, and angular pressure, thereby enabling calculations of velocity and flow angularity. The rake is supported in the center with a vertical strut and at both ends by plates with a bolt pattern which enables positioning of the rake every 6-inches above and below vertical centerline. Additionally, the 9-ft survey rake probes are positioned at the axial center point of the model turn table seen in Figure 4. The axial position of the rake 179.3-inches (from tunnel station 0 to the probe tips). This has been the standard position used starting in 2004. Figure 3 illustrates the left handed X-Y-Z coordinate system that is used with the points of origin as follows. The origin for the X-axis is at the bellmouth to test section weld seam. The origin for the Y-axis is the bottom of the inner wall where the wall meets the floor. The origin for the Z-axis is at the floor where the floor meets the inner wall.

The 9-Foot survey rake pressure probes are mounted through the main structure of the survey rake, as illustrated in Figure 5, and are nominally positioned in 9-inch increments. The hemispherical-head, 5-hole pressure probes (Figure 5) have a single total pressure port at the center front of the probe to measure total pressure, and 4 additional pressure ports in 90° increments around the probe head at 45° offsets to measure pitch and yaw angle of the airflow. In addition there are 4 static pressure ports 5.75-inches downstream of the head, at 90° increments (Figure 5). The probes were all calibrated at the NASA Glenn 3.5-inch diameter free jet calibration facility [4].

Figure 3: The 9-foot horizontal survey rake installed at vertical centerline in the IRT test section

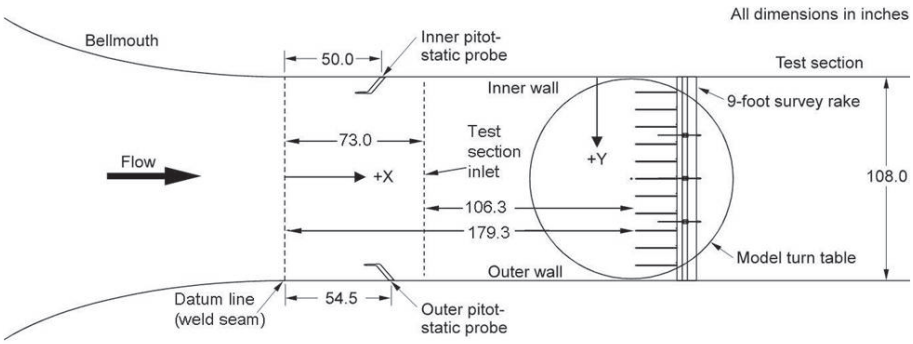

Figure 4: The 9-foot horizontal survey rake installed at vertical centerline in the IRT test section

2D Resistive Temperature Detector (RTD) Array

The 2D Resistive Temperature Detector (RTD) Survey Array is a grid of RTDs, as shown in Figure 6. The 7x7 grid positions the probes at 0%, ±25%, ±50%, and ±75% of the test section both horizontally and vertically (Figure 7). Probes extend 7-inches forward of the leading edge of the support members of the 2D RTD array. The probe heads are positioned 15-inches downstream of the model turn table center.

Figure 8 illustrates the details of the RTD probe that is used in the array. The total temperature probes used in the array are 4-wire RTDs with a ceramic capsule sensor. Total temperature recovery testing occurred in 2005 [5]. Figure 9 shows the cross section of the RTD survey array vertical member which has a 0.75-inche channel for instrumentation wiring. It also illustrates how the RTD probes extend 7-inches forward.

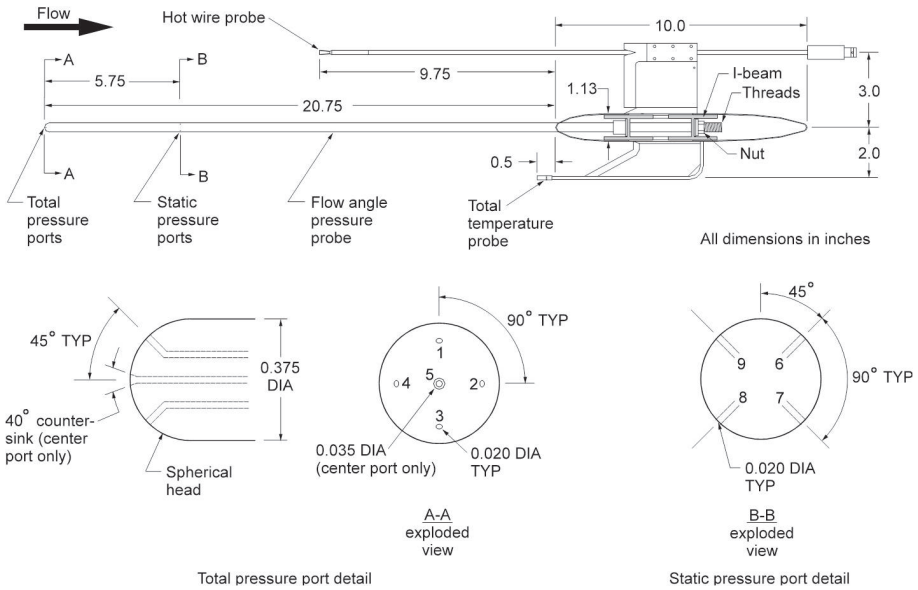

Figure 5: Hemispherical head probe total pressure ports. (A-A) total pressure port detail, (B-B) static pressure port detail.

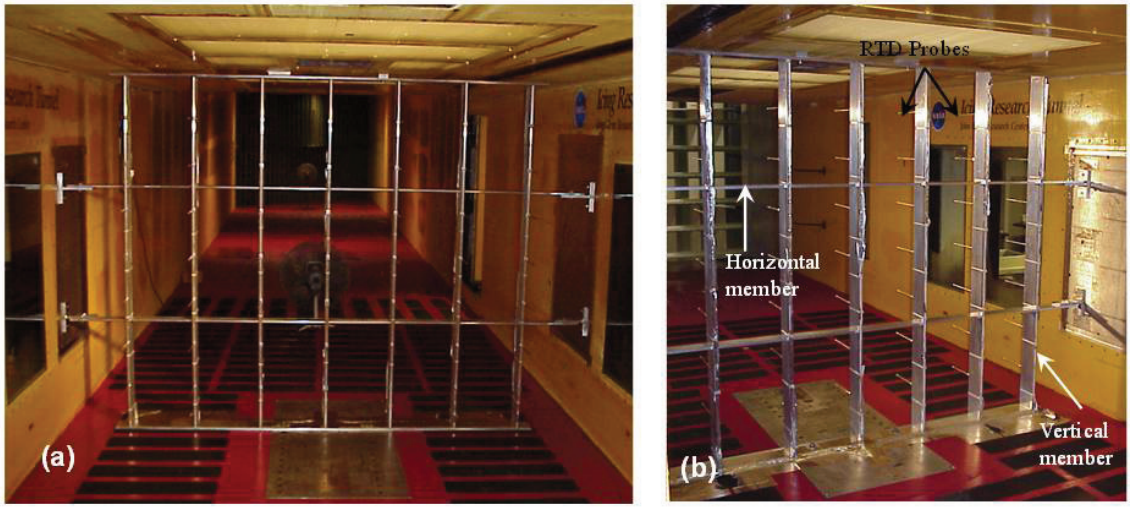

Figure 6: RTD Array installed in the IRT test section. (a) View looking downstream. (b) View looking upstream.

Facility Instrumentation

Standard facility instrumentation includes the north and south bellmouth pitot-static probes and an array of RTDs in D-corner. Facility total temperature measurements were acquired from a 24-probe array (4 rows of 6 RTD probes, Figure 10) mounted on the leading edge of the D-corner turning vanes. The north and south pitot-static probes measure total pressure and delta pressure, and are heated to prevent icing due to their position downstream of the spraybars.

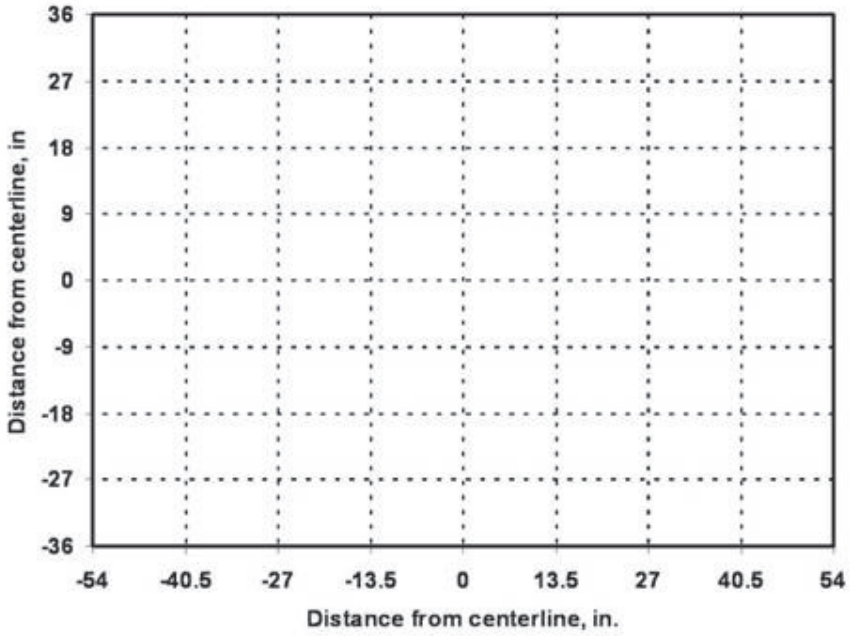

Figure 7: Grid arrangement of the 7x7 RTDs

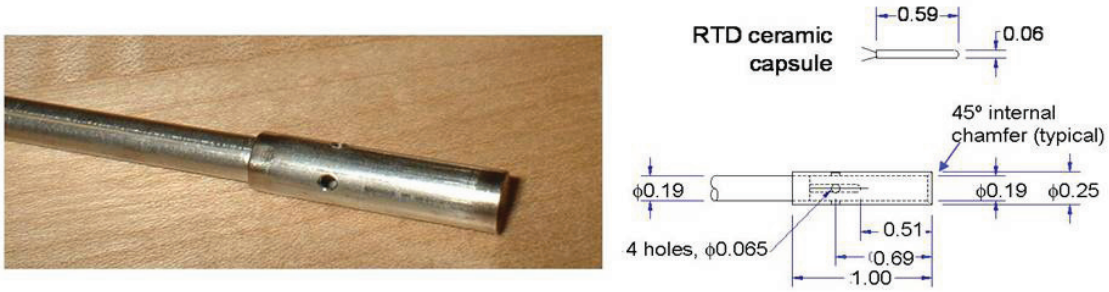

Figure 8: Details of the 2D RTD survey array probes (dimensions are in inches)

Steady-State Data Acquisition System

Real time steady-state data acquisition and display are provided by the IRT Escort Alpha System. This is the standard data acquisition and data display system used in the large test facilities at NASA Glenn. The system accommodates inputs from the Electronically Scanned Pressure (ESP) System, the facility distributed process control system, and any analog devices such as thermocouples, RTDs and pressure transducers. This system records all steady-state pressures and temperatures from the standard facility instrumentation and test specific hardware including the 9-ft survey rake, the 2D RTD survey array, and the quick-check rake. It also records facility operational parameters such as spraybar air pressure and drive fan speed. An Escort program was specifically written to support the aero-thermal calibration in the IRT.

The ESP system used during the test program utilized thirty-two port, rack mounted

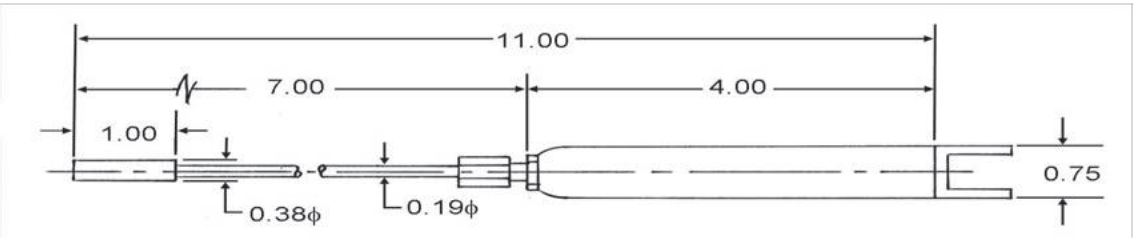

Figure 9: RTD Array vertical member cross section

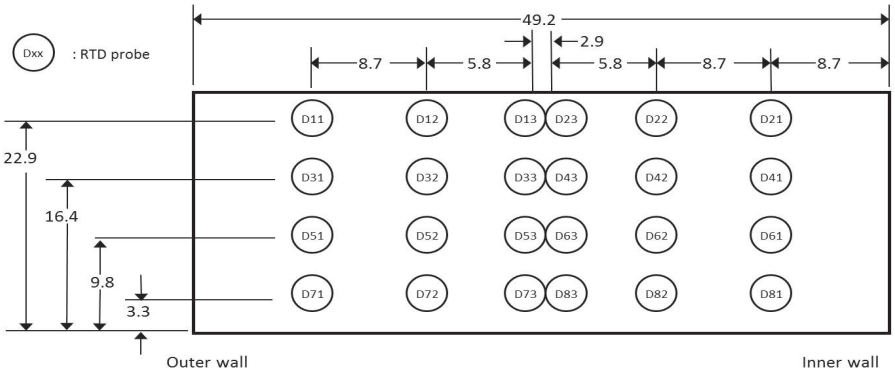

Figure 10: Arrangement of RTD Probes mounted on the D-corner turning vanes

modules. For this test program ±5 psid modules were used. The accuracy in the pressure measurements made with the ESP System is ±0.1 percent of full-scale of the module, or ±0.005 psia for the ±5 psid modules used.

Hot-Wire Survey Rake and Instrumentation

A custom hot-wire system has been developed for use at NASA GRC and is shown in Figure 11(a). The hot-wire or film is connected to the TSI Incorporated (Shoreview, MN) IFA-100 Anemometer, Model 150 Transducer module. The output from the anemometer is fed into the National Instruments (NI) Corporation (Austin, TX) Data Acquisition (DAQ) System which is connected to a laptop with NI Labview software. A custom Labview program was written for the hot-wire/film sensors which has the capability to accommodate up to 16 sensors across 4 PXI-6115 DAQ cards. A button trigger is connected between the hot-wire data system and the facility steady-state data acquisition system, Escort, which enables both systems to be triggered simultaneously.

Turbulence intensity data were acquired with the hot-wire/film survey rake shown in 11(b). The hot-wire/film was installed so as to position the wire/film horizontally or along the Y-axis with respect to the test section. Prior to the construction of this rake the hot-wires were mounted to the top of the 9-ft survey rake. Calibrations for the hot-wires/films are performed in situ in the wind tunnel test section from minimum to maximum velocity at the beginning of testing for each lateral position. Testing with the hot-wire rake is only done in the incompressible regime, $M < 0.3$. Only single wires/films normal to the axial velocity are used as the calibration is conducted in situ.

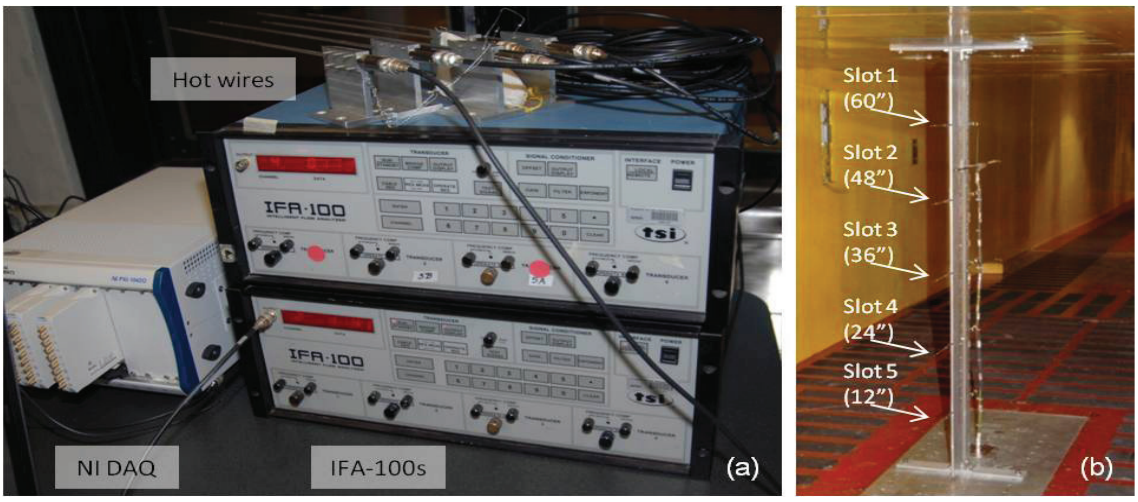

Figure 11: Hot-wire/film anemometry system: (a) NI DAQ and IFA-100 (b) hot-wire rake installed in the IRT test section with five hot-wires and a pitot-static probe

Quick-Check Rake

The quick-check rake was utilized on the last day of testing. Data is acquired but typically not looked at unless an issue is found with data from other hardware. Figure 12 shows the quick-check rake as installed in the IRT. It also shows the probe positions on the quick-check rake.

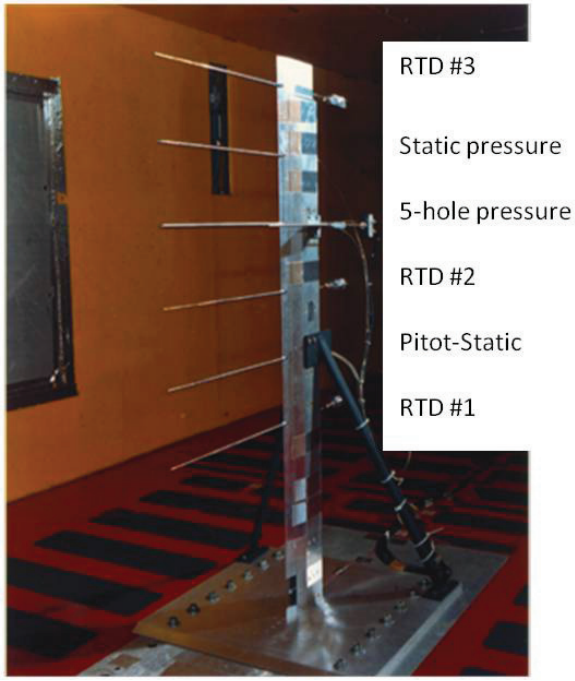

Figure 12: Quick-check rake

Procedures and Test Matrix

The IRT was operated using standard test procedures during the aero-thermal calibration. At each test condition, two data readings were acquired. Each reading was an average of 10 scans at a rate of 1 scan per second. For the 9-ft survey rake, and the hot-wire survey rake, prior to taking a reading, the spatial standard deviation of the D-corner RTDs was verified to be within $\pm 0.5\,^{\circ}$C. During testing of the 2D RTD array, the spatial standard deviation was verified to be within $\pm 0.1\,^{\circ}$C and, the temporal standard deviation of the D-corner RTDs was verified to be within $\pm 0.1\,^{\circ}$C.

Test Matrix

Table 1 lists the data points that were acquired with the 9-ft survey rake. During testing static temperature was held at $4.0\,^{\circ}$C [1].

Table 2 summarizes the data points that were recorded for the 2D RTD Array. During testing of the 2D RTD array, total temperature was set instead of static temperature. The operators were then instructed to go "hands off" of the temperature controls. To allow for a manageable total temperature swing of approximately $\pm 5.0\,^{\circ}$C, for each new sequence, total temperature was stabilized at the target temperature, i.e. $-10.0\,^{\circ}$C, at 220 knots prior to acquiring data. The data at the remaining velocities were acquired in the order of 50, 130, and 300 knots. Additionally, the spraybar air pressures were tested in the sequence of 0, 60, 30 psig. This was done so the spraybars would stabilize at their normal operating temperature of $80 - 85\,^{\circ}$C more quickly.

The hot-wire survey rake test points are illustrated in Table 3. Turbulence data were collected at a tunnel total temperature of $7.8\,^{\circ}$C to prevent the tunnel static temperature from dropping below freezing.

Table 4 shows the data points that were acquired with the quick-check rake. It is seen that the quick-check rake collected data at the lateral centerline position, at a subset of data points.

Table 1: Test matrix for the 9-ft survey rake.

Rake Position (horizontal)	Static temperature, $T_{T,ts}\,^{\circ}$C	Test Section Airspeed, $U_{ts} knots$	Spraybar air pressure, $P_{air}, psig$
CL	4.0	50,90,120,150,170,200,250	0,30,60
CL-6″	4.0	50,90,120,150,170,200,250,300	0,30,60
CL+6″	4.0	50,90,120,150,170,200,250,300	0,30,60
CL-12″	4.0	50,90,120,150,170,200,250,300	0,30,60
CL+12″	4.0	50,90,120,150,170,200,250,300	0,30,60
CL-18″	4.0	50,90,120,150,170,200,250,300	0,30,60
CL+18″	4.0	50,90,120,150,170,200,250,300	0,30,60
CL-24″	4.0	50,90,120,150,170,200,250,300	0,30,60
CL+24″	4.0	50,90,120,150,170,200,250,300	0,30,60

Table 2: Test matrix for the RTD Array.

Test Section total temperature, $T_{T,ts}$ °C	Test Section Airspeed, $U_{ts} knots$	Spraybar air pressure, $P_{air}, psig$
-30	50,130,220,300	0,30,60
-20	50,130,220,300	0,30,60
-10	50,130,220,300	0,30,60
-3	50,130,220,300	0,30,60
-2	50,130,220,300	0,30,60
-1	50,130,220,300	0,30,60
0	50,130,220,300	0,30,60
1	50,130,220,300	0,30,60
2	50,130,220,300	0,30,60
3	50,130,220,300	0,30,60
5	50,130,220,300	0,30,60

Table 3: Test matrix for the hot-wire survey rake.

Rake Position (lateral)	Test Section total temperature, $T_{T,ts}$ °C	Test Section Airspeed, $U_{ts} knots$	Spraybar air pressure, $P_{air}, psig$
CL	7.8	50,90,120,150,170	0,30,60
CL-18″	7.8	50,90,120,150,170	0,30,60
CL-36″	7.8	50,90,120,150,170	0,30,60
CL+18″	7.8	50,90,120,150,170	0,30,60
CL+36″	7.8	50,90,120,150,170	0,30,60

Table 4: Test matrix for the quick-check rake.

Rake Position (lateral)	Test Section Static Temperature, $T_{T,ts}$ °C	Test Section Airspeed, $U_{ts} knots$	Spraybar air pressure, $P_{air}, psig$
CL	4	50, 130, 220, 300	0, 30, 60
CL	-10	50, 130, 220, 300	0, 30, 60
CL	-25	50, 130, 220, 300	0, 30, 60
CL	-40	50, 130, 220, 300	0, 30, 60

Data Reduction and Analysis

U.S. customary units of measurement are used in the following data reduction. However, the icing community prefers a mixed set of units including airspeed in knots and temperature in degrees Celsius (°C). Therefore, the details on the data reduction are presented as they are carried out in English units. The final results have been converted to and are presented in the units used by the icing community.

For the following calculations, the *bm* subscript refers to measured or calculated parameters associated with the two bellmouth pitot-static probes. The subscript *rake* refers to measured or calculated parameters associated with any of the probes on the 9-ft survey rake. Additionally, the subscript *local* refers to the measured or calculated corrected *rake* parameters which have been corrected by individual probe calibration coefficients and represent the true local properties in the test section. All of the local total pressures, static pressures, and Mach numbers are normalized by bellmouth parameters to arrive at recovery ratios. All of the equations utilized in the data reduction were compressible flow equations [6].

Facility Calculations

The bellmouth pitot-static probes in the IRT measure total pressure and delta pressure. Equation 1 shown below calculates the average that is taken of the bellmouth total pressure between the north and south pitot-static probes.

$$P_{T,bm} = \frac{(P_{T,north} + P_{T,south})}{2} \tag{1}$$

Static pressure was computed by the difference of total pressure from delta pressure. The north and south probes were calculated separately.

$$P_{S,north} = P_{T,north} - \Delta P_{north}, \qquad P_{S,south} = P_{T,south} - \Delta P_{south} \tag{2}$$

The static pressure of the bellmouth was then averaged using the static pressure readings from the north and south bellmouth pitot-static probes, equation 3.

$$P_{S,bm} = \frac{(P_{S,north} + P_{S,south})}{2} \tag{3}$$

Facility total temperature, equation 4, was calculated based on the average of the 24 RTDs on the leading edge of the D-corner turning vanes.

$$T_{T,davg} = \frac{1}{24} \sum_{i=1}^{24} T_{T,d,i} \tag{4}$$

Utilizing the bellmouth total pressure and static pressure, Mach number at the bellmouth is computed using equation 5.

$$M_{bm} = \sqrt{\frac{2}{\gamma - 1} \left[\left(\frac{P_{T,bm}}{P_{S,bm}} \right)^{\frac{\gamma-1}{\gamma}} - 1 \right]} \tag{5}$$

Facility dynamic pressure, equation 6 is then calculated using bellmouth Mach number, M_{bm} and bellmouth static pressure $P_{S,bm}$.

$$q_{bm} = \frac{\gamma}{2} P_{S,bm} \cdot M_{bm}^2 \tag{6}$$

9-foot Survey Rake Calculations

Data collected by the 9-ft survey rake are used to construct Mach number and static pressure calibration curves. Additionally, the collected data are examined to check for flow quality in the facility.

The average of the four static pressure taps on each of the 11 probes was used to calculate the rake static pressure for each probe.

$$P_{S,rake} = \frac{(P_6 + P_7 + P_8 + P_9)}{4} \tag{7}$$

Mach number was computed based on the rake total pressure to static pressure ratio.

$$M_{rake} = \sqrt{\frac{2}{\gamma - 1}\left[\left(\frac{P_{T,rake}}{P_{S,rake}}\right)^{\frac{\gamma-1}{\gamma}} - 1\right]} \tag{8}$$

The correction equations or local values for total and static pressure are based on the rake Mach number. C_o and C_q are functions of M_{rake} and are experimentally determined during calibration of the pressure probe flow-angle [4]. Local static and total pressure are computed as shown.

$$P_{T,local} = P_{T,rake} - C_o(M_{rake})\left[P_{T,rake} - P_{S,rake}\right] \tag{9}$$

$$P_{S,local} = P_{T,local} - \frac{(P_{T,rake} - P_{S,rake})}{C_q(M_{rake})} \tag{10}$$

The local test section Mach number (equation 11) for each probe is determined using $P_{S,local}$ and $P_{T,local}$.

$$M_{local} = \sqrt{\frac{2}{\gamma - 1}\left[\left(\frac{P_{T,local}}{P_{S,local}}\right)^{\frac{\gamma-1}{\gamma}} - 1\right]} \tag{11}$$

Local dynamic pressure in the test section is calculated per equation 12 below.

$$q_{local} = \frac{\gamma}{2} P_{S,local} \cdot M_{local}^2 \tag{12}$$

Flow Angularity

The following equations are used to calculate pitch and yaw flow-angle data from the pressure data obtained from the 45 ° offset pressure ports on the front of the hemispherical head probe. The average of these four 45 ° offset pressure ports is used to calculate P_{avg}, equation 13.

$$P_{avg} = \frac{(P_1 + P_2 + P_3 + P_4)}{4} \tag{13}$$

The pressure coefficients C_α and C_β are calculated for both pitch and yaw. The pitch pressure coefficient, C_α, equation 14 is calculated using the 45 ° offset pressure ports in the pitch plane, P_1 and P_3 and the difference between the total pressure in the center of the hemispherical probe, P_5, and the average of all four 45 ° offset pressure ports. Similarly, the yaw pressure coefficient, C_β, equation 15 is calculated using the 45 ° offset pressure ports in the yaw plane, P_2 and P_4, and the difference between the total pressure in the center of the hemispherical probe, P_5, and the average of all four 45 ° offset pressure ports.

$$C_\alpha = \frac{(P_3 - P_1)}{(P_5 - P_{avg})} \tag{14}$$

$$C_\beta = \frac{(P_4 - P_2)}{(P_5 - P_{avg})} \tag{15}$$

Pitch angle, α, and yaw angle, β, are calculated using previously determined pitch and yaw pressure coefficients and M_{rake}.

$$\alpha = K_{0,\alpha}(M_{rake}) + K_{1,\alpha}(M_{rake})C_\alpha + \Delta_{\alpha,arm} + \Delta_{\alpha,level} \tag{16}$$

$$\beta = K_{0,\beta}(M_{rake}) + K_{2,\beta}(M_{rake})C_\beta + \Delta_{\beta,arm} + \Delta_{\beta,ruler} \tag{17}$$

The coefficients $K_{0,\alpha}$, $K_{1,\alpha}$, $K_{0,\beta}$, and $K_{2,\beta}$ were experimentally determined [4]. The delta coefficients are measurements made using a computer-aided inspection arm, an inclinometer, and a ruler.

Turbulence Intensity

During this particular test entry one hot-wire and four hot film probes were used. The hot-wire was positioned near the ceiling at 60-inches and the hot films were places in the remaining four slots below the hot-wire. The hot-wire and film probes were calibrated in situ in the IRT at the beginning of testing at each new position. In situ calibration data sweeps were completed at velocities of 50, 90, 120, 150, and 170 knots and with the spraybar air pressure at 0 psig. These in situ calibration data sweeps and a known velocity from a 5-hole hemispherical head probed attached to the side of the rake were used to develop coefficients A, B and n seen in King's Law [7] below, (equation 18).

$$E^2 = A + B \cdot Q^n \qquad or \qquad Q = \left[\frac{(E^2 - A)}{B}\right]^{1/n} \tag{18}$$

Once the coefficients were developed, King's Law was again used to calculate measured velocity from the hot-wire/film voltages for each acquired data point. The variable Q is the measured velocity, and since single wires or films were used, it is assumed that Q equals the axial component only. Using the now calculated velocity values, a temporal mean velocity and standard deviation for each steady state data point, acquired at a rate of 1kHz for 10 seconds, is calculated. Dividing the root mean square of the instantaneous velocity by the mean velocity yields turbulence intensity.

2D RTD Array Calculations

Total temperature data recorded by the 2D RTD array requires a temperature recovery correction, equation 19. Experiments to determine the recovery coefficients for the RTDs on the 2D RTD array were performed in 2005 [5].

$$T_{T,local} = (C_0 + C_1 M_{ts} + C_2 M_{ts}^2) T_{T,array} \tag{19}$$

This local total temperature is then used to develop a calibration curve between the 2D RTD array in the test section and the D-corner RTDs.

Discussion of Results

The following section will discuss the results of the 2012 IRT Aero-Thermal Calibration. This section will begin by discussing a pressure discrepancy that was found during the course of testing and how it was resolved. The aero-thermal calibration curves used for determining the operating conditions in the IRT will be discussed. Flow quality results will be presented with respect to flow quality goals for icing wind tunnels.

Pressure Discrepancy

No pressure data is being reported out for the January 2012, 300 knots test points. The calibration team intended to recollect the data in May 2012 but was unable to, due to schedule conflicts. The following is a description of why the 300 knots test points were not used for this calibration. Therefore, the calibration curves presented in the next section are only good to 250 knots.

During post processing of the data it was found that at the 300 knots test points, data acquired by the 9-foot survey rake showed an unusual drop in static pressure. This drop was seen only in the 300 knots case. The pressure data that had been collected with the quick-check rake was then examined and the static pressure drop was seen again by this second piece of hardware. Investigation ensued at the facility and it was found that the reference pressure 90 degree elbow line, shown in Figure 13(a), was not properly connected. This resulted in the balance chamber leakage flow to skew all ESP pressure readings low whenever the IRT was operated at greater than 250 knots. The extra pipe length shown in Figure 13(b) allows for the pressure to be read without an influence from outside sources including a fan and other equipment in the room.

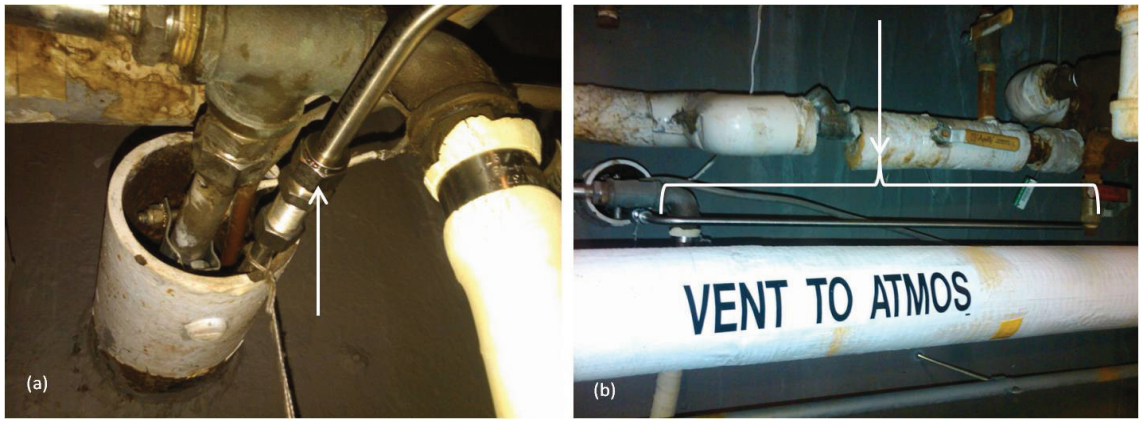

Figure 13: (a)The pipe exiting the balance chamber of the IRT and the joint at which the 90 degree elbow was disconnected. (b)The 90 degree elbow as installed.

Aero-Thermal Calibration Curves

As mentioned, one of the primary goals of this calibration cycle was to update the aero-thermal calibration curves used in the computing subroutine IRTAT which is used to set conditions in the test section. Figure 14, Figure 15, and Figure 16 are the updated calibration relationships for Mach number, static pressure, and total temperature. It can been seen that the curves are linear in nature which is what is most desirable for calibration relationships.

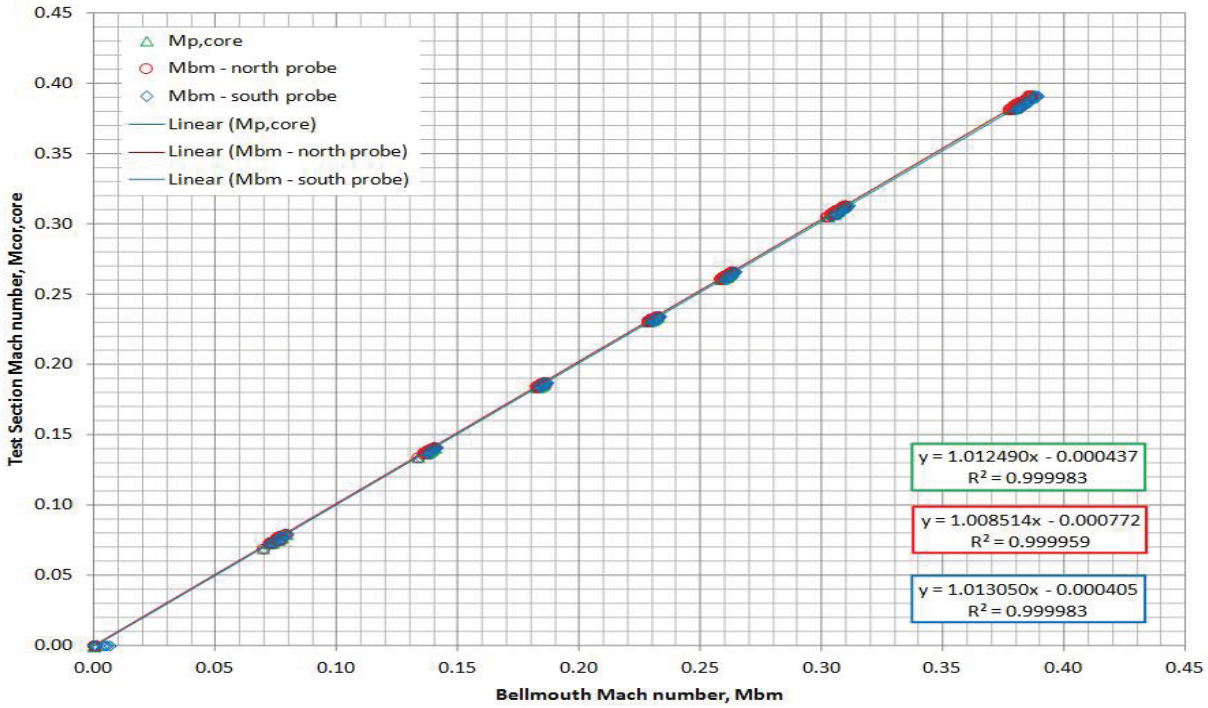

Figure 14: Mach number calibration for the IRT from the 2012 full aero-thermal calibration.

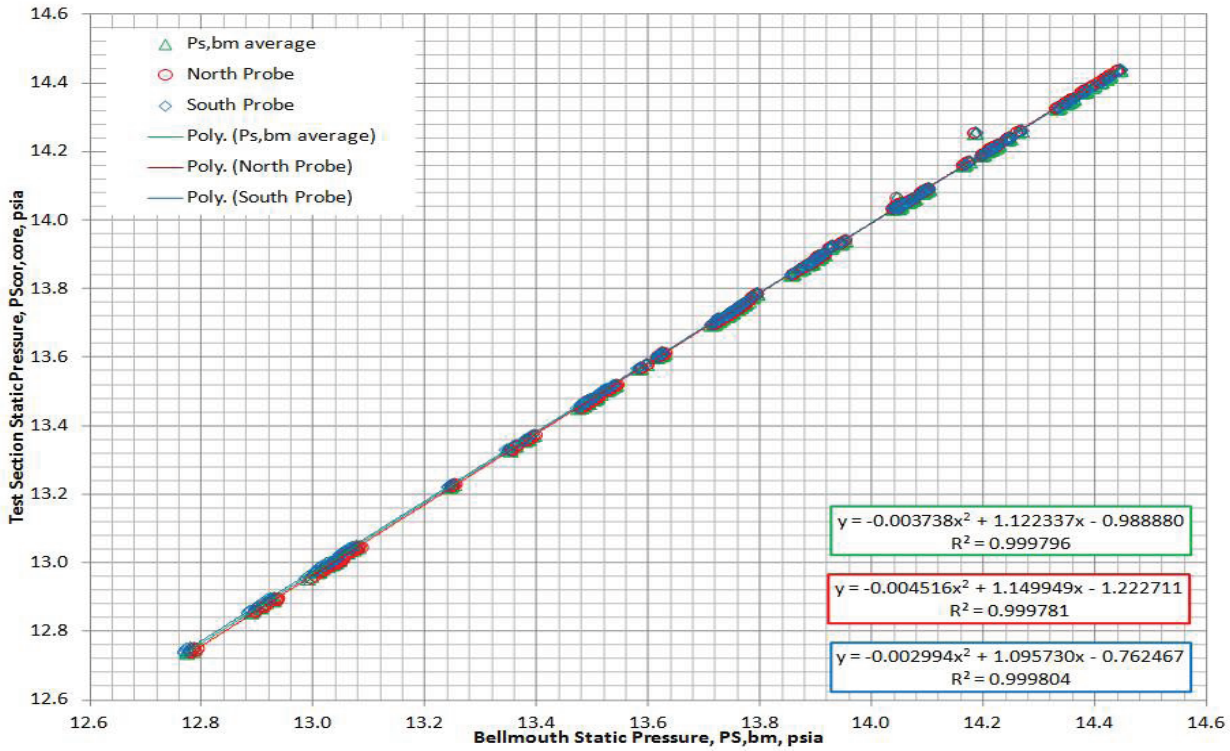

Figure 15: Static pressure calibration for the IRT from the 2012 full aero-thermal calibration.

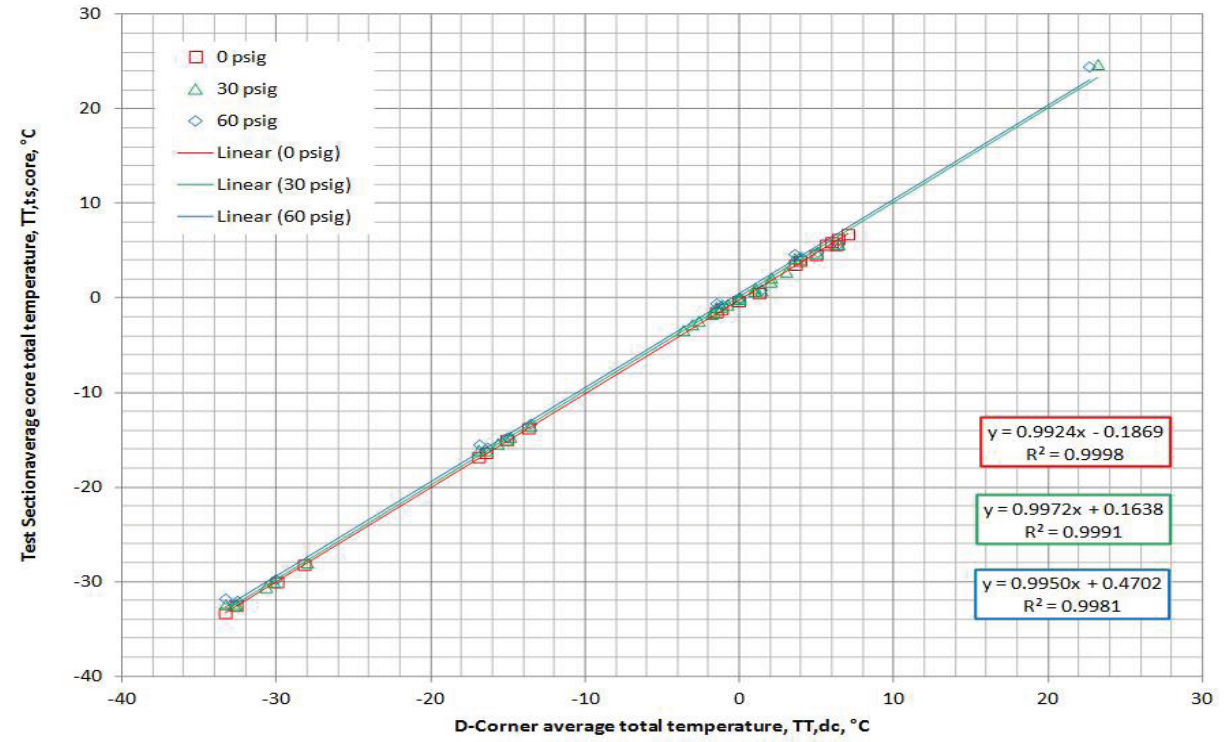

Figure 16: Total temperature calibration for the IRT from the 2012 full aero-thermal calibration.

Flow Quality Goals

Table 5 is a summary of Aero-Thermal flow quality goals for an icing wind tunnel [1]. The IRT flow quality with respect to the flow quality goals will be discussed in the subsequent sections.

Table 5: Aero-thermal flow quality goals for an icing tunnel test section.

Parameter	Measurement Uncertainty	Test Section Spatial Uniformity	Tunnel Centerline Temporal Stability
Airspeed	±1%	±2%	±2%
Static air temperature, -30 through +5 °C	±0.5 °C	±1 °C	±0.5 °C
Static air temperature, below −30 °C	±2 °C	±2 °C	±2 °C
Flow Angularity	±0.25 °	±2 °	N/A
Turbulence ($P_{air} = 0psig$)	±0.25%	< 2%	±2%
Turbulence ($P_{air} = 60psig$)	±0.25%	< 2%	±2%

Only test section spatial uniformity will be discussed for the 2012 data. Data was acquired for 10 seconds then averaged, not the minimum required 30 seconds to determine temporal stability, therefore temporal stability will not be discussed for the 2012 aero-thermal calibration. It is recommended that data be acquired in future calibrations to enable temporal stability to be calculated. Measurement uncertainty will nt be discussed for the 2012 aero-thermal calibration either. A measurement uncertainty analysis (MUA) effort is currently under way for the facilities at GRC and a report will be written upon completion of this work.

Flow quality data for Mach number, total pressure, static pressure, and total temperature are presented in x-y plots to facilitate the viewing of as many features of the flow field as possible. For easier visual comparison the surface plots of the temperature of the test section is presented next to the surface plot of the temperature of D-corner.

Turbulence Intensity

Data shown in Figure 17 illustrates the turbulence intensity seen at the horizontal and vertical centerline of the test section with a spraybar air pressure of 0 psig. Turbulence intensity, u'/U, is shown plotted with respect to test section velocity, $U(kts)$. Facility changes that could affect turbulence intensity are summarized in the bottom right of Figure 17. The standard deviations shown on the 2009 and 2012 data are from 4 time traces taken at the same condition. The data is not available to develop standard deviations for data from 2005 and before. A full aero-thermal calibration was completed in 2006, but the data has not been reduced to be added to Figure 17 at the time of this publication.

Results for turbulence intensity is shown in Figure 18. The turbulence intensity, u'/U, is plotted with respect to the turn table centerline survey plane. A higher turbulence at centerline is typically seen due to the spray bar center support. While the total number

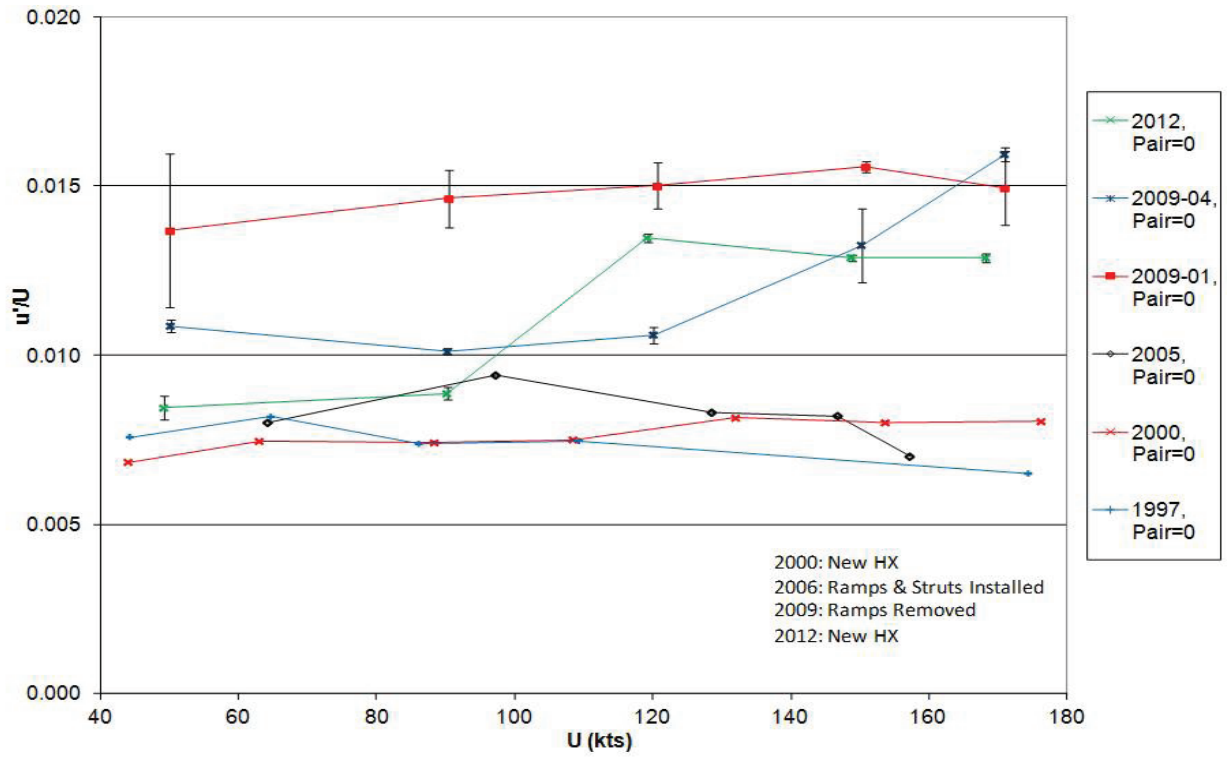

Figure 17: IRT Turbulence Intensity, Historical Comparison at horizontal and vertical centerline, $P_{air} = 0psig$.

of nozzles were reduced, 7 air-only atomizing nozzles located at the bottom center of the spraybars were added to mix out the icing cloud, thereby increasing turbulence intensity. The IRT will not have the low-turbulence levels of a wind tunnel used for aerodynamics testing. This is a result of the lack of flow manipulators like screens and honeycomb straighteners due to the icing conditions.

Table 6 illustrates the measured turbulence intensity with respect to test section spatial uniformity. It can be seen that most test section spatial uniformity test points meet the SAE flow quality goal of $< 2\%$. The test points that do not meet the $< 2\%$ criteria is the 50 knots, 30 psi and 60 psi spray bar air pressure conditions.

Table 6: Turbulence Intensity Test Section Spatial Uniformity

	0 psi	30 psi	60 psi
50 knots	0.844%	2.004%	2.784%
90 knots	0.905%	1.299%	1.659%
120 knots	1.231%	1.394%	1.567%
150 knots	1.188%	1.284%	1.411%
170 knots	1.173%	1.240%	1.33%

Flow Angularity

Results for the test section flow angularity as measured by the 5-hole probes mounted on the 9-ft survey rake is shown in Figure 19. The vectors shown in Figure 19 only reflect the magnitude and direction of the local air flow, but not airspeed. For reference, $+1^\circ$ in pitch and yaw is noted on each figure. The wall flow angularity behaviour has been seen in previous data sets as far back as 2004. Most of the variation in the flow-angle orientation is probably due to disturbances generated by the spraybars

Table 7 illustrates the flow angularity test section spatial uniformity for the test conditions acquired. The 90 to 250 knots cases meet the SAE flow quality goals as laid out in Table 5. The 50 knots test conditions does not meet the SAE flow quality goal of $\pm 2^\circ$. Tunnel centerline spatial uniformity is not examined as part of the SAE flow quality goals for an icing wind tunnel.

Table 7: Flow Angularity Test Section Spatial Uniformity

	0 psi	30 psi	60 psi
50 knots	$\pm 2.562^\circ$	$\pm 2.464^\circ$	$\pm 2.433^\circ$
90 knots	$\pm 0.919^\circ$	$\pm 0.877^\circ$	$\pm 0.781^\circ$
120 knots	$\pm 0.648^\circ$	$\pm 0.472^\circ$	$\pm 0.531^\circ$
150 knots	$\pm 0.594^\circ$	$\pm 0.538^\circ$	$\pm 0.465^\circ$
170 knots	$\pm 0.622^\circ$	$\pm 0.581^\circ$	$\pm 0.578^\circ$
200 knots	$\pm 0.654^\circ$	$\pm 0.583^\circ$	$\pm 0.578^\circ$
250 knots	$\pm 0.626^\circ$	$\pm 0.785^\circ$	$\pm 0.645^\circ$

Mach Number

Results for Mach number are shown in Figure 20. Mach number in the test section, M_{ts}, is normalized by Mach number at the bellmouth, M_{bm}, and plotted with respect to the width of the test section in inches. The normalization of the test section to bellmouth for each condition is done to remove run-to-run variations. Delta Mach number, each major division on the vertical axis in Figure 20 helps to illustrate the absolute Mach number variation seen in the data. Also, examining Figure 20, it is seen that the spraybar air injection has a minimal affect on Mach number.

Table 8 illustrates the airspeed test section spatial uniformity. All of the acquired test conditions meet the test section spatial uniformity flow quality goal of $\pm 2\%$, as laid out in Table 5.

Total Pressure

Results for total pressure are shown in Figure 21. Total pressure in the test section, $P_{T,ts}$, is normalized by total pressure at the bellmouth, $P_{T,bm}$, and plotted with respect to the width of the test section in inches. The normalization of the test section to bellmouth for each condition is done to remove run-to-run variations. A delta total pressure is seen

Table 8: Airspeed Test Section Spatial Uniformity

	0 psi	30 psi	60 psi
50 knots	±0.846%	±1.476%	±0.922%
90 knots	±0.518%	±0.585%	±0.506%
120 knots	±0.623%	±0.513%	±0.564%
150 knots	±0.563%	±0.491%	±0.522%
170 knots	±0.483%	±0.518%	±0.522%
200 knots	±0.620%	±0.504%	±0.506%
250 knots	±0.553%	±0.581%	±0.517%

in the bottom right corner of the plots to help relate the ratios presented to the absolute quantity of each y-axis division in Figure 21. Further examining Figure 21, it is seen that the spraybar air injection does have an affect on the total pressure distribution in the test section. The largest effects of the spray bars are seen at lower test section airspeeds and near the test section boundaries. For example the effect of the spraybars is more pronounced at the inner wall (0-24 inches) and the outer wall (84-108 inches). The flow in the core of the test section is seen to be minimally affected.

Static Pressure

Results for static pressure is shown in Figure 22. Static pressure in the test section, $P_{S,ts}$, is normalized by static pressure at the bellmouth, $P_{S,bm}$, and plotted with respect to the width of the test section in inches. The normalization of the test section to bellmouth for each condition is done to remove run-to-run variations. A delta static pressure is shown in the bottom right corner of the plots to help relate the quantity of one tick in Figure 22 to the ratio presented. Also, examining Figure 22 further, it is seen that the spraybar air injection does not have a significant effect on the static pressure distribution in the test section.

Total Temperature

Results for total temperature is shown in Figure 23. Test section total temperature, $T_{T,ts,array}$,°C, is shown plotted with respect to the width of the test section in inches, Figure 23.

Table 9 lists the test section spatial uniformity for the test conditions that were acquired. At a total temperature test point of −1°C the test section temperature variation is approximately ±0.25°C. However, at colder total temperature test points of −30°C and below, the test section variation is approximately ±0.5°C to ±1.3°C. This larger variation is seen because the $80-85$°C spraybar air is more pronounced in the test section at the much colder temperatures near the bottom of the IRT operating range. The last ten rows of Table 9 are hysteresis test points. All of the data in Table 9 meets its respective criteria as laid out in Table 5 when referenced to test section temperature.

Table 9: Temperature Test Section Spatial Uniformity

	0 psi	30 psi	60 psi
$T_{T,davg} = 7\,°C$, 200 knots	$\pm 0.299\,°C$	N/A	N/AC
$T_{T,davg} = 6\,°C$, 150 knots	$\pm 0.287\,°C$	N/A	N/A
$T_{T,davg} = 6\,°C$, 100 knots	$\pm 0.273\,°C$	N/A	N/A
$T_{T,davg} = 6\,°C$, 50 knots	$\pm 0.435\,°C$	N/A	N/A
$T_{T,davg} = 5\,°C$, 220 knots	$\pm 0.241\,°C$	$\pm 0.246\,°C$	$\pm 0.263\,°C$
$T_{T,davg} = 4\,°C$, 50 knots	$\pm 0.394\,°C$	$\pm 0.564\,°C$	$\pm 0.704\,°C$
$T_{T,davg} = 4\,°C$, 130 knots	$\pm 0.209\,°C$	$\pm 0.197\,°C$	$\pm 0.320\,°C$
$T_{T,davg} = 6\,°C$, 300 knots	$\pm 0.263\,°C$	$\pm 0.283\,°C$	$\pm 0.292\,°C$
$T_{T,davg} = 3\,°C$, 220 knots	N/A	$\pm 0.243\,°C$	N/A
$T_{T,davg} = 2\,°C$, 130 knots	N/A	$\pm 0.340\,°C$	N/A
$T_{T,davg} = 2\,°C$, 220 knots	N/A	$\pm 0.264\,°C$	N/A
$T_{T,davg} = 1\,°C$, 130 knots	N/A	$\pm 0.311\,°C$	N/A
$T_{T,davg} = 1\,°C$, 220 knots	N/A	$\pm 0.257\,°C$	N/A
$T_{T,davg} = 0\,°C$, 130 knots	N/A	$\pm 0.197\,°C$	N/A
$T_{T,davg} = 0\,°C$, 220 knots	$\pm 0.234\,°C$	$\pm 0.194\,°C$	$\pm 0.163\,°C$
$T_{T,davg} = -2\,°C$, 50 knots	$\pm 0.303\,°C$	$\pm 0.559\,°C$	$\pm 0.450\,°C$
$T_{T,davg} = -1\,°C$, 130 knots	$\pm 0.210\,°C$	$\pm 0.229\,°C$	$\pm 0.296\,°C$
$T_{T,davg} = 1\,°C$, 300 knots	$\pm 0.611\,°C$	$\pm 0.984\,°C$	$\pm 0.935\,°C$
$T_{T,davg} = -15\,°C$, 220 knots	$\pm 0.403\,°C$	$\pm 0.359\,°C$	$\pm 0.380\,°C$
$T_{T,davg} = -17\,°C$, 50 knots	$\pm 0.883\,°C$	$\pm 0.820\,°C$	$\pm 1.007\,°C$
$T_{T,davg} = -16\,°C$, 130 knots	$\pm 0.315\,°C$	$\pm 0.306\,°C$	$\pm 0.697\,°C$
$T_{T,davg} = -14\,°C$, 300 knots	$\pm 0.436\,°C$	$\pm 0.488\,°C$	$\pm 0.516\,°C$
$T_{T,davg} = -30\,°C$, 220 knots	$\pm 0.512\,°C$	$\pm 0.485\,°C$	$\pm 0.503\,°C$
$T_{T,davg} = -33\,°C$, 50 knots	$\pm 1.378\,°C$	$\pm 1.009\,°C$	$\pm 1.300\,°C$
$T_{T,davg} = -33\,°C$, 130 knots	$\pm 0.417\,°C$	$\pm 0.421\,°C$	$\pm 0.945\,°C$
$T_{T,davg} = -28\,°C$, 300 knots	$\pm 0.594\,°C$	$\pm 0.604\,°C$	$\pm 0.614\,°C$
$T_{T,davg} = -31\,°C$, 220 knots	N/A	$\pm 0.312\,°C$	N/A
$T_{T,davg} = -33\,°C$, 130 knots	N/A	$\pm 0.800\,°C$	N/A
$T_{T,davg} = -15\,°C$, 220 knots	N/A	$\pm 0.566\,°C$	N/A
$T_{T,davg} = -16\,°C$, 130 knots	N/A	$\pm 0.397\,°C$	N/A
$T_{T,davg} = -3\,°C$, 220 knots	N/A	$\pm 0.373\,°C$	N/A
$T_{T,davg} = -4\,°C$, 130 knots	N/A	$\pm 0.859\,°C$	N/A
$T_{T,davg} = -2\,°C$, 220 knots	N/A	$\pm 0.339\,°C$	N/A
$T_{T,davg} = -3\,°C$, 130 knots	N/A	$\pm 0.372\,°C$	N/A
$T_{T,davg} = -1\,°C$, 220 knots	N/A	$\pm 0.311\,°C$	N/A
$T_{T,davg} = -2\,°C$, 130 knots	N/A	$\pm 0.311\,°C$	N/A

Test section to D-corner comparison

Figure 24 allows for an easier visual comparison of the temperature distribution in the test section with respect to the temperature distribution at D-corner at a test condition. This

surface plot presentation was requested so customers have a better understanding of what the temperature distribution in the test section looks like with respect to the temperature distribution seen in D-corner. Figure 24 test section surface plots represent the difference of the temperature of the individual RTD in the array from the average of the RTD array temperature. Figure 24 D-corner surface plots represent the difference of the temperature of the individual D-corner temperature measurement from the average of D-corner.

Study around 0°C

An abridged study was conducted around 0°C. Some airspeed data points were omitted in the interest of time. D-corner total temperatures from 3°C to −3°C were considered for this study. Test cases 130 knots and above were found to have an appearance of mixing in the test section, with more of a temperature gradient behaviour seen in D-corner. The 50 knot test cases showed temperature gradient behaviour in both the test section and D-corner. The 300 knots, D-corner total temperature of 1°C case has the most pronounced case of mixing in the test section. This case is seen in Figure 24 (ff, gg, and hh). It is believed that this mixing behaviour is directly related the spraybar behaviour and therefore the icing cloud behaviour in the test section around 0°C.

Summary of Test Results

Aero-thermal calibration testing was completed in January and May 2012. Calibration testing was conducted to remap the test section flow quality and to re-develop the aero-thermal calibration curves which relate the test section properties to the bellmouth pitot-static probes and the D-corner RTD array. This testing occurred as a result of the major modifications that occurred to the heat exchanger and the refrigeration plant. This modification resulted in a lower achievable temperature in the test section. This is reflected in the total temperature data that was presented in this report.

A pressure discrepancy was found at 300 knots and resolved. Overall, the IRT meets most of the test section spatial uniformity flow quality goals set forth. There are a few specific test points that do not meet the test section spatial uniformity criteria depicted in Table 5. The tunnel centerline temporal stability will be examined as part of the next calibration. Also, measurement uncertainty analysis will be presented in a separate paper upon completion of the work that is currently in progress. At this time, an interim calibration is planned for February 2013. When the interim calibration data is collected, it will be compared with full calibration data set as validation.

Recommendations

The following recommendations were developed following the calibration entry. Their implementation is suggested prior to the next calibration entry into the IRT.

- Acquire data for at least 30 seconds to enable the establishment of temporal stability at tunnel centerline.

- Include instrument uncertainties upon completion of the analysis.
- Update or replace the 9-foot rake hardware. If possible, develop a method to translate the hardware to improve efficiency during the test entry.

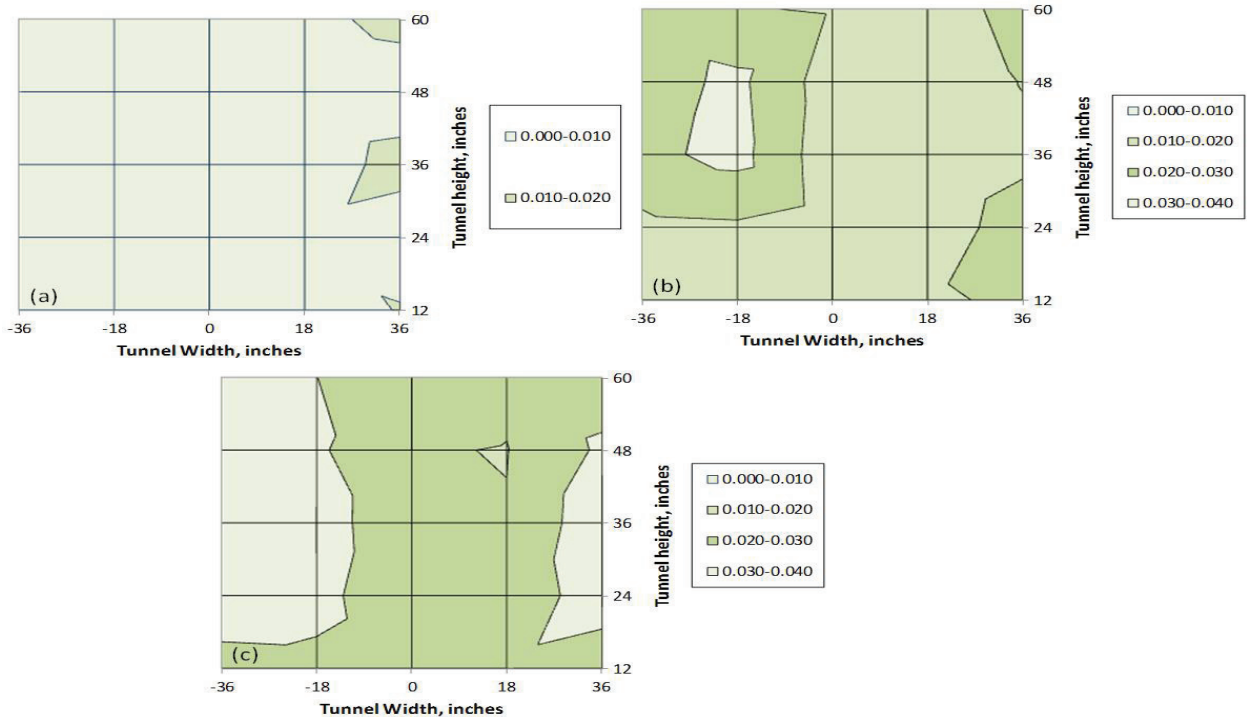

Figure 18: Test section turbulence intensity, as collected by the hot wire/film survey rake. (a) $U_{ts} = 50$ knots, $P_{air} = 0$ psig. (b) $U_{ts} = 50$ knots, $P_{air} = 30$ psig. (c) $U_{ts} = 50$ knots, $P_{air} = 60$ psig.

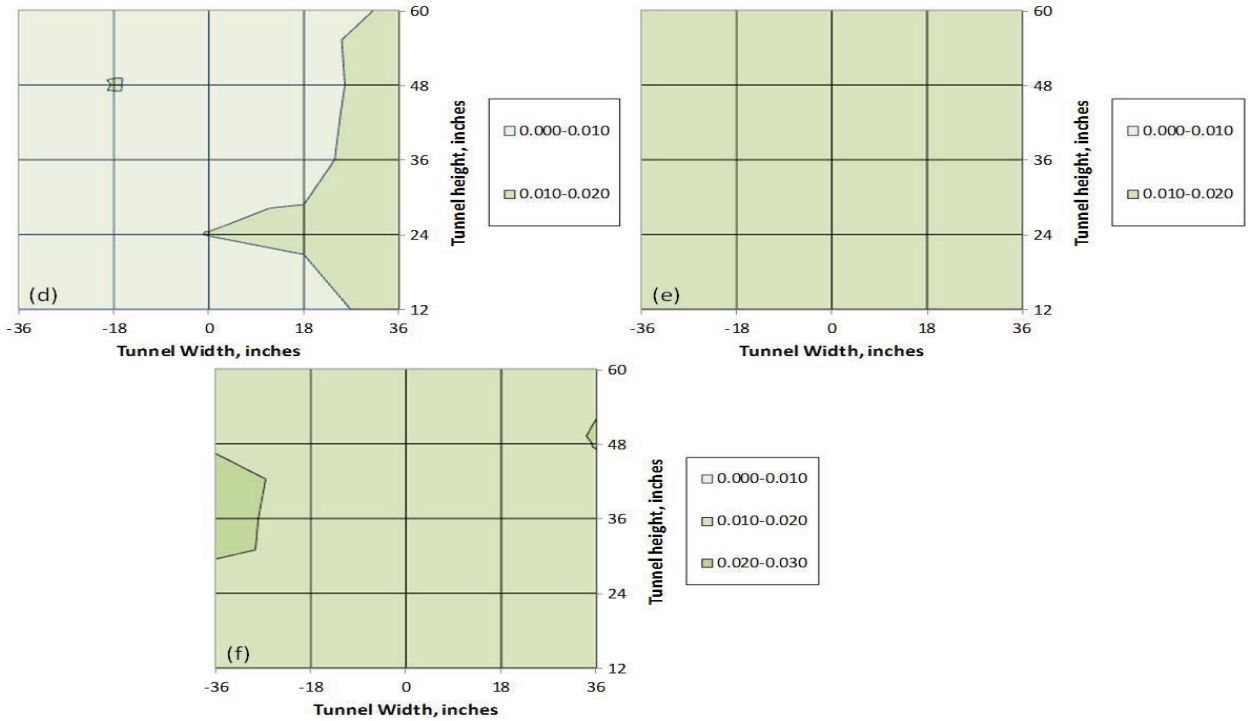

Continued Figure 18: (d) $U_{ts} = 90$ knots, $P_{air} = 0$ psig. (e) $U_{ts} = 90$ knots, $P_{air} = 30$ psig. (f) $U_{ts} = 90$ knots, $P_{air} = 60$ psig.

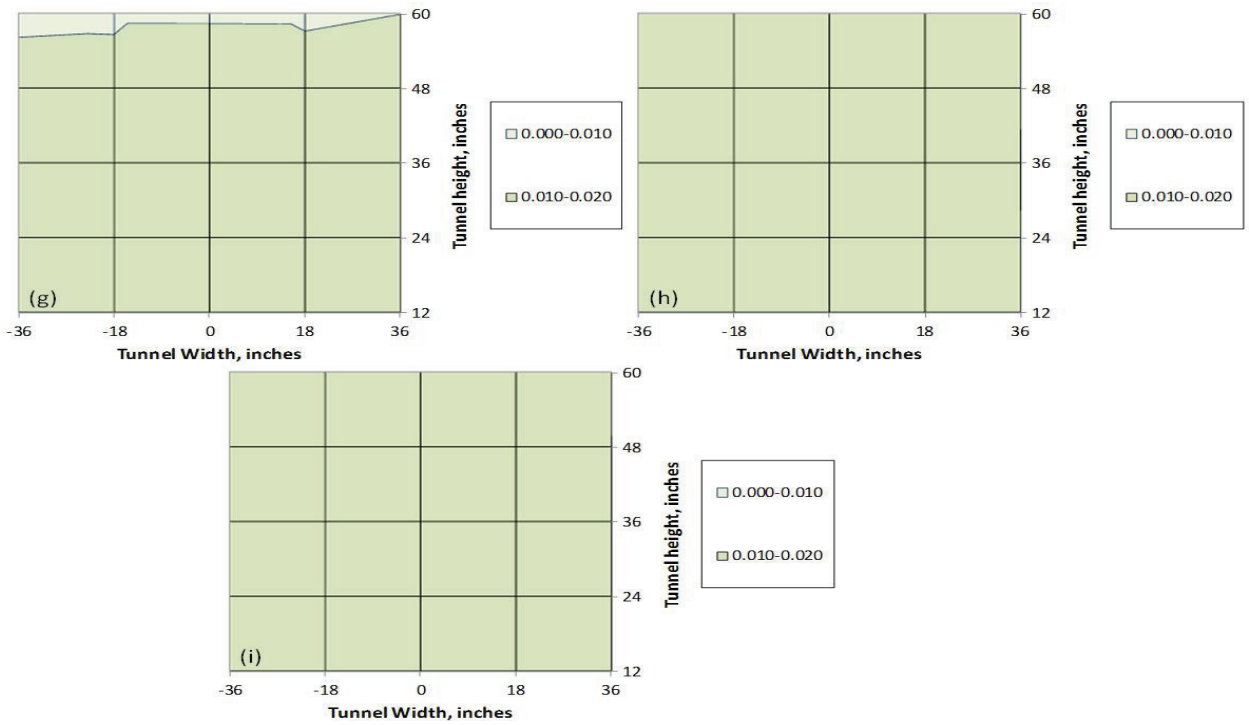

Continued Figure 18: (g) $U_{ts} = 120$ knots, $P_{air} = 0$ psig. (h) $U_{ts} = 120$ knots, $P_{air} = 30$ psig. (i) $U_{ts} = 120$ knots, $P_{air} = 60$ psig.

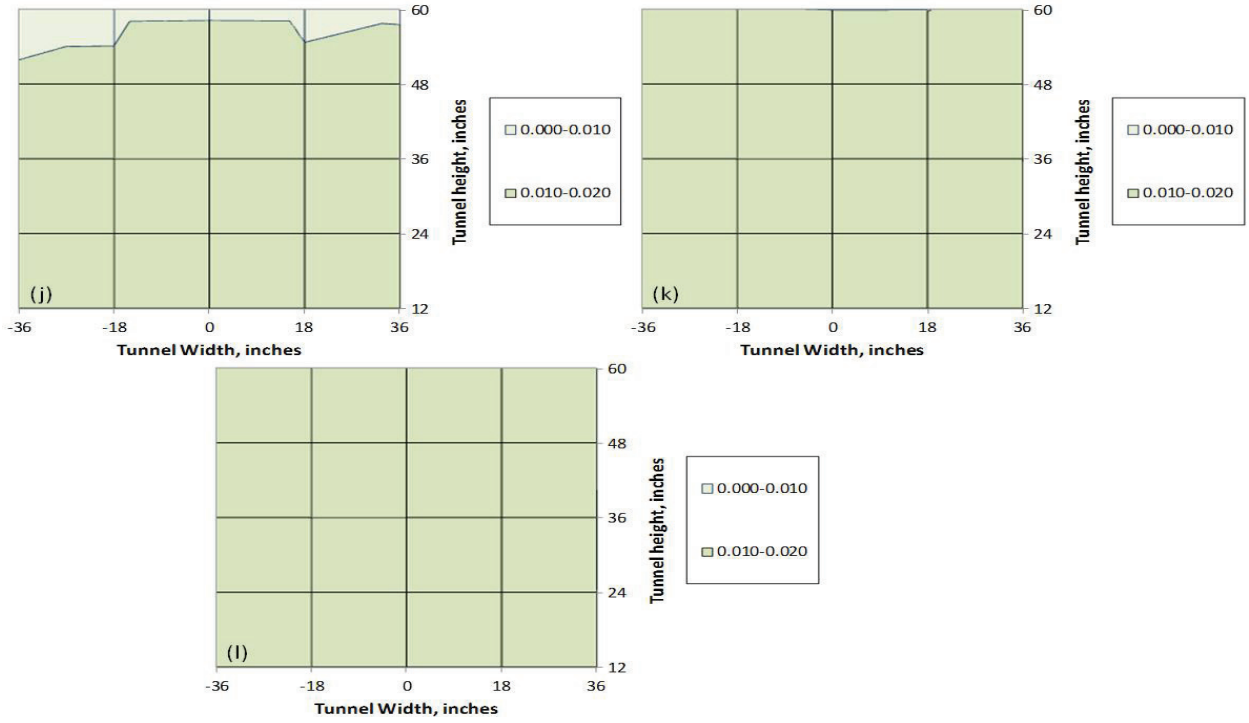

Continued Figure 18: (j) $U_{ts} = 150$ knots, $P_{air} = 0$ psig. (k) $U_{ts} = 150$ knots, $P_{air} = 30$ psig. (l) $U_{ts} = 150$ knots, $P_{air} = 60$ psig.

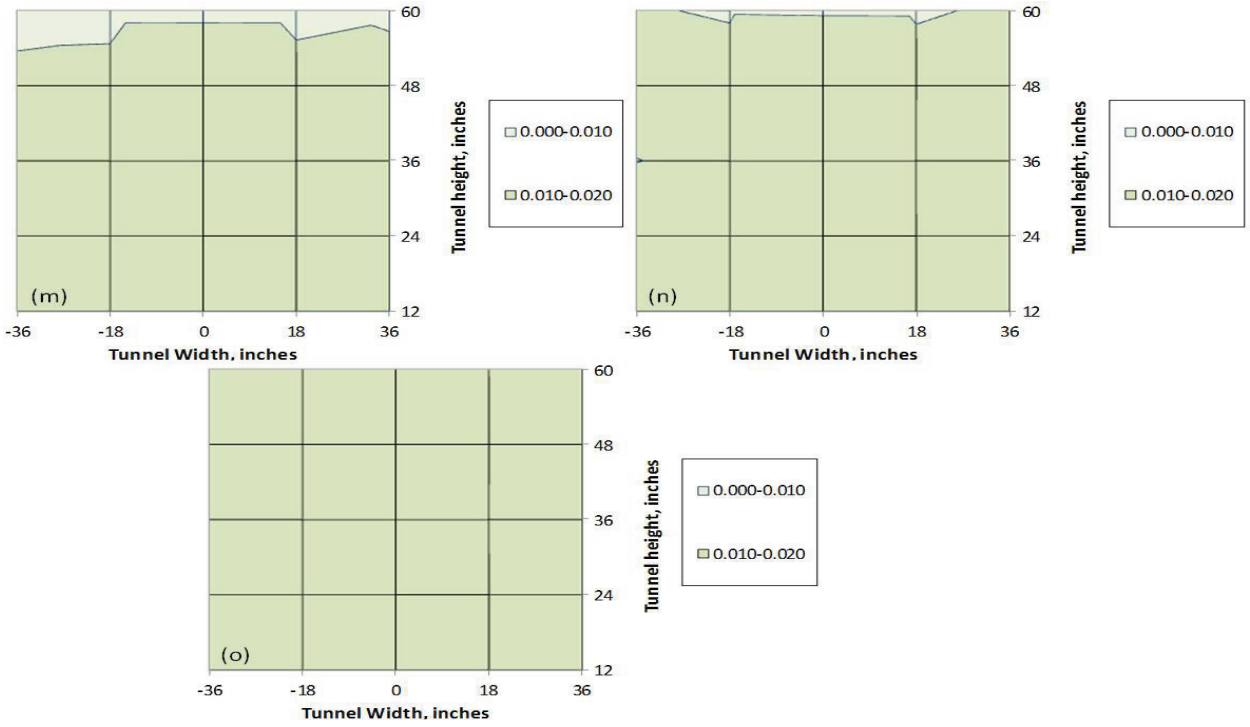

Continued Figure 18: (m) U_{ts} = 170 knots, P_{air} = 0 psig. (n) U_{ts} = 170 knots, P_{air} = 30 psig. (o) U_{ts} = 170 knots, P_{air} = 60 psig.

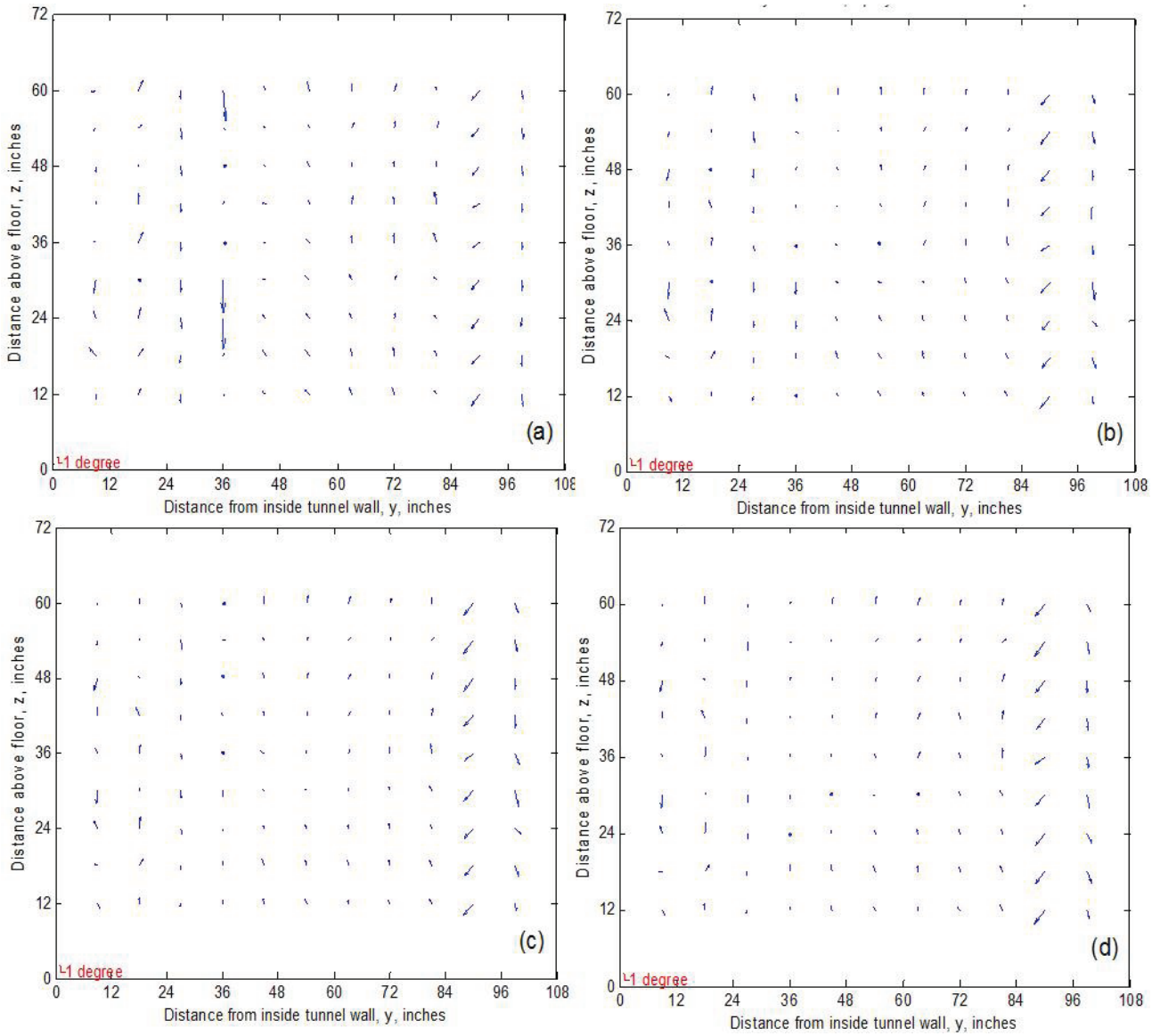

Figure 19: (a) $U_{ts} = 50$ knots, $P_{air} = 0$ psig. (b) $U_{ts} = 90$ knots, $P_{air} = 0$ psig. (c) $U_{ts} = 120$ knots, $P_{air} = 0$ psig. (d) $U_{ts} = 150$ knots, $P_{air} = 0$ psig.

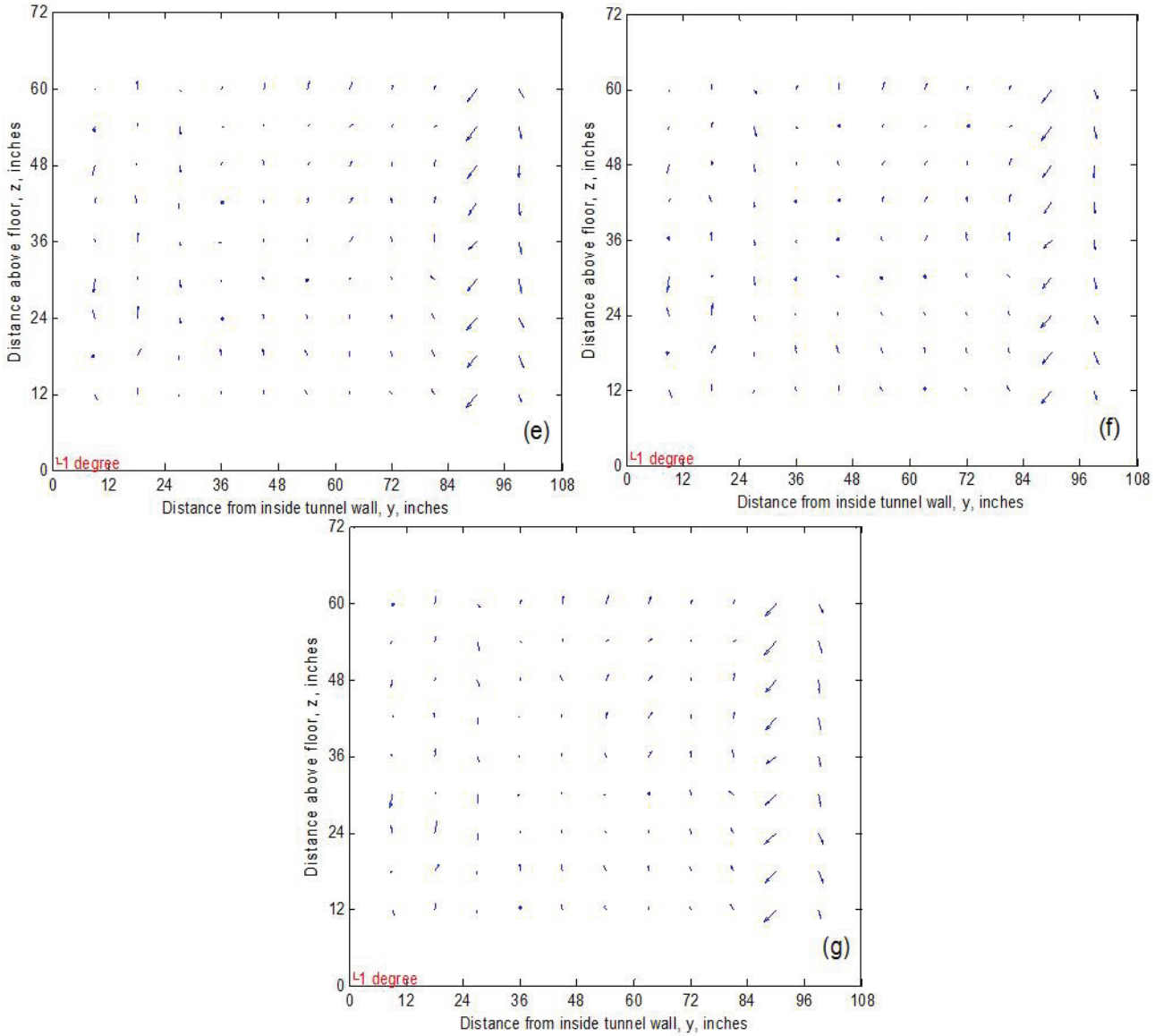

Continued Figure 19: (e) $U_{ts} = 170$ knots, $P_{air} = 0$ psig. (f) $U_{ts} = 200$ knots, $P_{air} = 0$ psig. (g) $U_{ts} = 250$ knots, $P_{air} = 0$ psig.

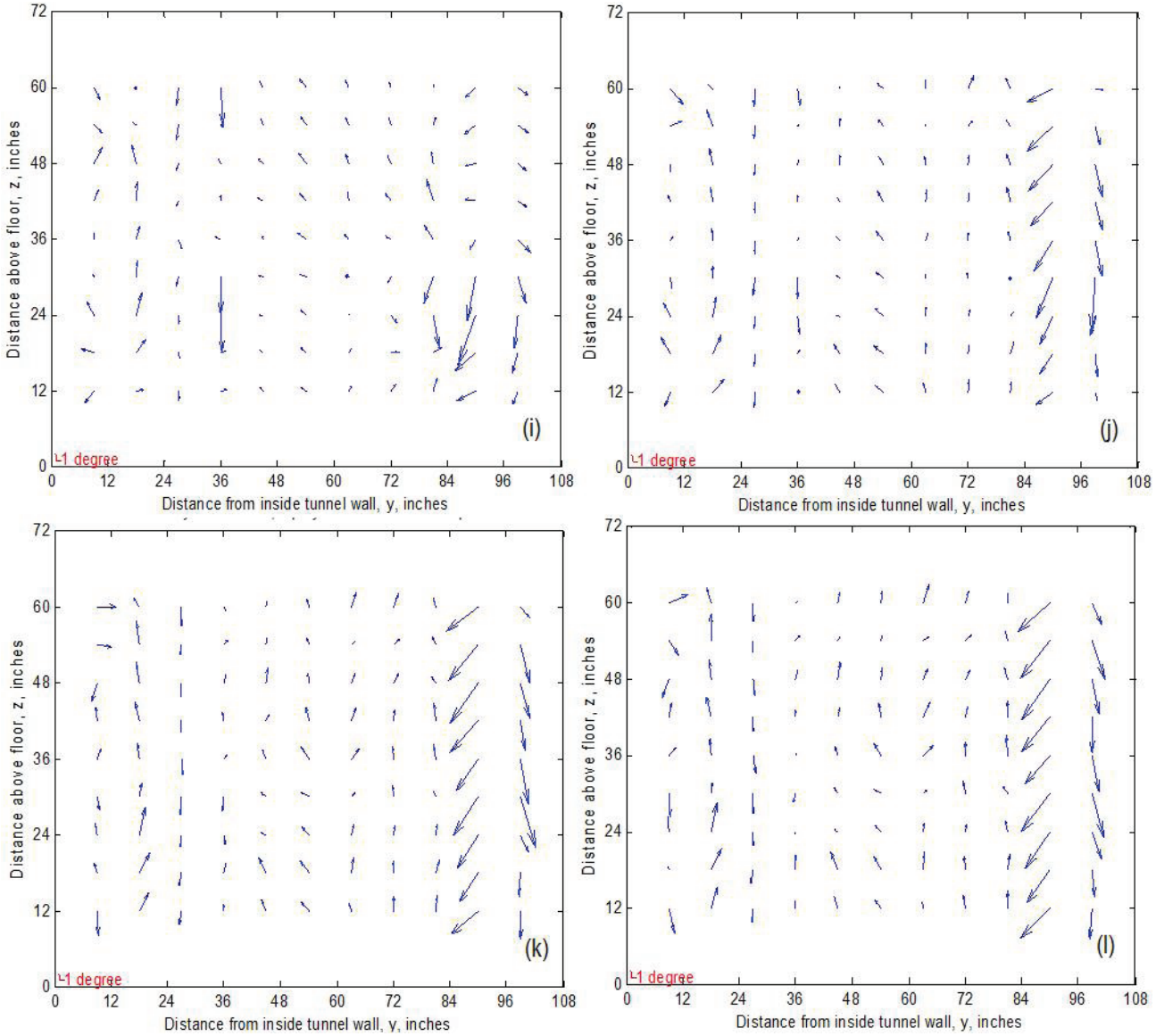

Continued Figure 19: (i) $U_{ts} = 50$ knots, $P_{air} = 30$ psig. (j) $U_{ts} = 90$ knots, $P_{air} = 30$ psig. (k) $U_{ts} = 120$ knots, $P_{air} = 30$ psig. (l) $U_{ts} = 150$ knots, $P_{air} = 30$ psig.

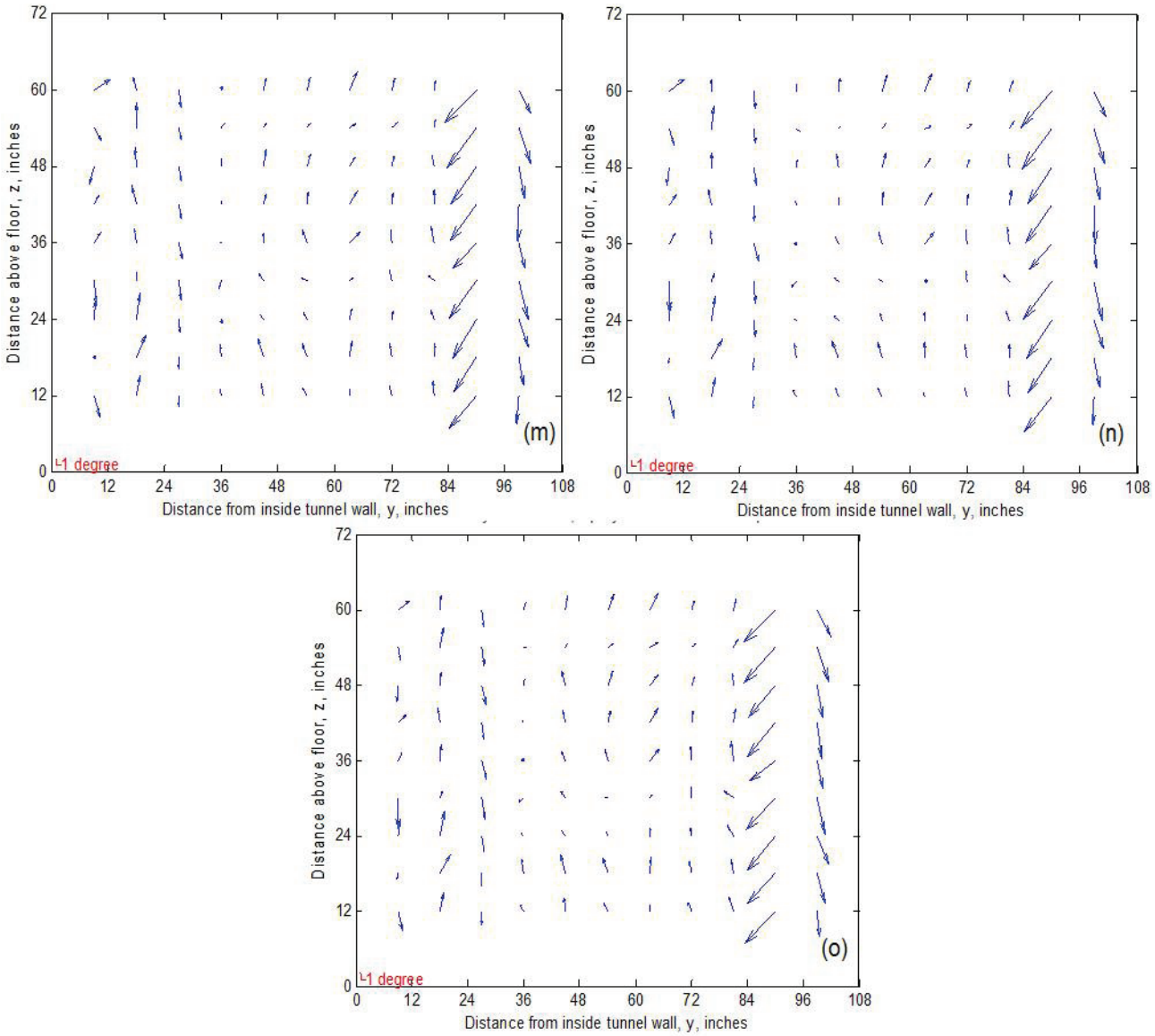

Continued Figure 19: (m) $U_{ts} = 170$ knots, $P_{air} = 30$ psig. (n) $U_{ts} = 200$ knots, $P_{air} = 30$ psig. (o) $U_{ts} = 250$ knots, $P_{air} = 30$ psig.

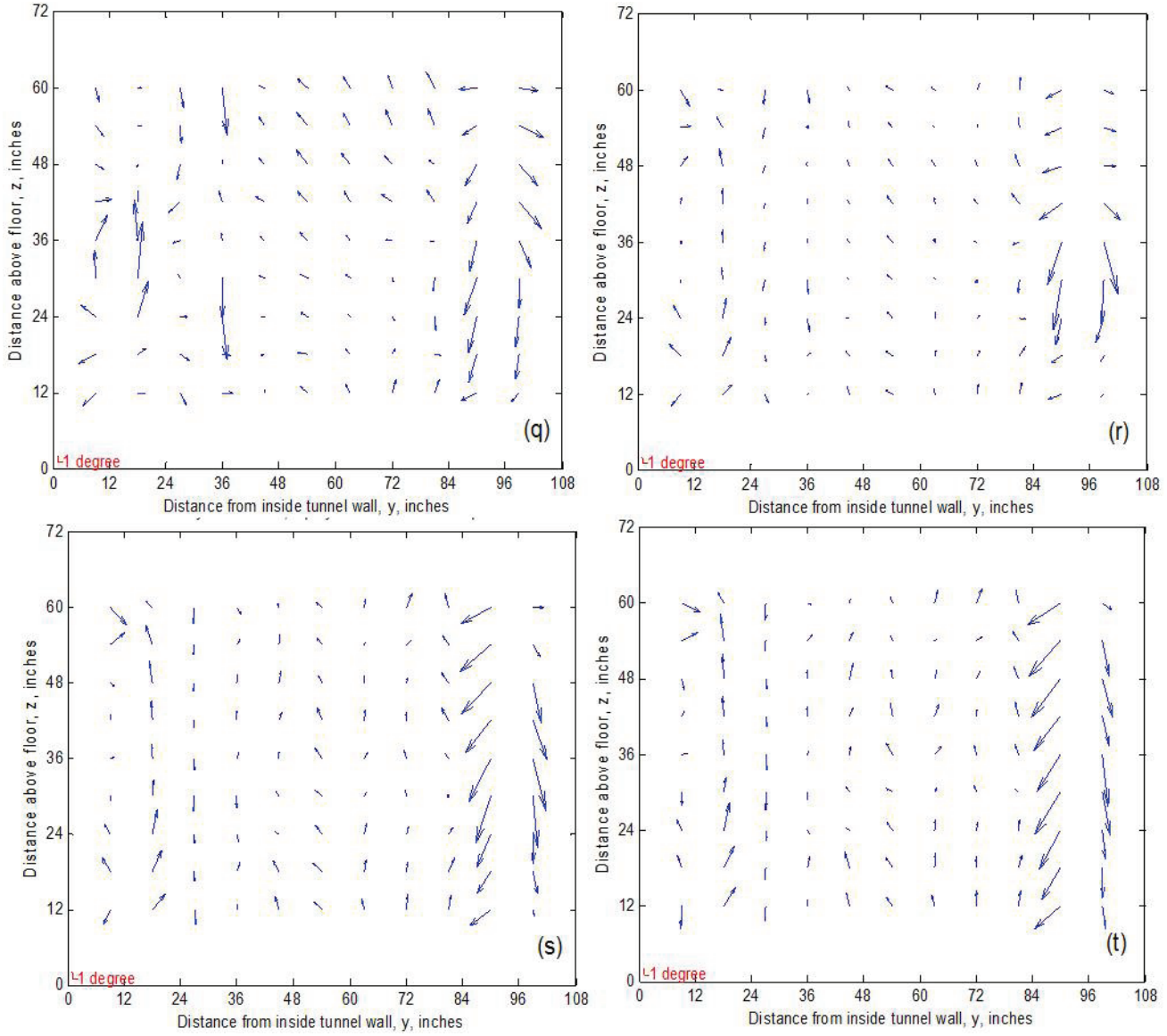

Continued Figure 19: (q) $U_{ts} = 50$ knots, $P_{air} = 60$ psig. (r) $U_{ts} = 90$ knots, $P_{air} = 60$ psig. (s) $U_{ts} = 120$ knots, $P_{air} = 60$ psig. (t) $U_{ts} = 150$ knots, $P_{air} = 60$ psig.

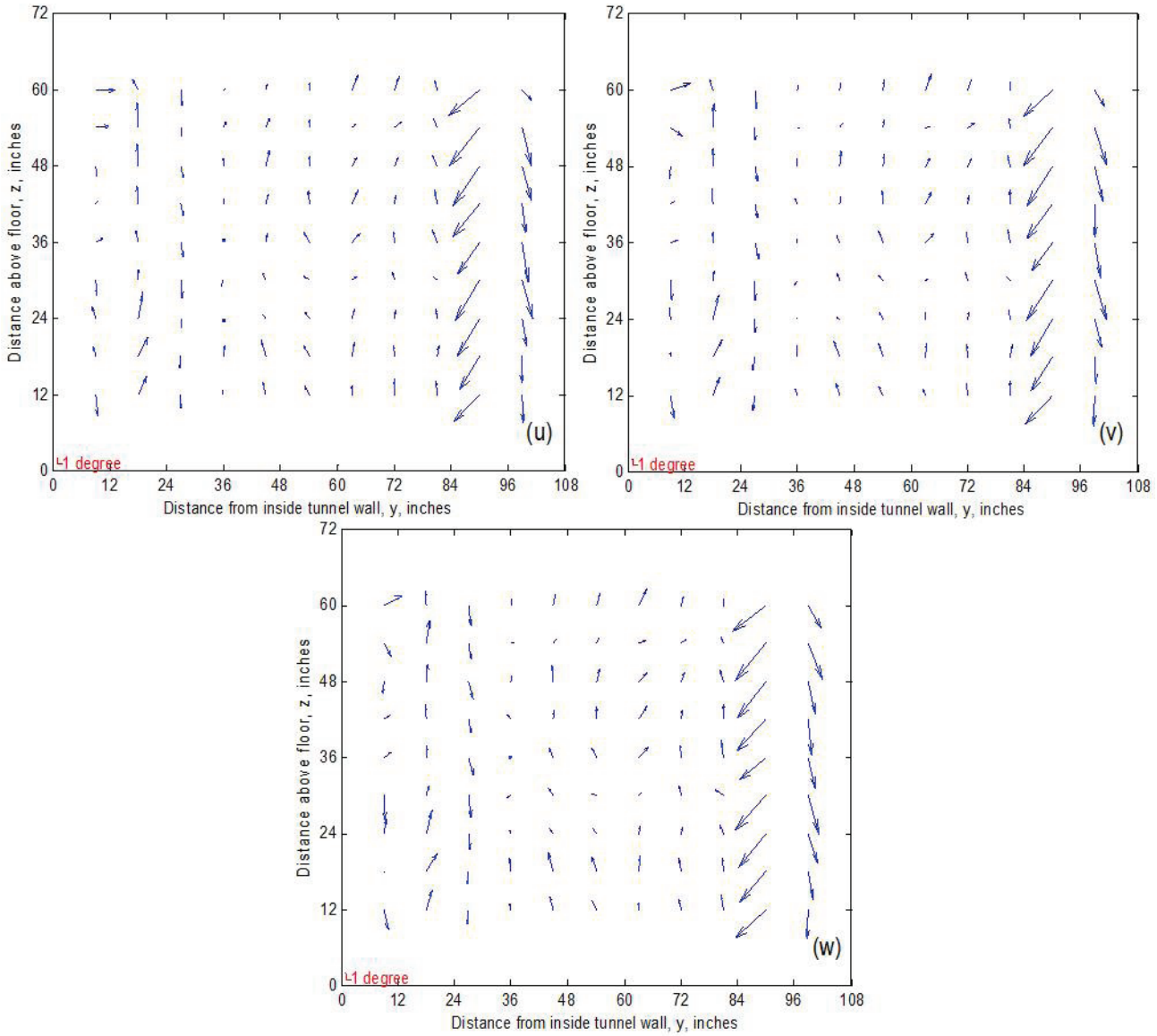

Continued Figure 19: (u) $U_{ts} = 170$ knots, $P_{air} = 60$ psig. (v) $U_{ts} = 200$ knots, $P_{air} = 60$ psig. (w) $U_{ts} = 250$ knots, $P_{air} = 60$ psig.

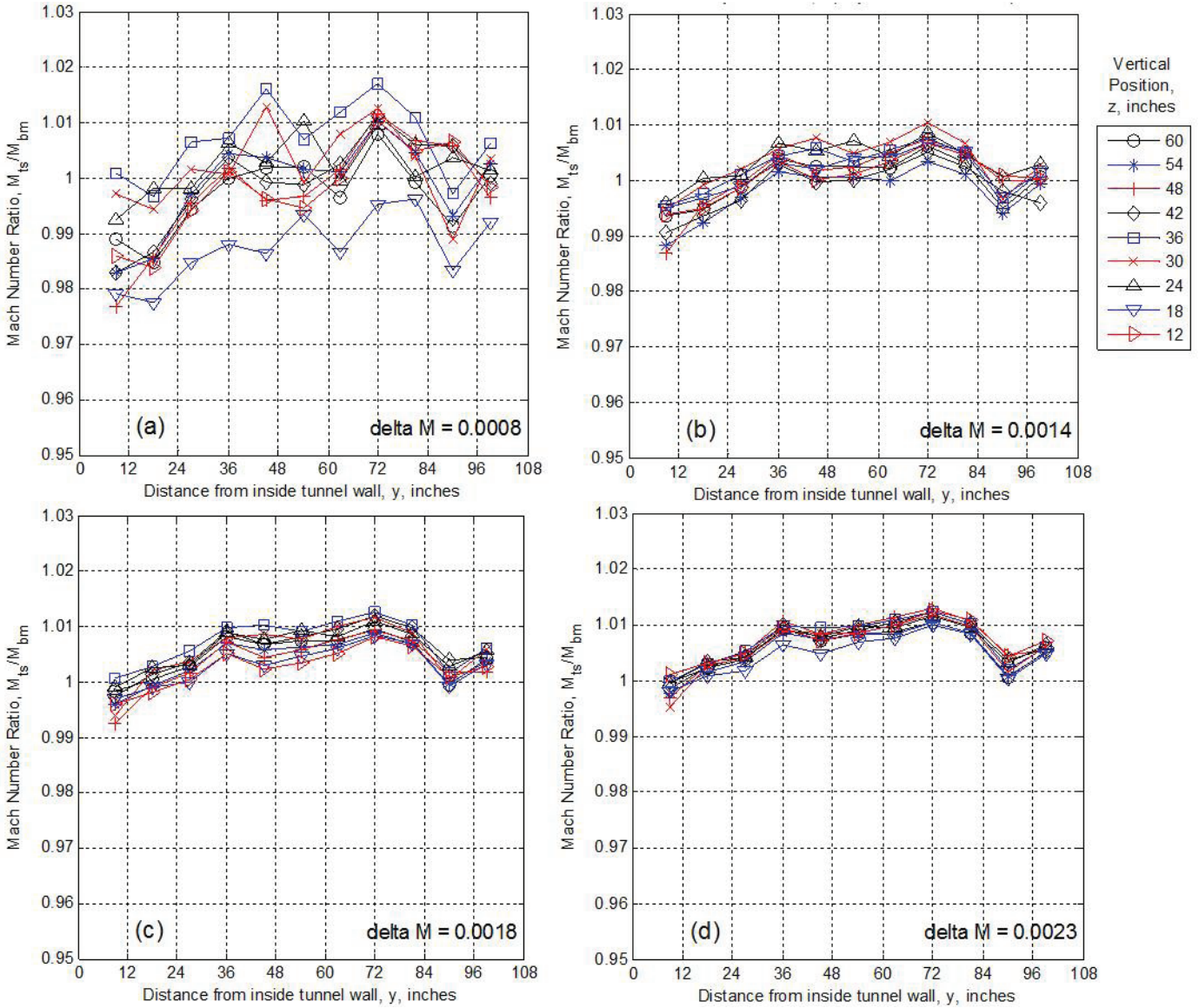

Figure 20: Mach number distribution data from the IRT test section. Data collected using the 9-ft survey rake mounted at 9 vertical positions over several tunnel runs. The test section Mach number data was normalized using the bellmouth Mach number measurement. Approximate Mach number delta is indicated for each test section setting. (a) $U_{ts} = 50$ knots, $P_{air} = 0$ psig. (b) $U_{ts} = 90$ knots, $P_{air} = 0$ psig. (c) $U_{ts} = 120$ knots, $P_{air} = 0$ psig. (d) $U_{ts} = 150$ knots, $P_{air} = 0$ psig.

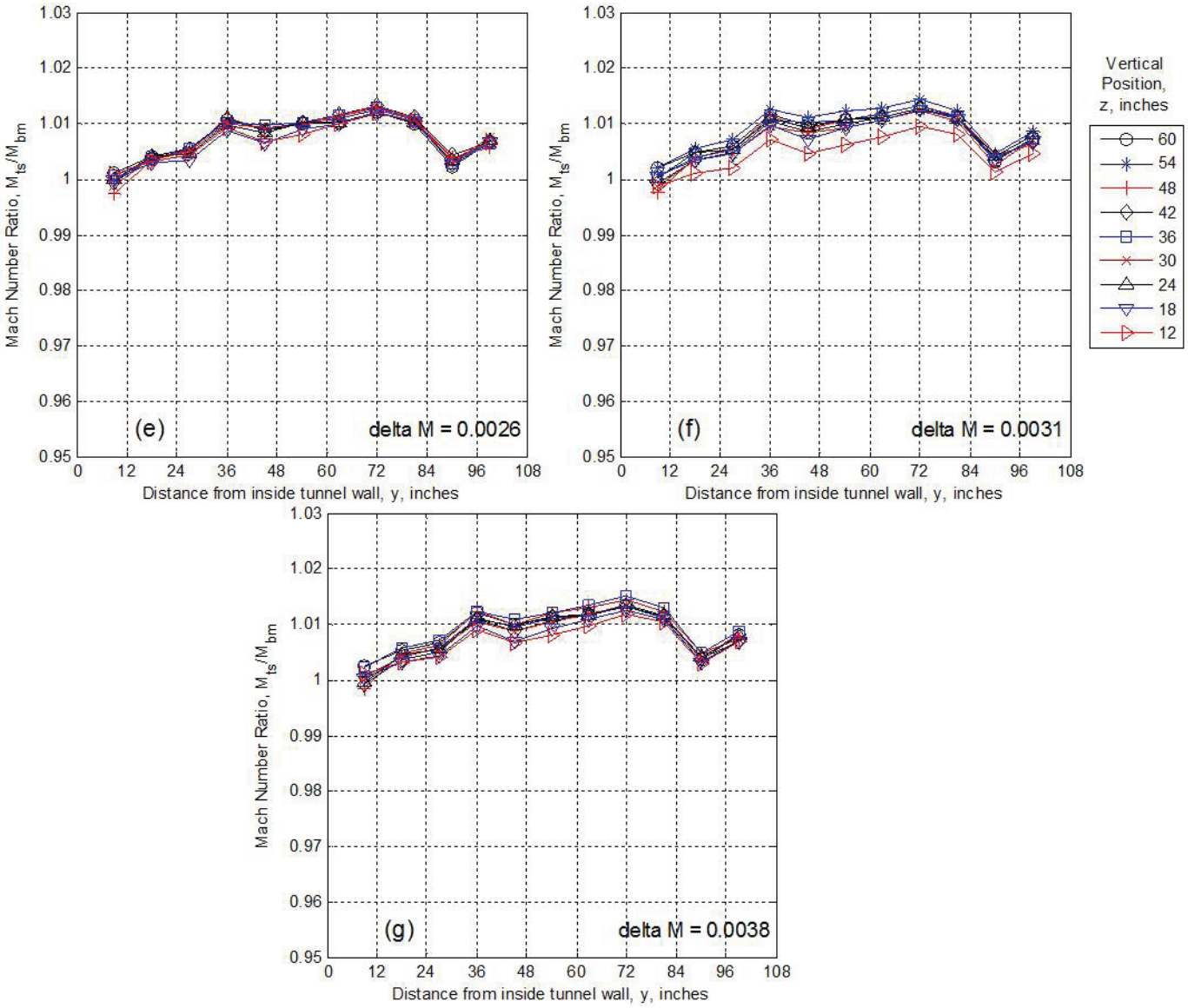

Continued Figure 20: (e) $U_{ts} = 170$ knots, $P_{air} = 0$ psig. (f) $U_{ts} = 200$ knots, $P_{air} = 0$ psig. (g) $U_{ts} = 250$ knots, $P_{air} = 0$ psig.

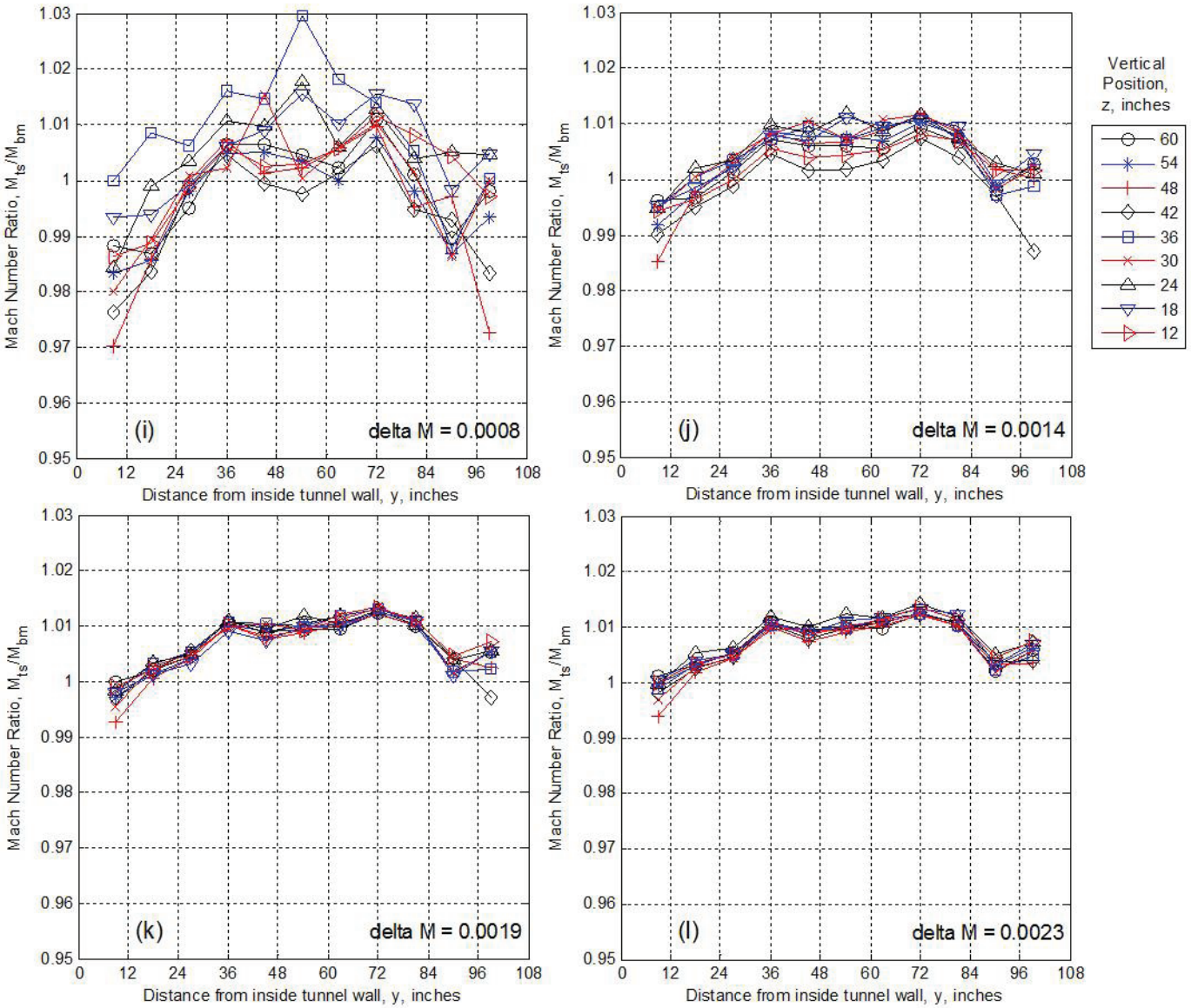

Continued Figure 20: (i) U_{ts} = 50 knots, P_{air} = 30 psig. (j) U_{ts} = 90 knots, P_{air} = 30 psig. (k) U_{ts} = 120 knots, P_{air} = 30 psig. (l) U_{ts} = 150 knots, P_{air} = 30 psig.

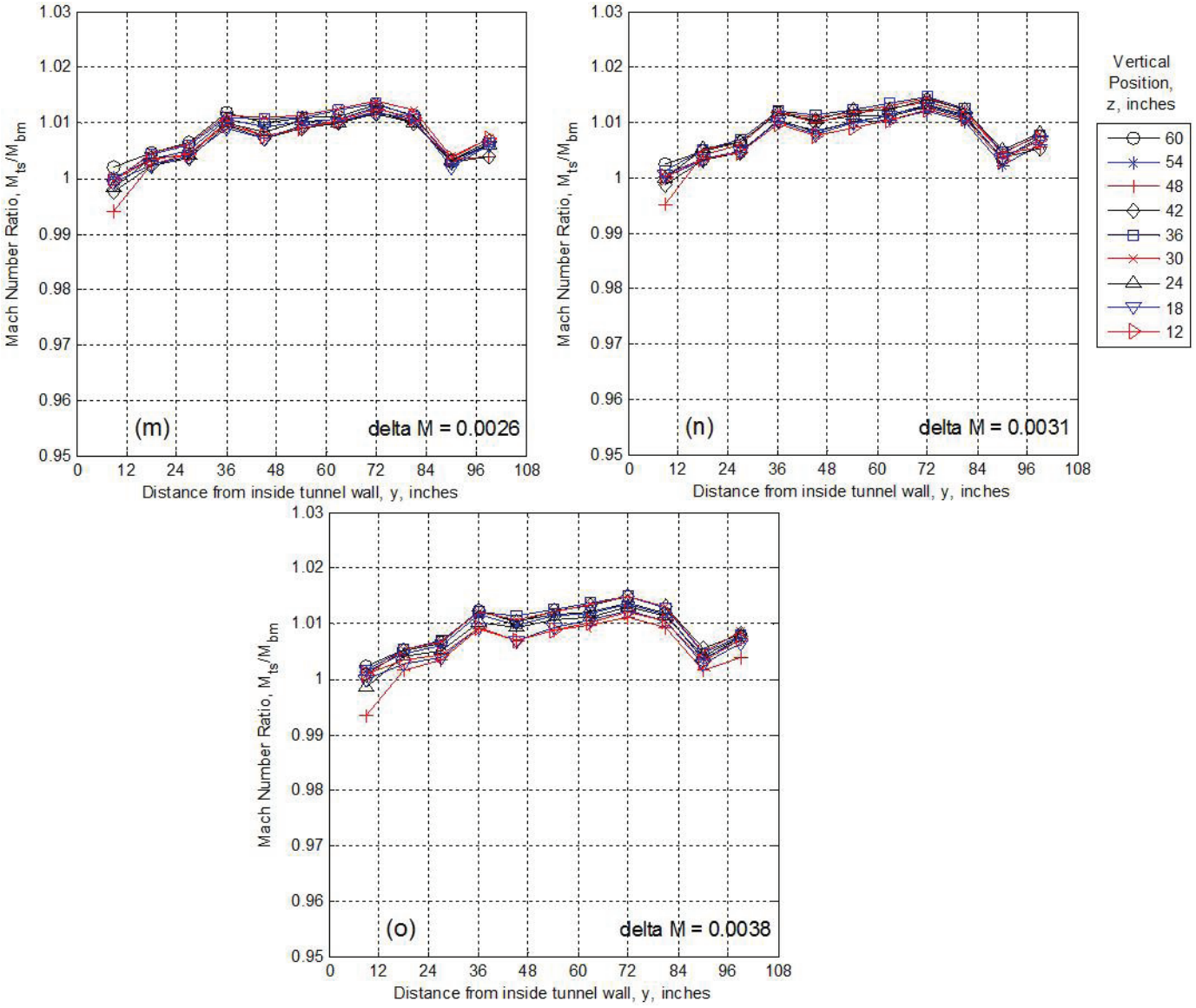

Continued Figure 20: (m) U_{ts} = 170 knots, P_{air} = 30 psig. (n) U_{ts} = 200 knots, P_{air} = 30 psig. (o) U_{ts} = 250 knots, P_{air} = 30 psig.

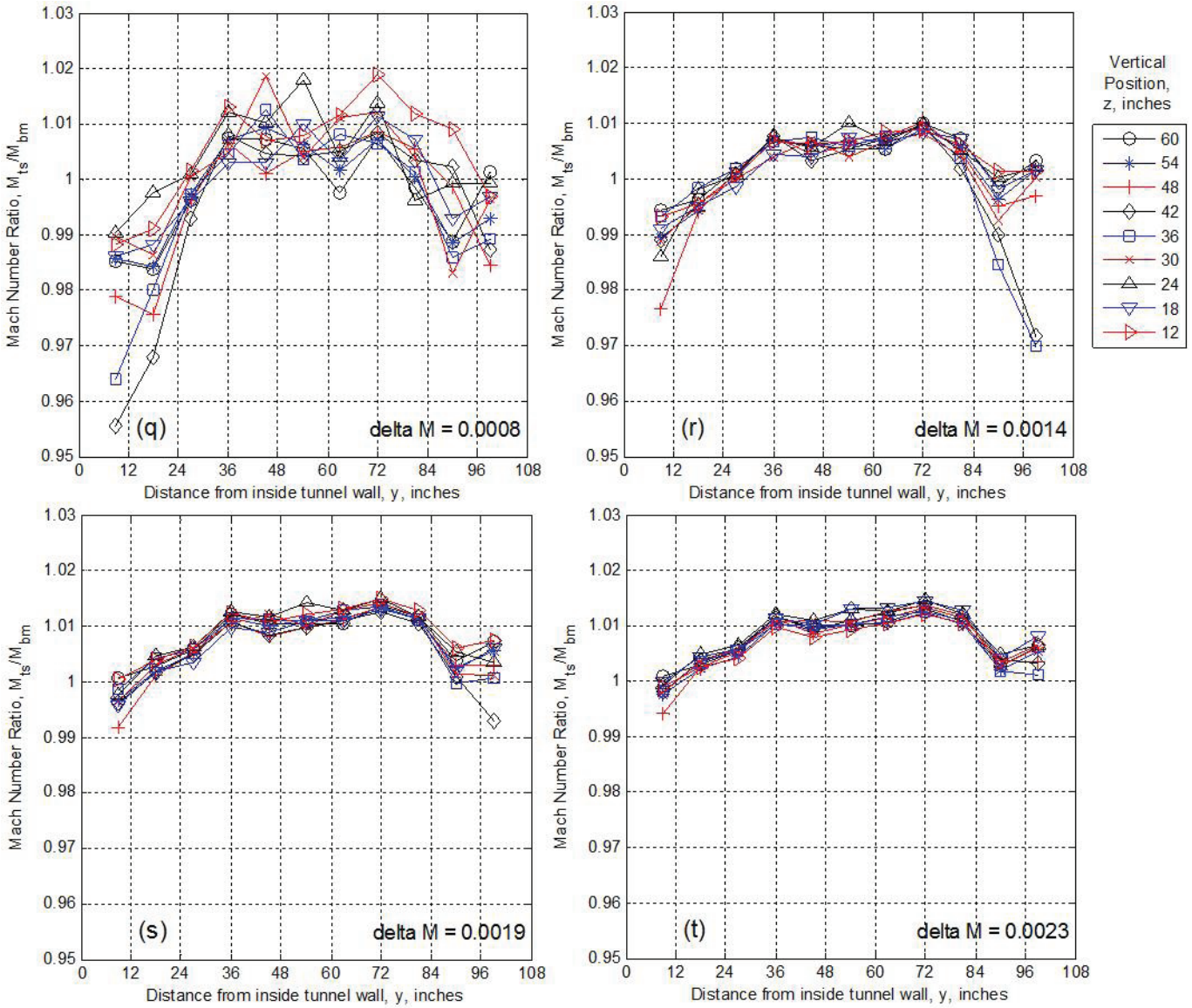

Continued Figure 20: (q) U_{ts} = 50 knots, P_{air} = 60 psig. (r) U_{ts} = 90 knots, P_{air} = 60 psig. (s) U_{ts} = 120 knots, P_{air} = 60 psig. (t) U_{ts} = 150 knots, P_{air} = 60 psig.

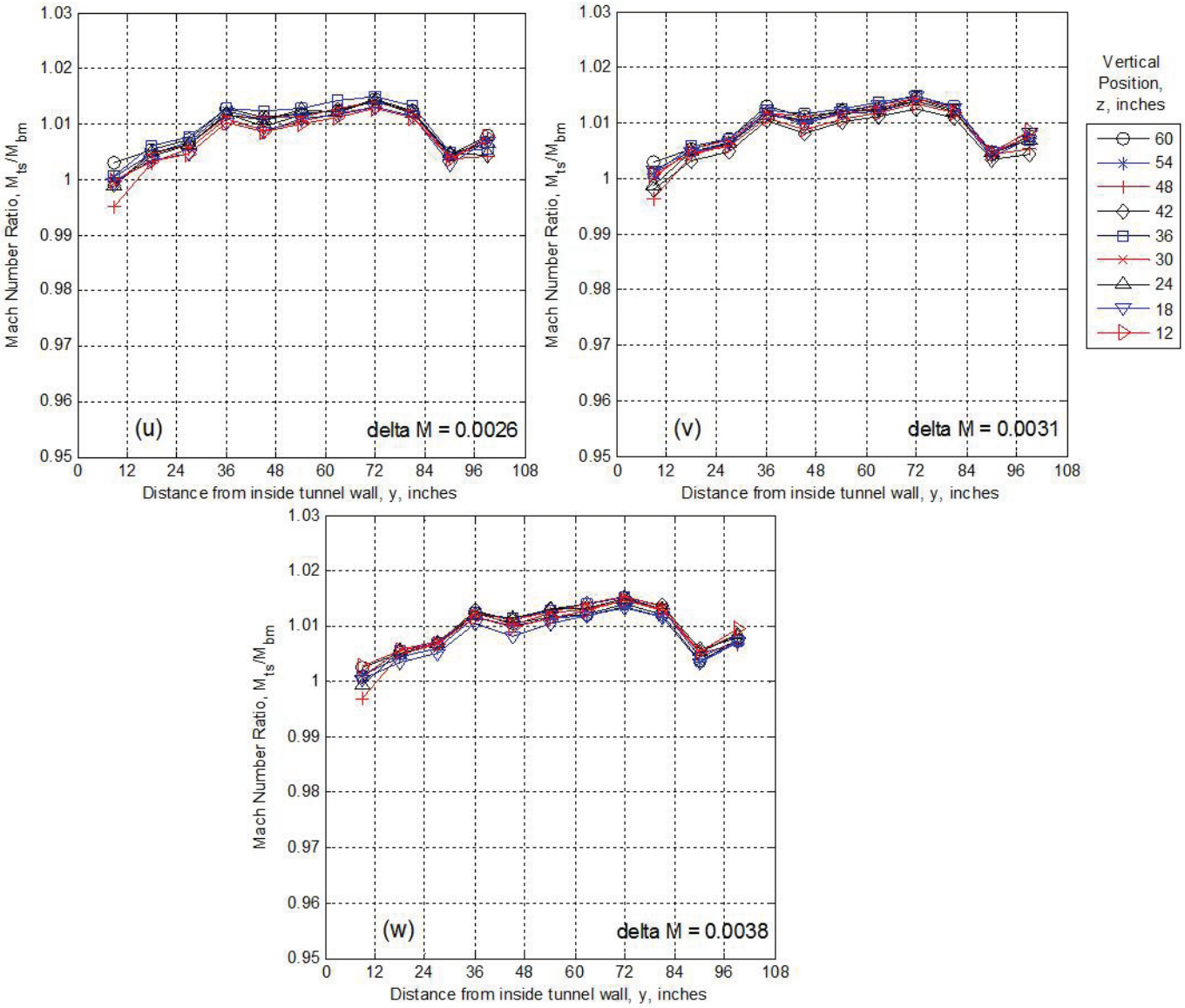

Continued Figure 20: (u) $U_{ts} = 170$ knots, $P_{air} = 60$ psig. (v) $U_{ts} = 200$ knots, $P_{air} = 60$ psig. (w) $U_{ts} = 250$ knots, $P_{air} = 60$ psig.

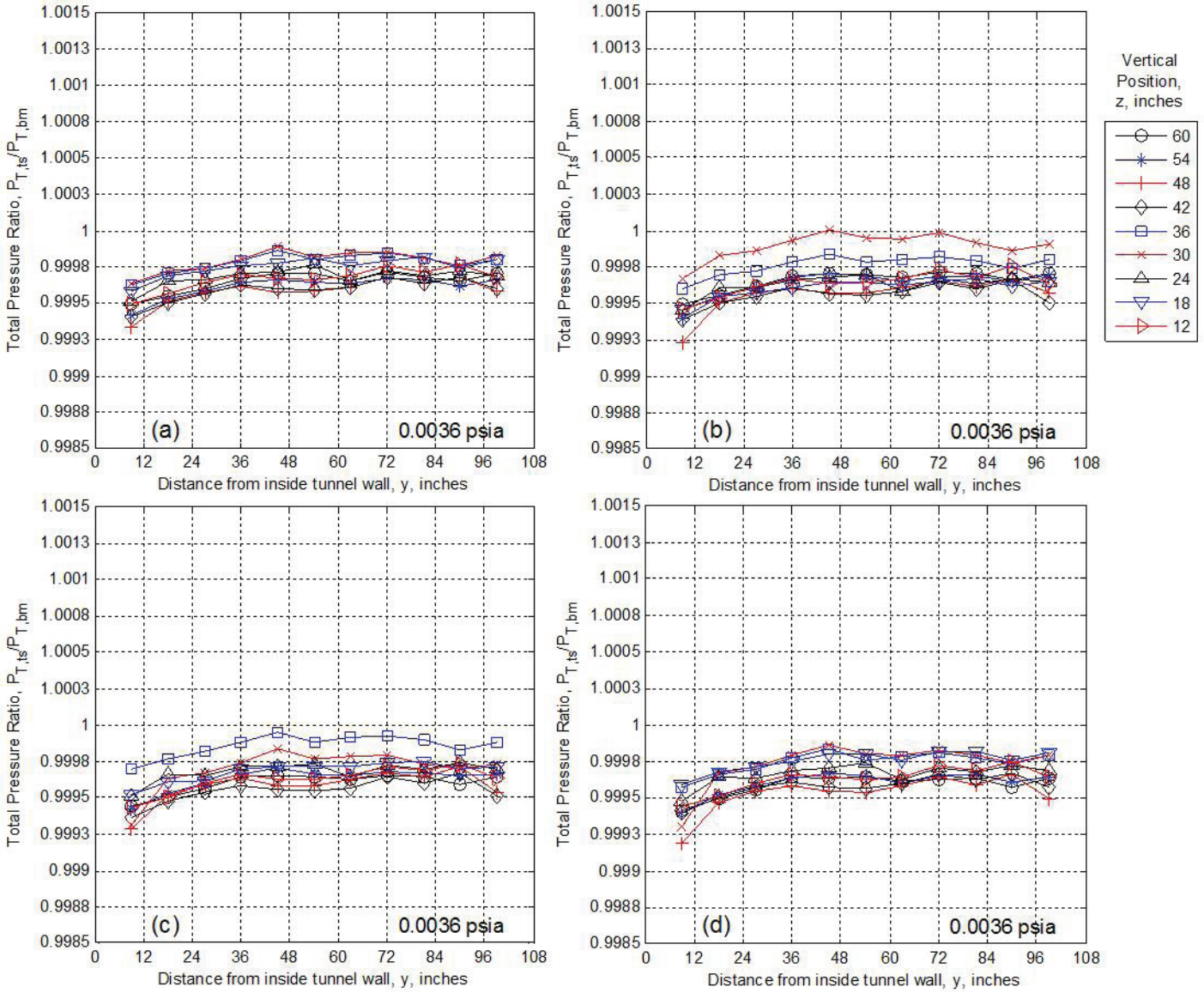

Figure 21: Total pressure distribution data from the IRT test section. Data collected using the 9-ft survey rake mounted at 9 vertical positions over several tunnel runs. The test section total pressure data is normalized using the bellmouth total pressure measurement. (a) U_{ts} = 50 knots, P_{air} = 0 psig. (b) U_{ts} = 90 knots, P_{air} = 0 psig. (c) U_{ts} = 120 knots, P_{air} = 0 psig. (d) U_{ts} = 150 knots, P_{air} = 0 psig.

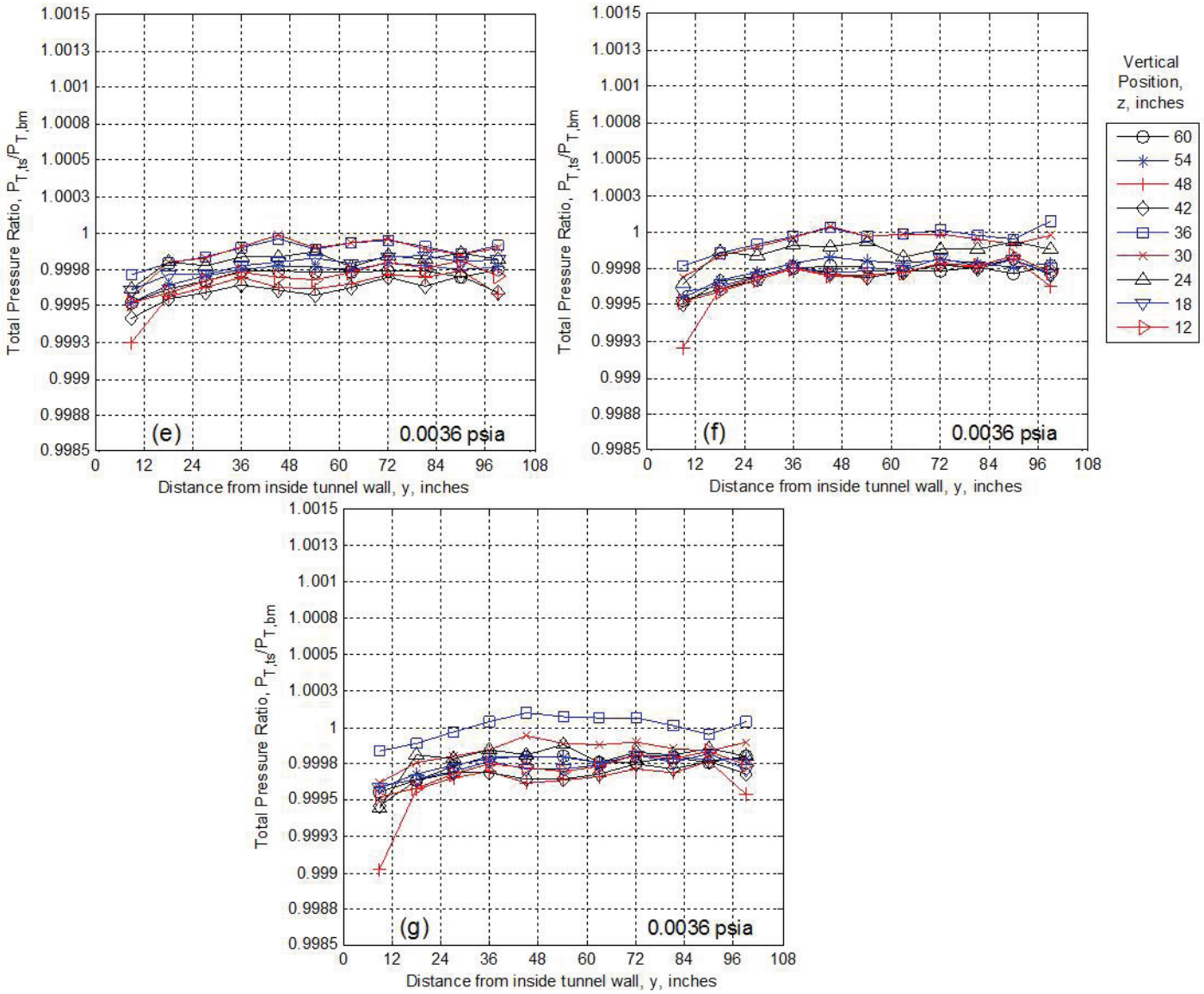

Continued Figure 21: (e) $U_{ts} = 170$ knots, $P_{air} = 0$ psig. (f) $U_{ts} = 200$ knots, $P_{air} = 0$ psig. (g) $U_{ts} = 250$ knots, $P_{air} = 0$ psig.

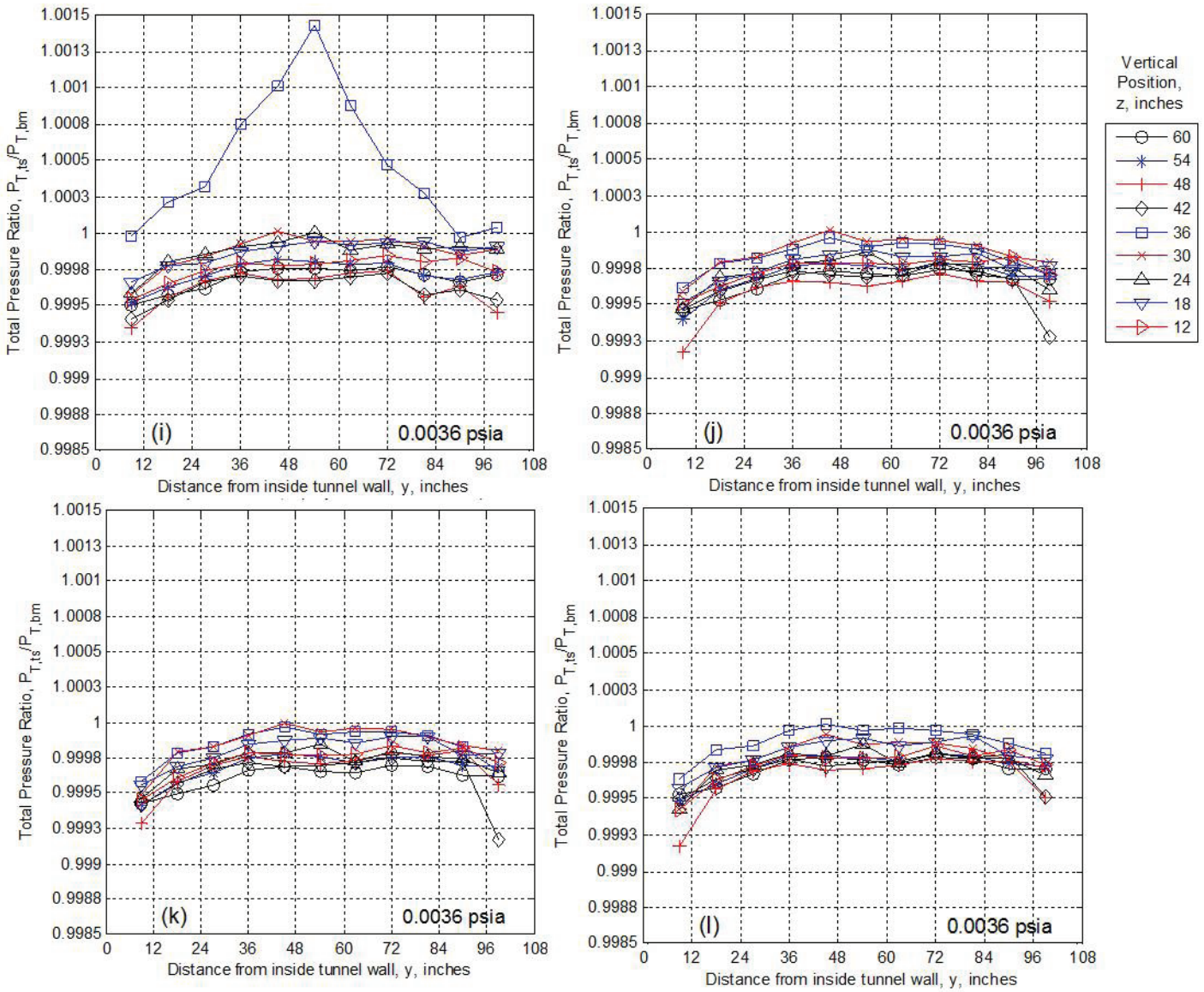

Continued Figure 21: (i) U_{ts} = 50 knots, P_{air} = 30 psig. (j) U_{ts} = 90 knots, P_{air} = 30 psig. (k) U_{ts} = 120 knots, P_{air} = 30 psig. (l) U_{ts} = 150 knots, P_{air} = 30 psig.

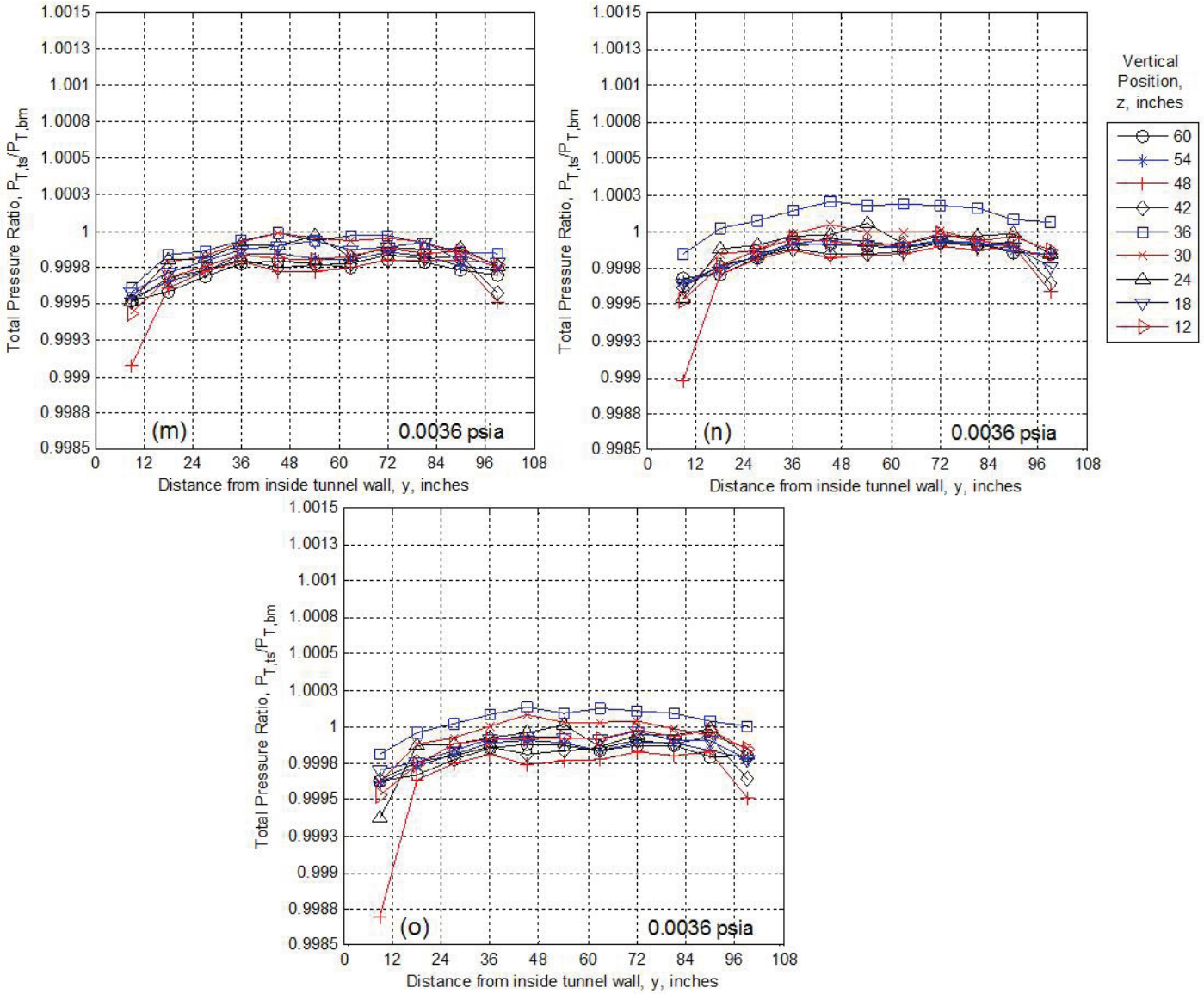

Continued Figure 21: (m) U_{ts} = 170 knots, P_{air} = 30 psig. (n) U_{ts} = 200 knots, P_{air} = 30 psig. (o) U_{ts} = 250 knots, P_{air} = 30 psig.

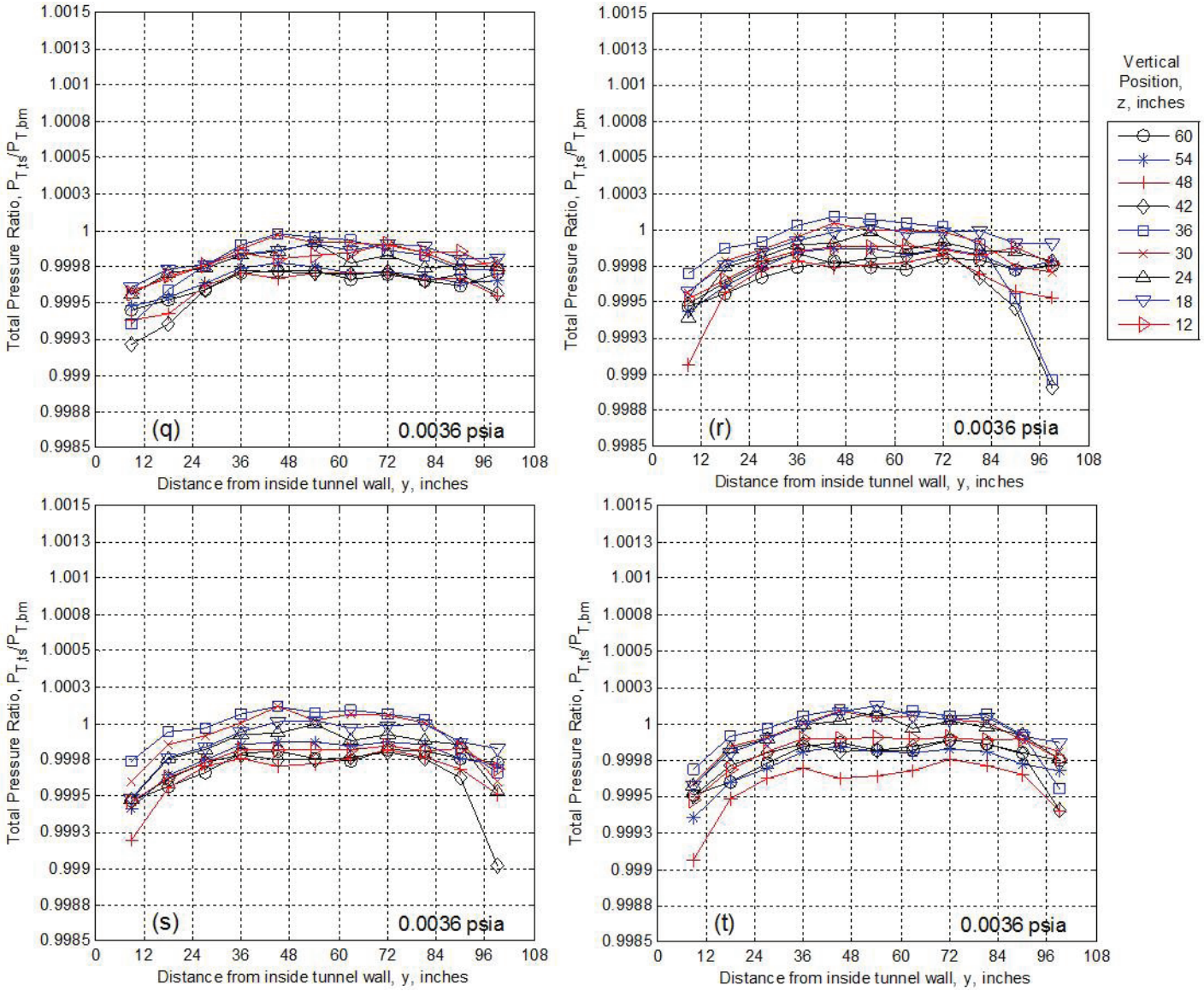

Continued Figure 21: (q) U_{ts} = 50 knots, P_{air} = 60 psig. (r) U_{ts} = 90 knots, P_{air} = 60 psig. (s) U_{ts} = 120 knots, P_{air} = 60 psig. (t) U_{ts} = 150 knots, P_{air} = 60 psig.

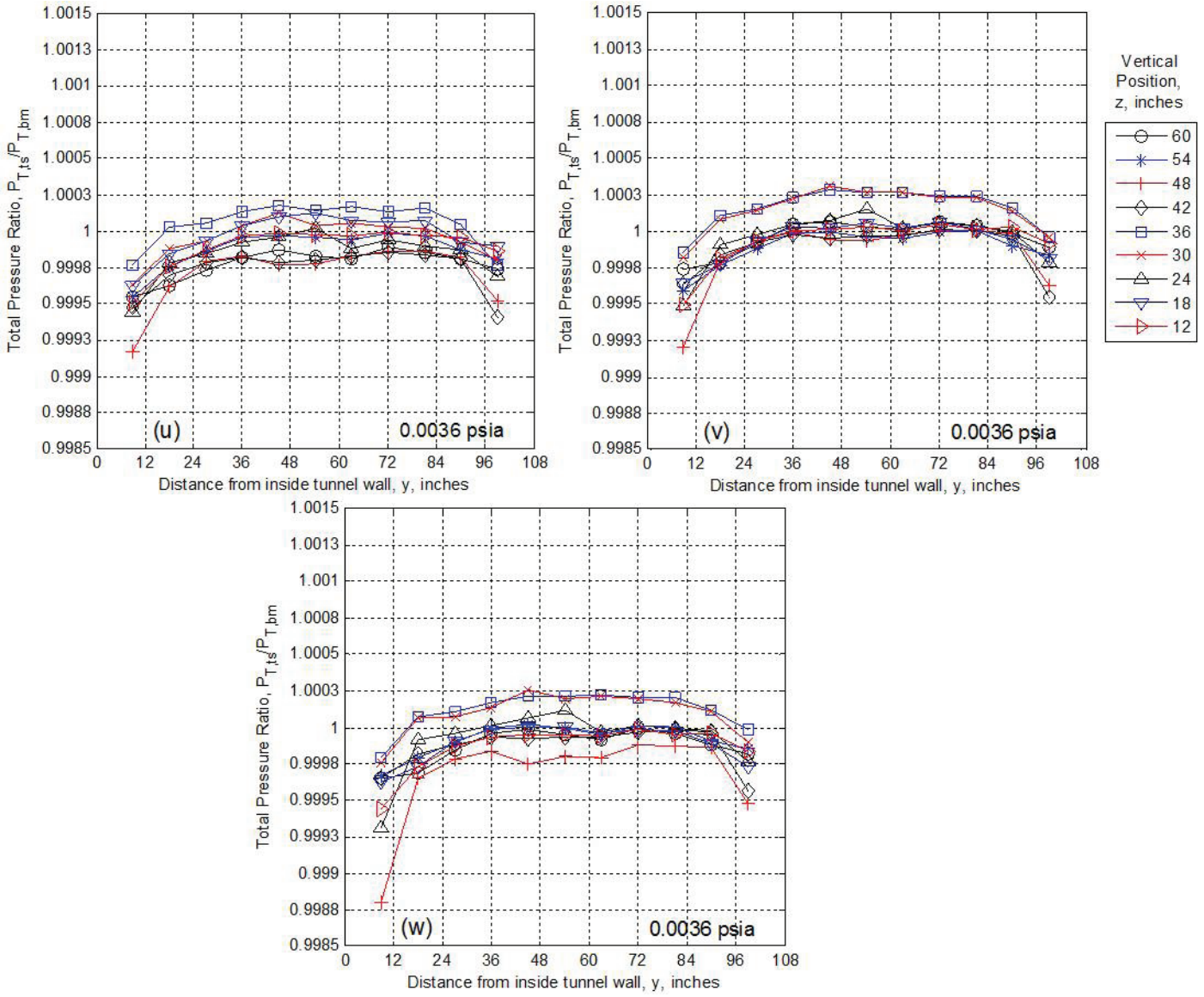

Continued Figure 21: (u) $U_{ts} = 170$ knots, $P_{air} = 60$ psig. (v) $U_{ts} = 200$ knots, $P_{air} = 60$ psig. (w) $U_{ts} = 250$ knots, $P_{air} = 60$ psig.

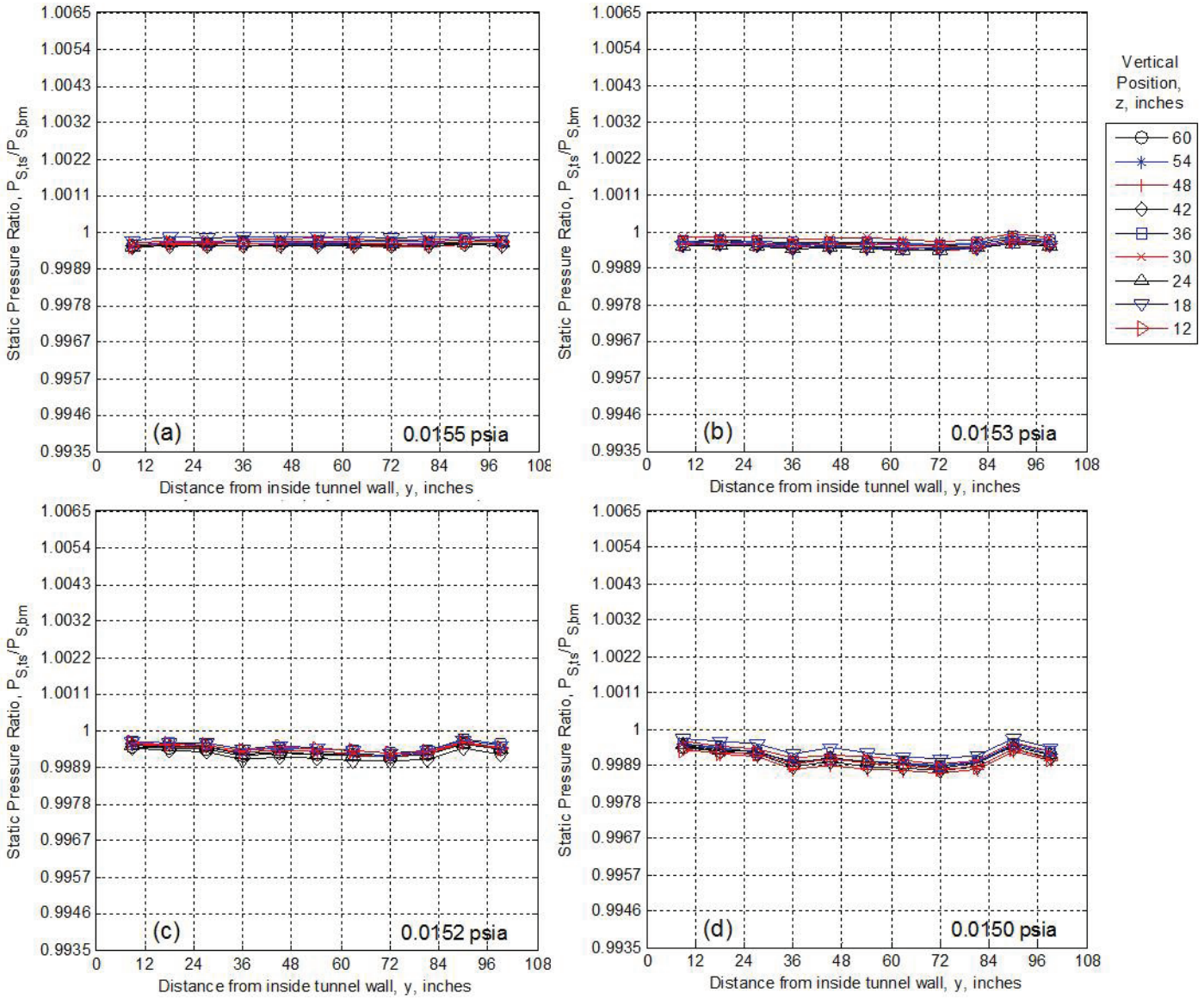

Figure 22: Static pressure distribution data from the IRT test section. Data collected using the 9-ft survey rake mounted at 9 vertical positions over several tunnel runs. (a) $U_{ts} = 50$ knots, $P_{air} = 0$ psig. (b) $U_{ts} = 90$ knots, $P_{air} = 0$ psig. (c) $U_{ts} = 120$ knots, $P_{air} = 0$ psig. (d) $U_{ts} = 150$ knots, $P_{air} = 0$ psig.

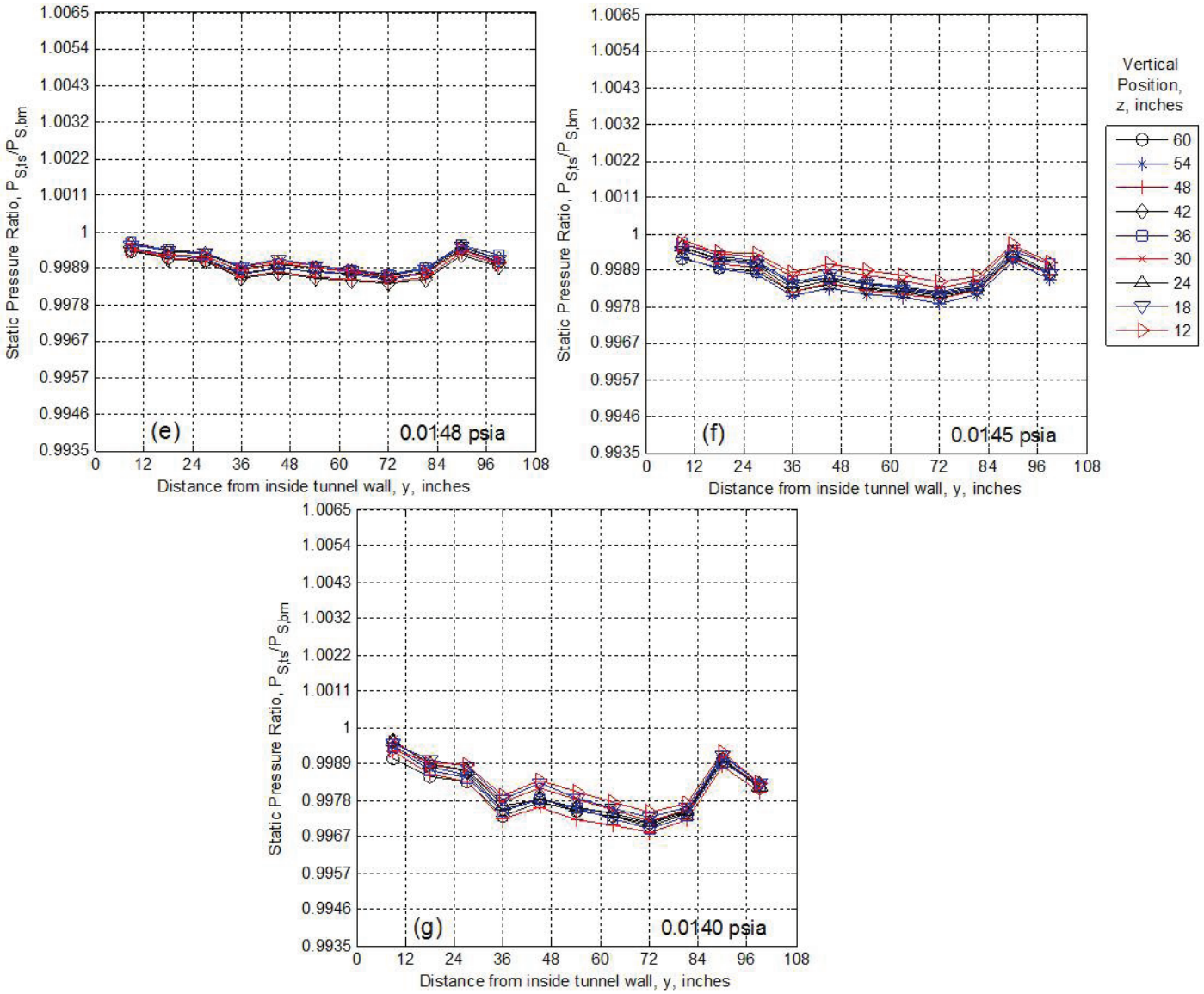

Continued Figure 22: (e) $U_{ts} = 170$ knots, $P_{air} = 0$ psig. (f) $U_{ts} = 200$ knots, $P_{air} = 0$ psig. (g) $U_{ts} = 250$ knots, $P_{air} = 0$ psig.

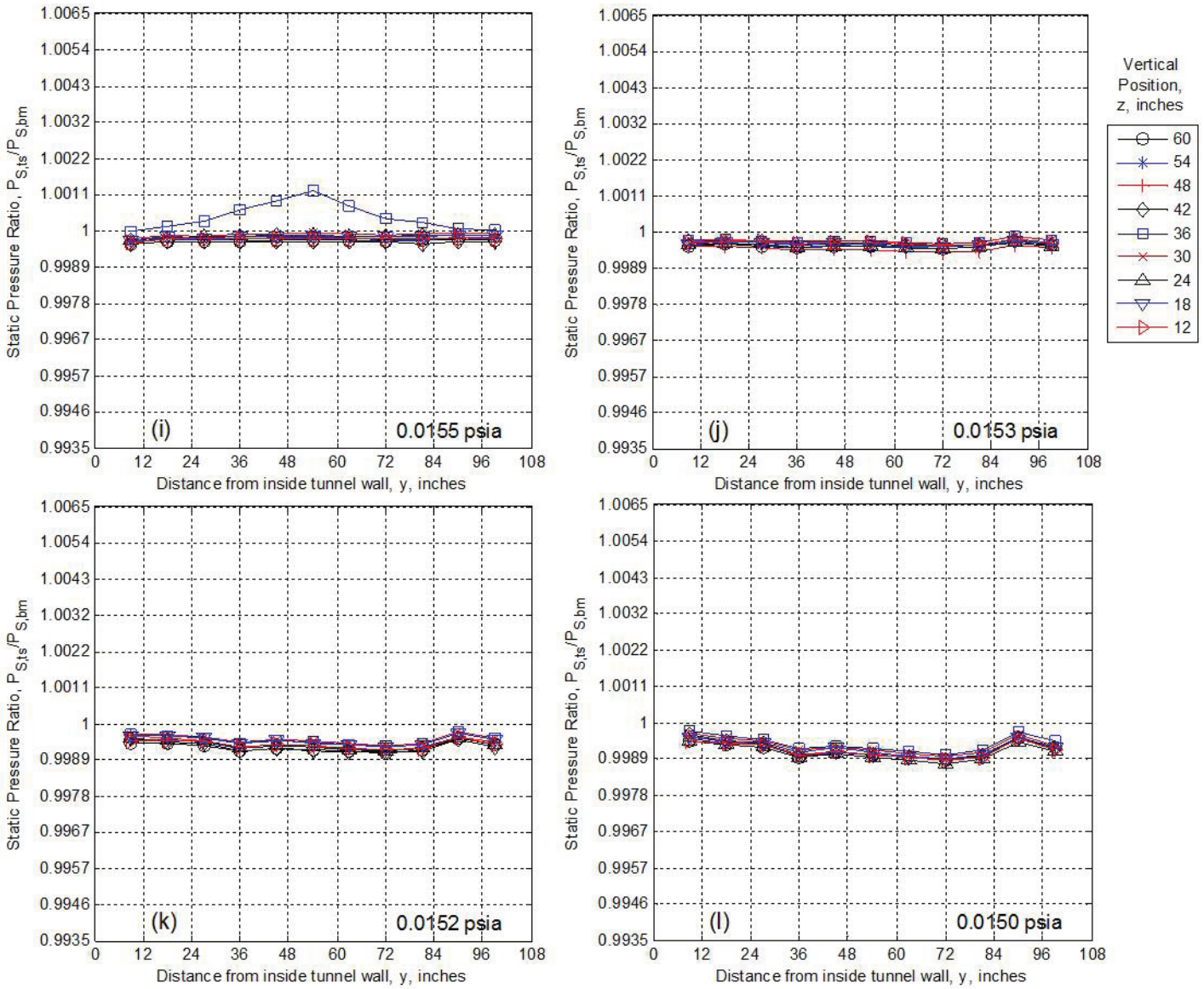

Continued Figure 22: (i) U_{ts} = 50 knots, P_{air} = 30 psig. (j) U_{ts} = 90 knots, P_{air} = 30 psig. (k) U_{ts} = 120 knots, P_{air} = 30 psig. (l) U_{ts} = 150 knots, P_{air} = 30 psig.

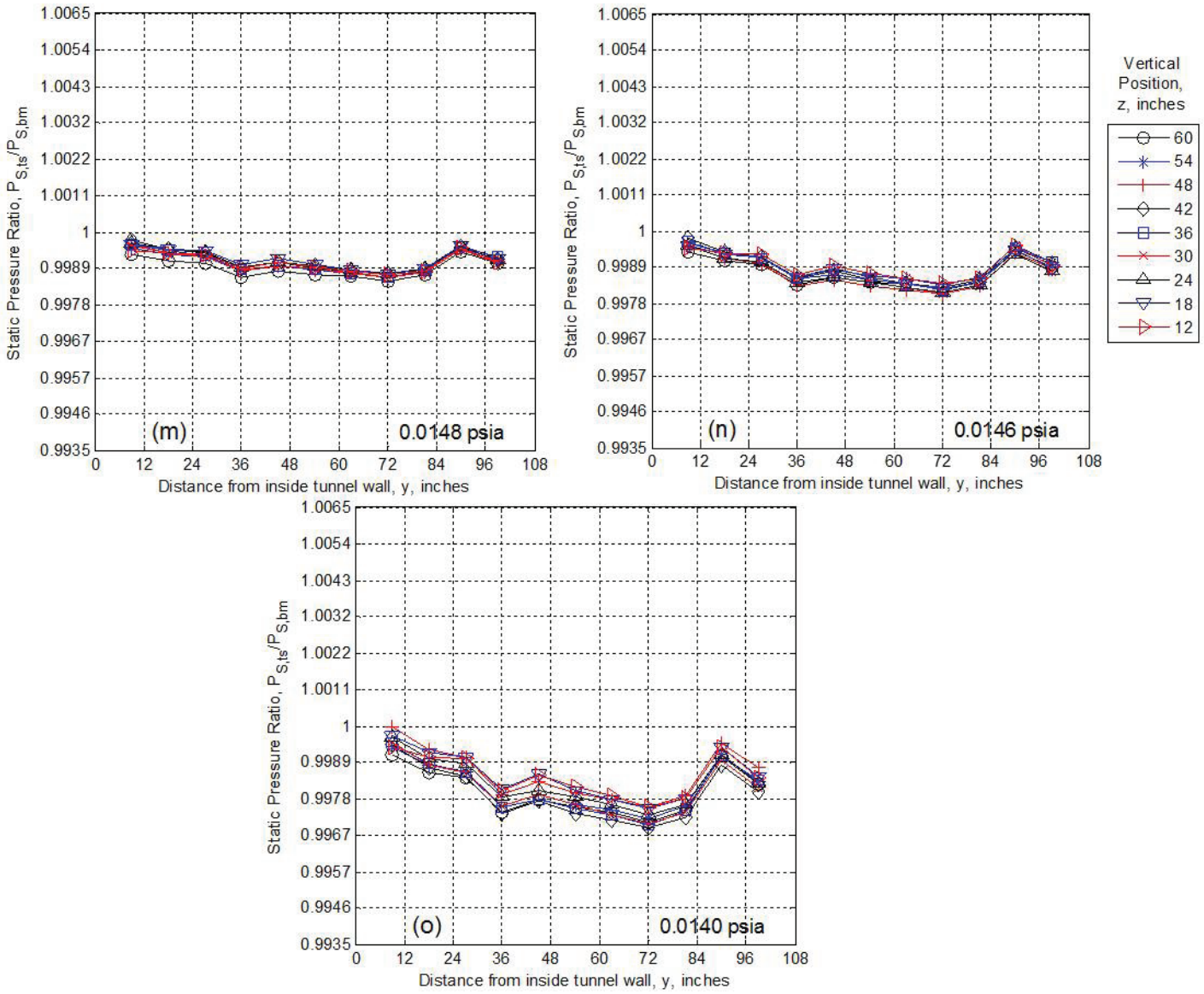

Continued Figure 22: (m) U_{ts} = 170 knots, P_{air} = 30 psig. (n) U_{ts} = 200 knots, P_{air} = 30 psig. (o) U_{ts} = 250 knots, P_{air} = 30 psig.

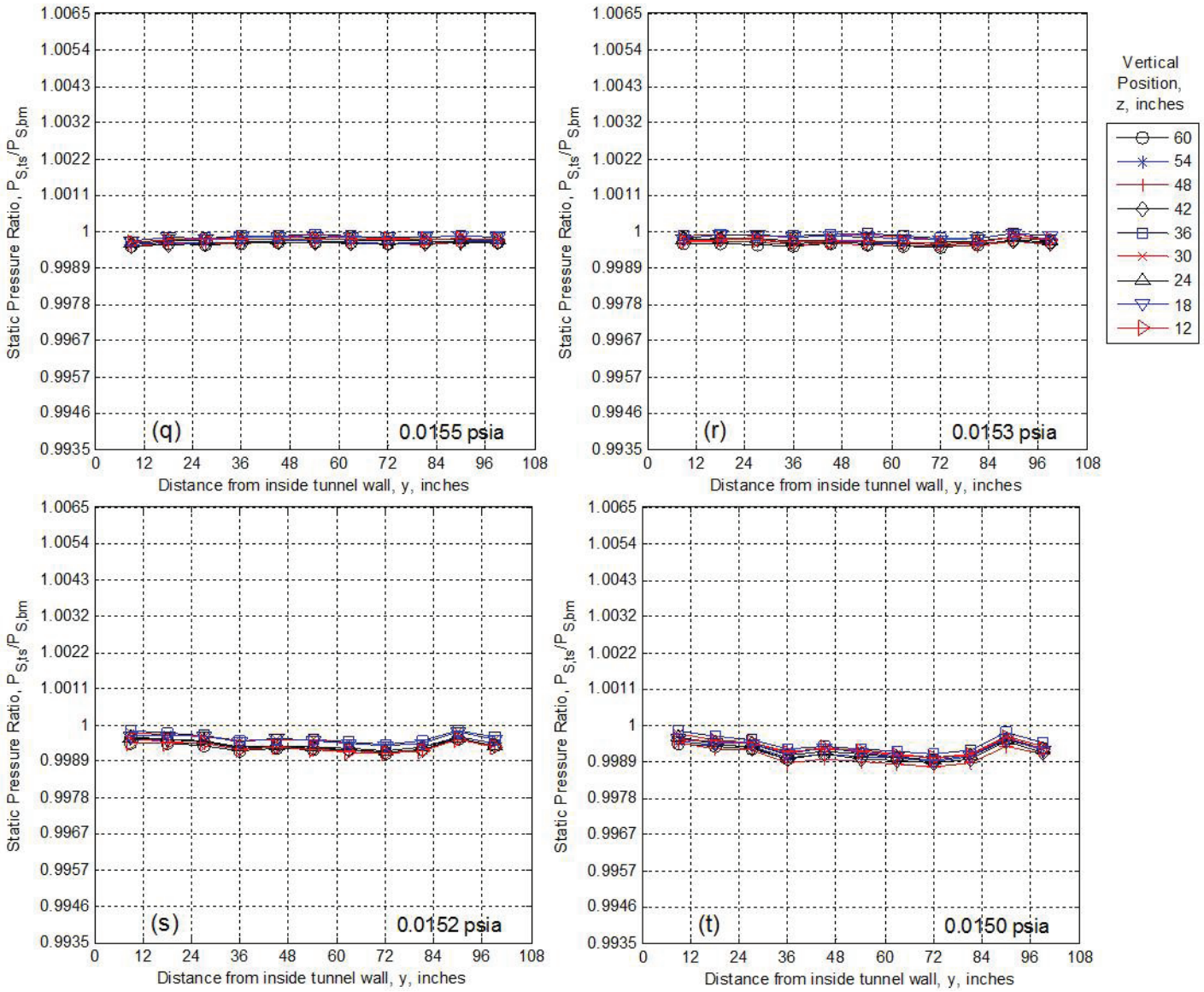

Continued Figure 22: (q) U_{ts} = 50 knots, P_{air} = 60 psig. (r) U_{ts} = 90 knots, P_{air} = 60 psig. (s) U_{ts} = 120 knots, P_{air} = 60 psig. (t) U_{ts} = 150 knots, P_{air} = 60 psig.

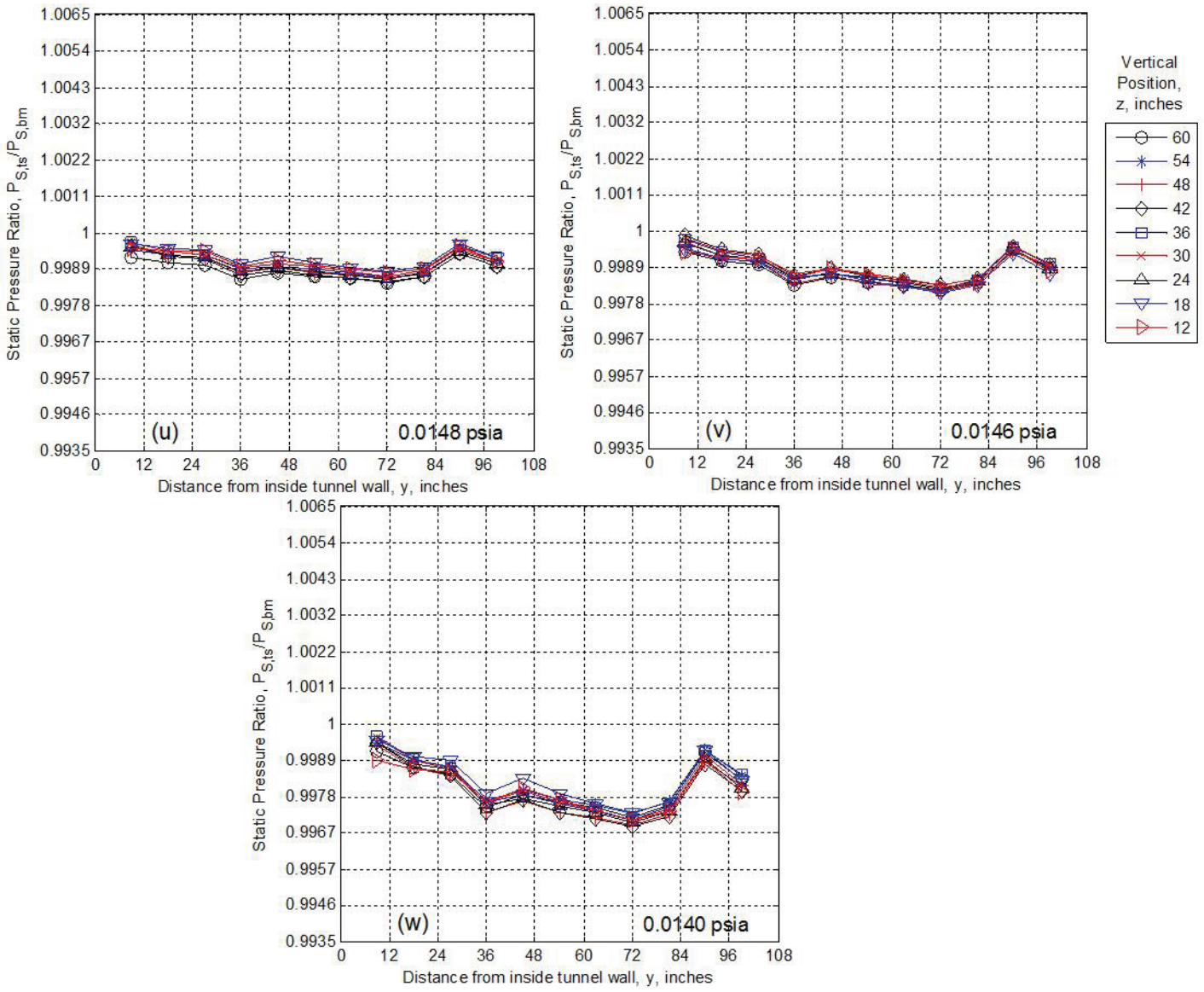

Continued Figure 22: (u) $U_{ts} = 170$ knots, $P_{air} = 60$ psig. (v) $U_{ts} = 200$ knots, $P_{air} = 60$ psig. (w) $U_{ts} = 250$ knots, $P_{air} = 60$ psig.

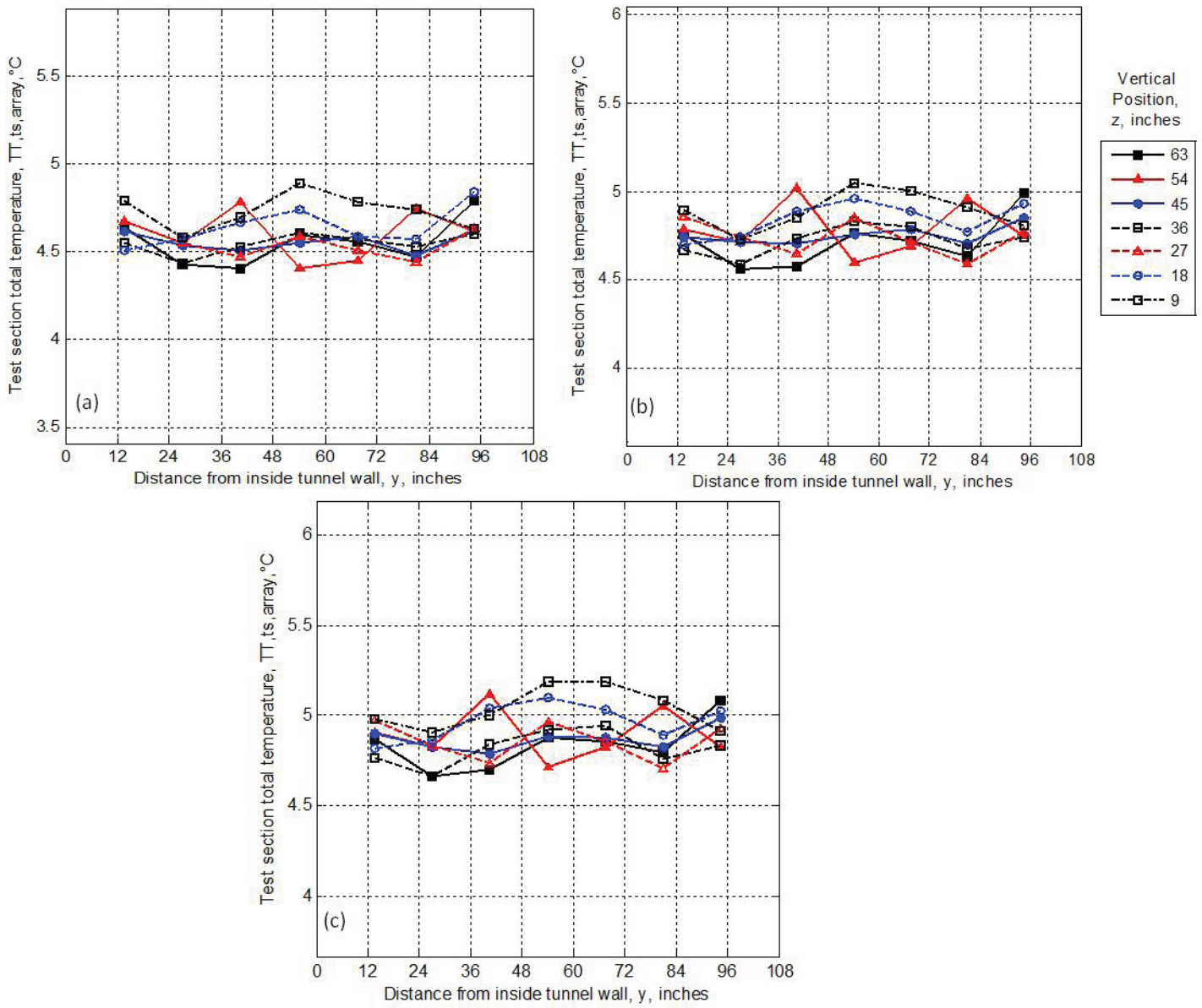

Figure 23: Total Temperature test section temperature distribution, as collected by the 2D RTD survey array. (a) $U_{ts} = 217$ knots, $T_{T,davg} = 5.0°C$, $P_{air} = 0$ psig (b) $U_{ts} = 217$ knots, $T_{T,davg} = 5.0°C$, $P_{air} = 30$ psig (c) $U_{ts} = 217$ knots, $T_{T,davg} = 5.0°C$, $P_{air} = 60$ psig

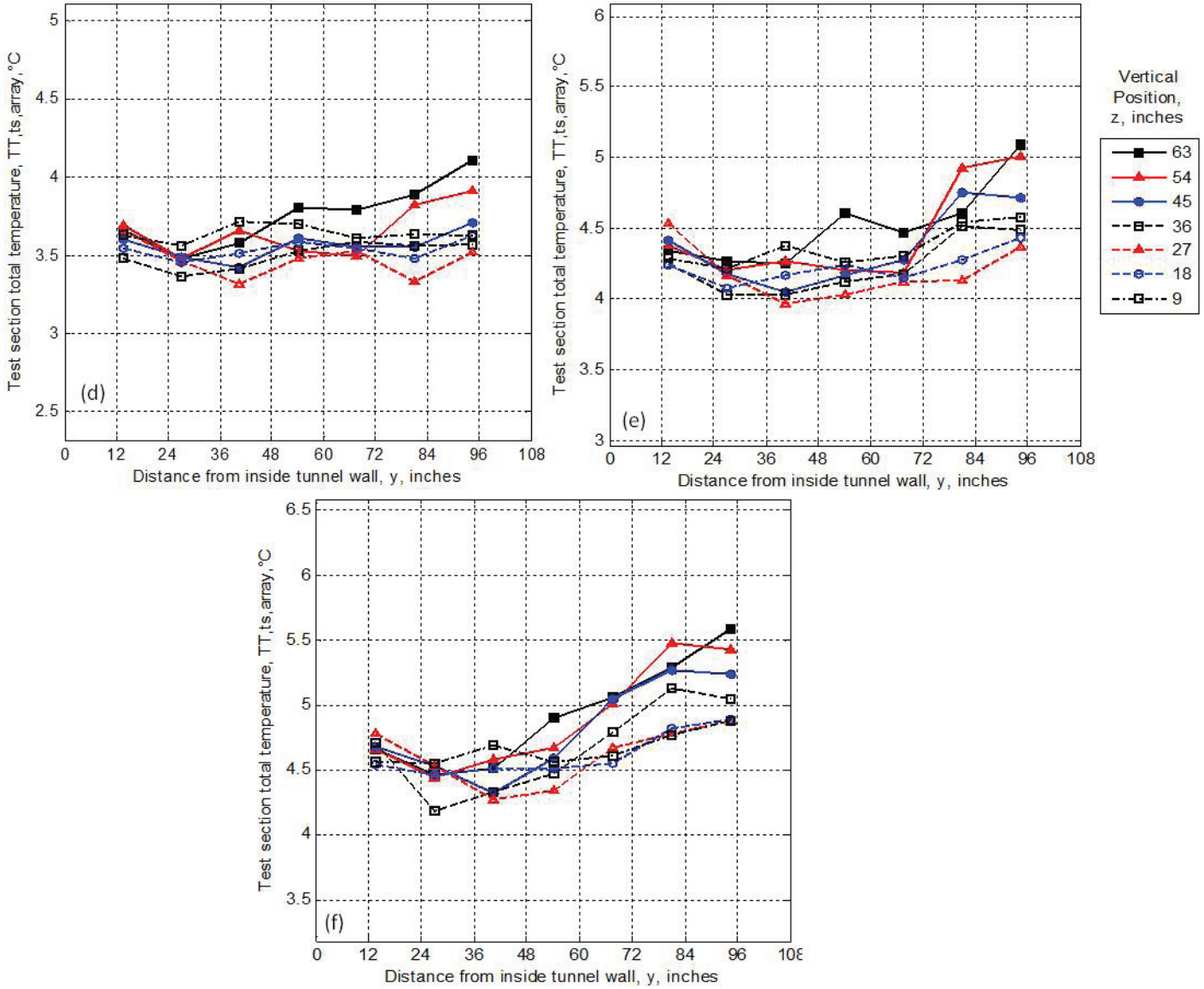

Continued Figure 23: (d) $U_{ts} = 50$ knots, $T_{T,davg} = 3.6°C$, $P_{air} = 0$ psig, (e) $U_{ts} = 50$ knots, $T_{T,davg} = 3.6°C$, $P_{air} = 30$ psig (f) $U_{ts} = 50$ knots, $T_{T,davg} = 3.6°C$, $P_{air} = 60$ psig

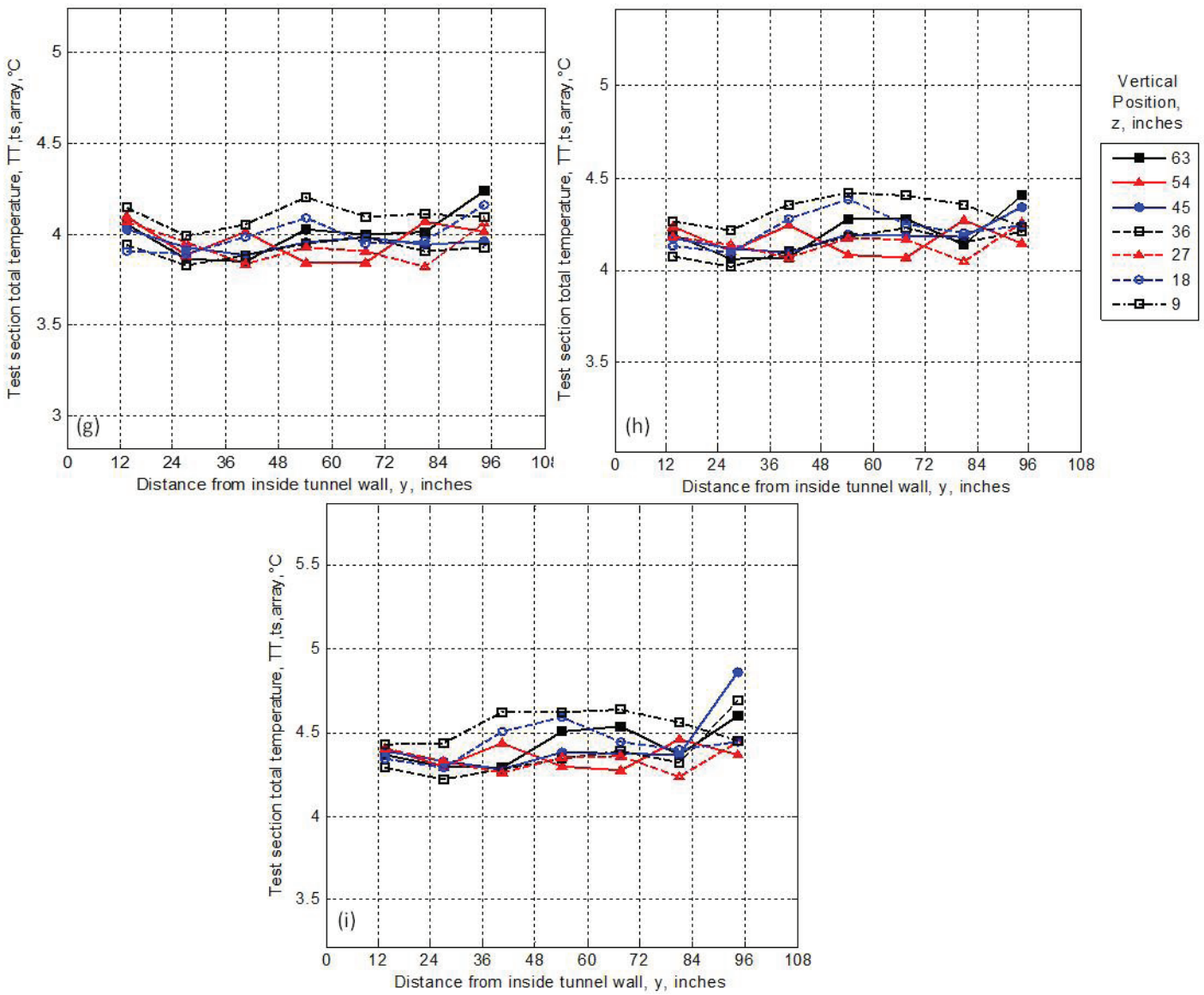

Continued Figure 23: (g) U_{ts} = 130 knots, $T_{T,davg} = 3.9°C$, P_{air} = 0 psig (h) U_{ts} = 130 knots, $T_{T,davg} = 3.9°C$, P_{air} = 30 psig (i) U_{ts} = 130 knots, $T_{T,davg} = 3.9°C$, P_{air} = 60 psig

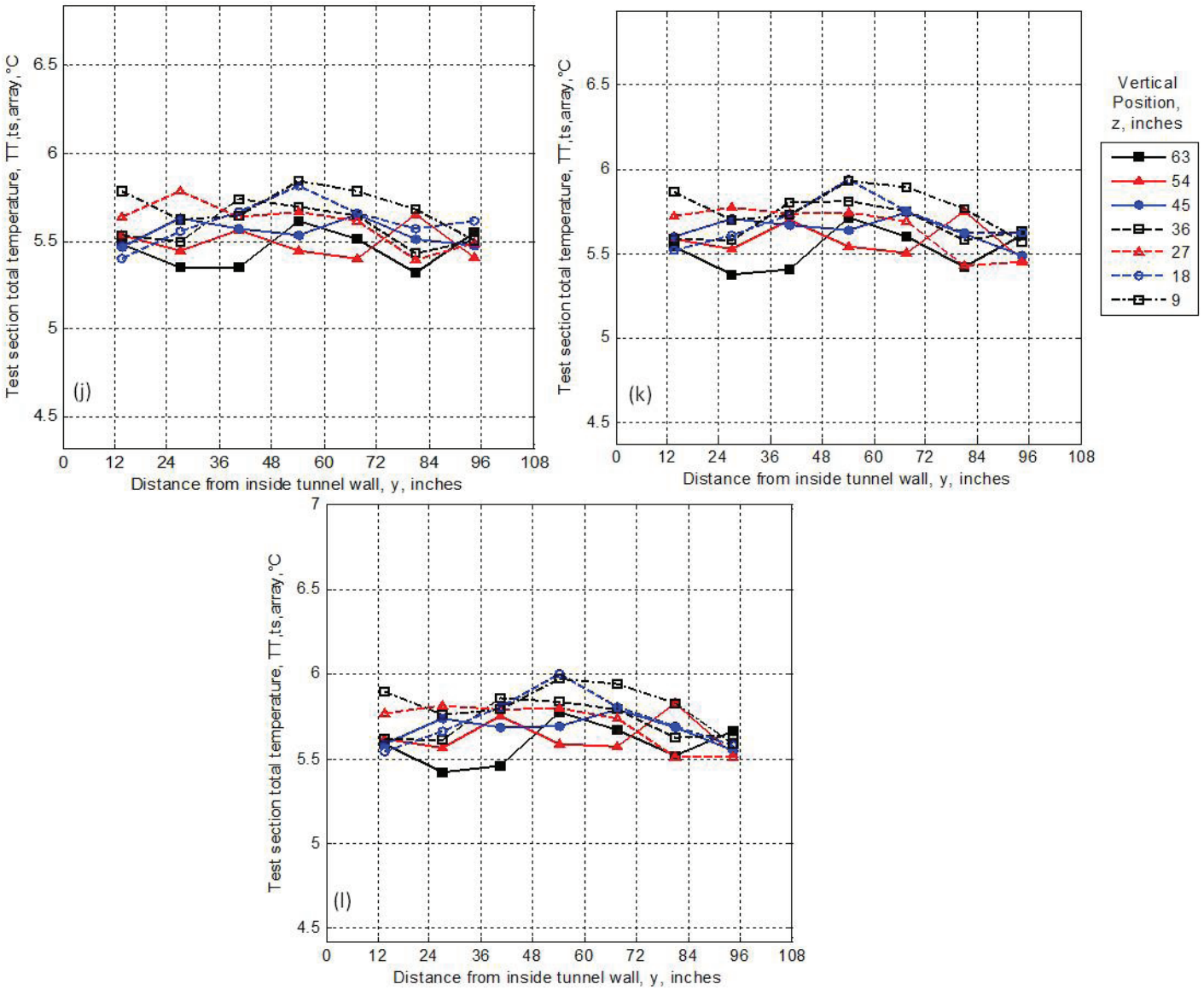

Continued Figure 23: (j) U_{ts} = 300 knots, $T_{T,davg} = 6.3°C$, P_{air} = 0 psig (k) U_{ts} = 300 knots, $T_{T,davg} = 6.4°C$, P_{air} = 30 psig (l) U_{ts} = 300 knots, $T_{T,davg} = 6.4°C$, P_{air} = 60 psig

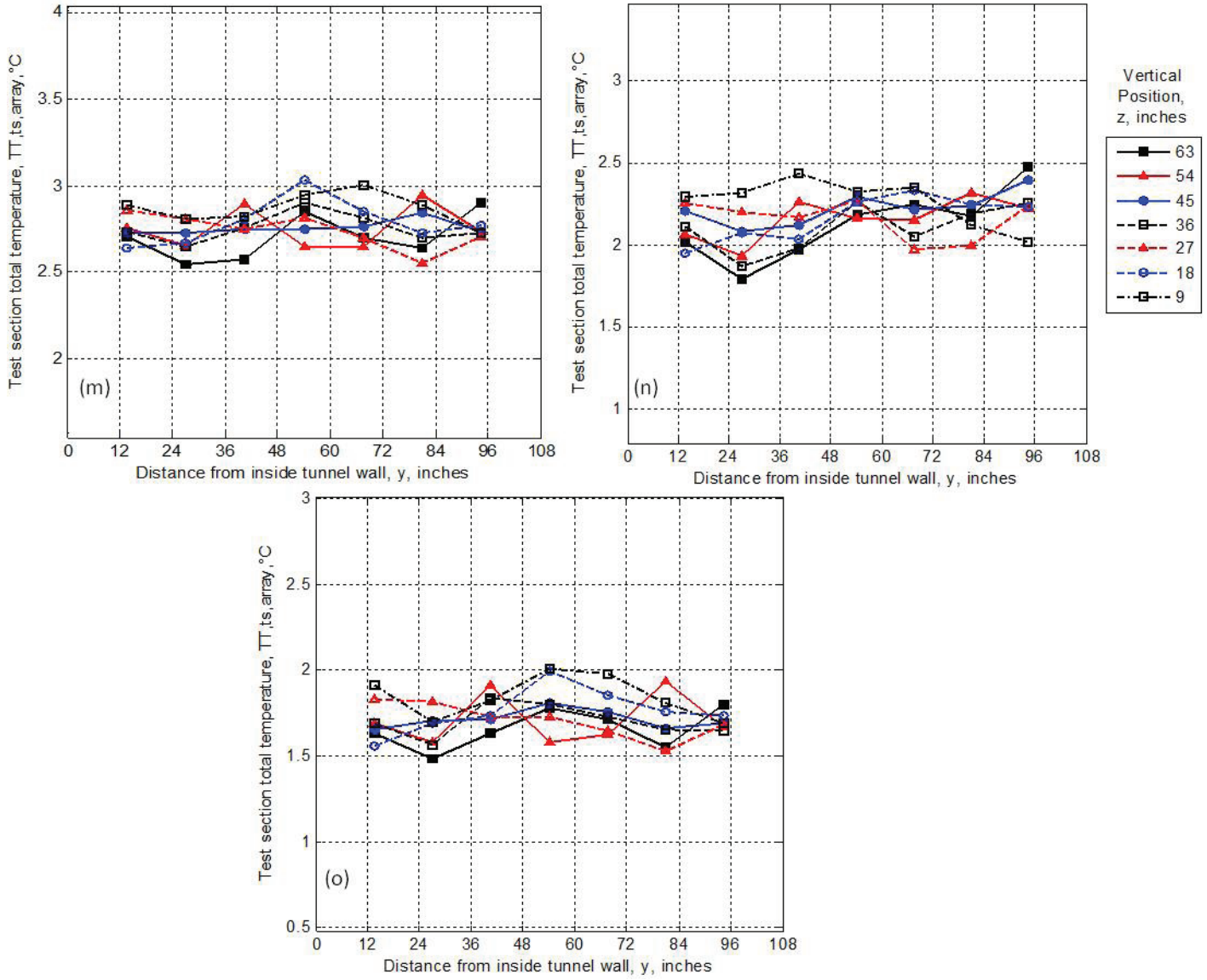

Continued Figure 23: (m) $U_{ts} = 220$ knots, $T_{T,davg} = 3.0°C$, $P_{air} = 30$ psig (n) $U_{ts} = 130$ knots, $T_{T,davg} = 2.1°C$, $P_{air} = 30$ psig (o) $U_{ts} = 220$ knots, $T_{T,davg} = 2.0°C$, $P_{air} = 30$ psig

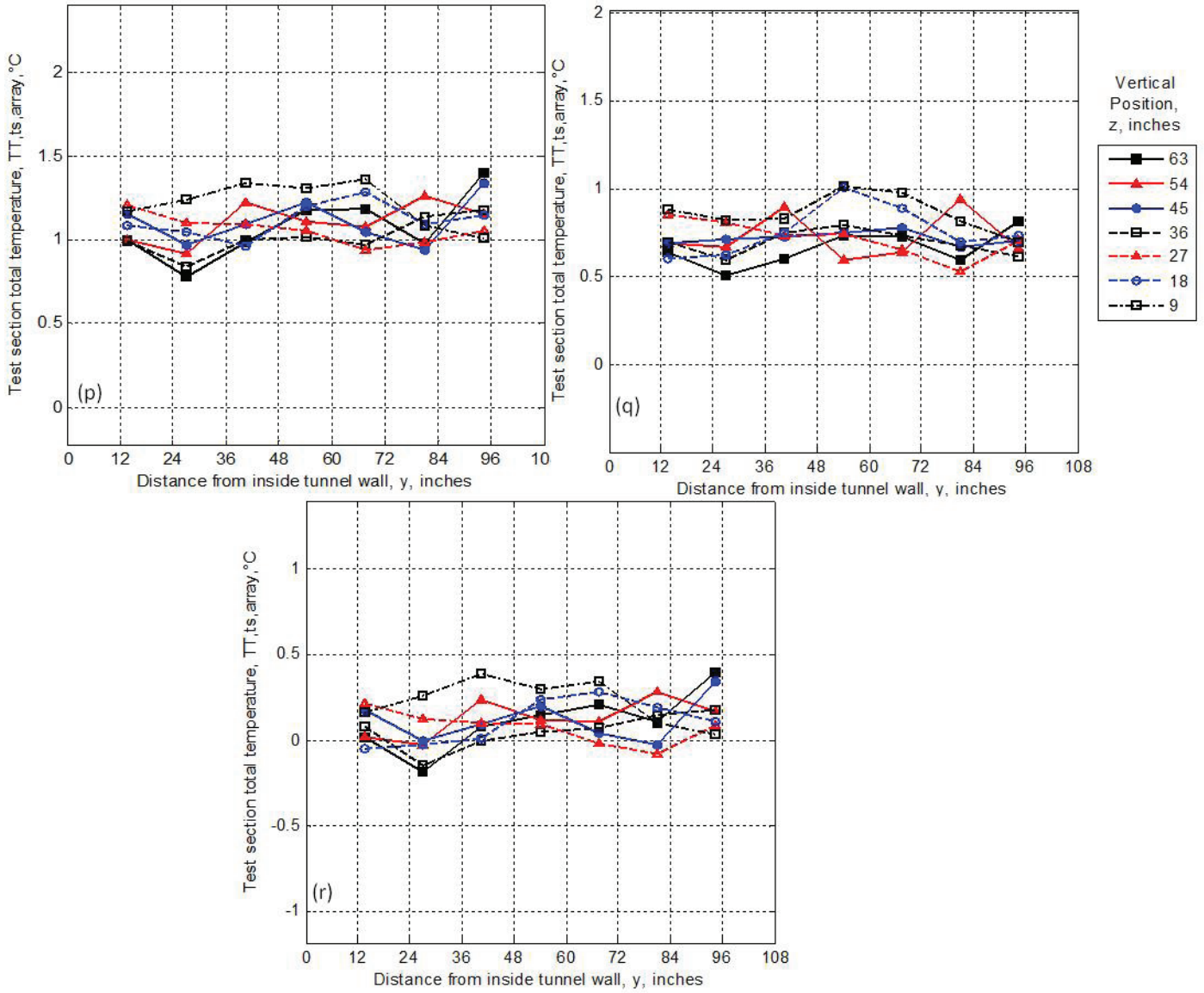

Continued Figure 23: (p) $U_{ts} = 130$ knots, $T_{T,davg} = 1.0°C$, $P_{air} = 30$ psig (q) $U_{ts} = 220$ knots, $T_{T,davg} = 1.0°C$, $P_{air} = 30$ psig (r) $U_{ts} = 130$ knots, $T_{T,davg} = 0.0°C$, $P_{air} = 30$ psig

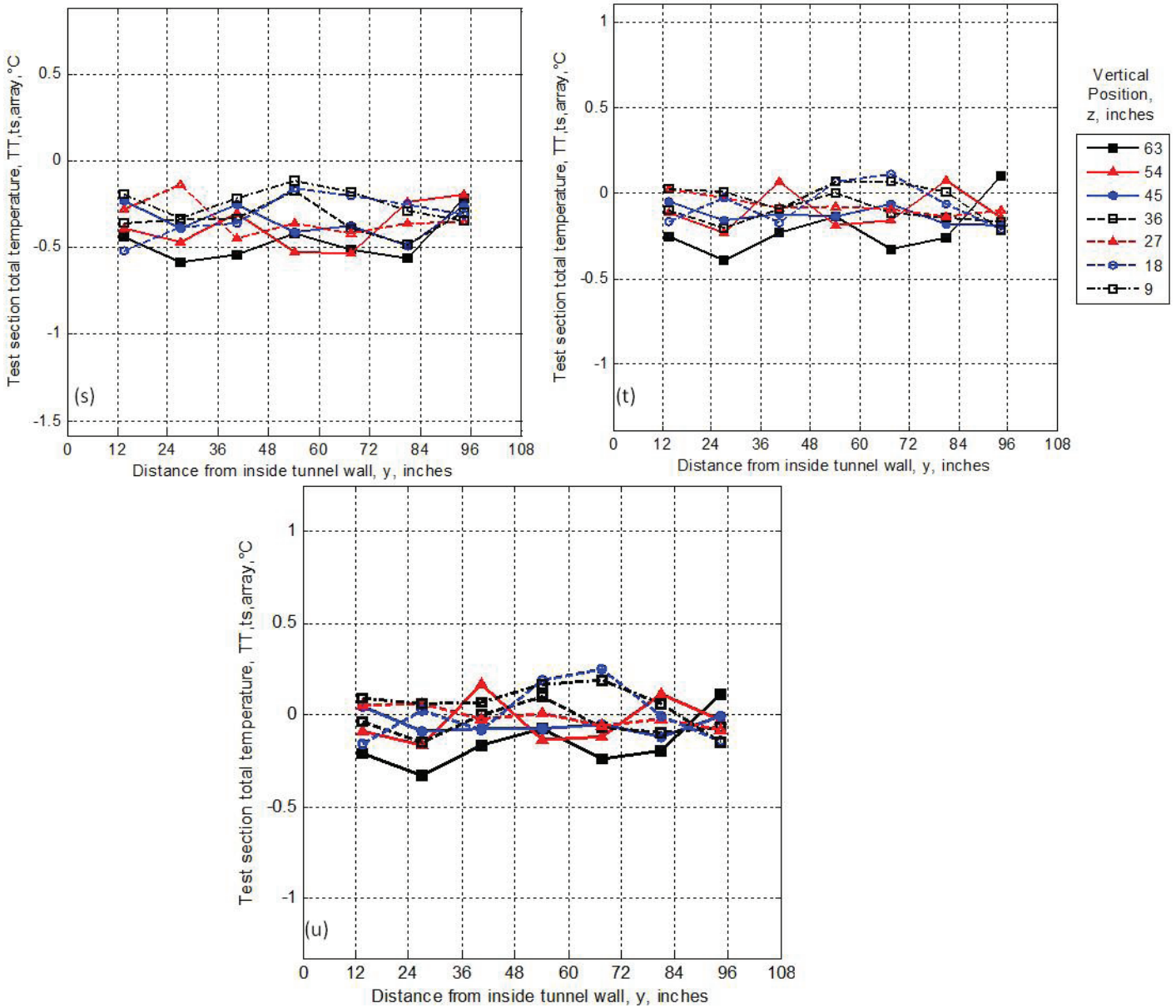

Continued Figure 23: (s) $U_{ts} = 220$ knots, $T_{T,davg} = 0.0°C$, $P_{air} = 0$ psig (t) $U_{ts} = 220$ knots, $T_{T,davg} = 0.0°C$, $P_{air} = 30$ psig (u) $U_{ts} = 220$ knots, $T_{T,davg} = 0.0°C$, $P_{air} = 60$ psig

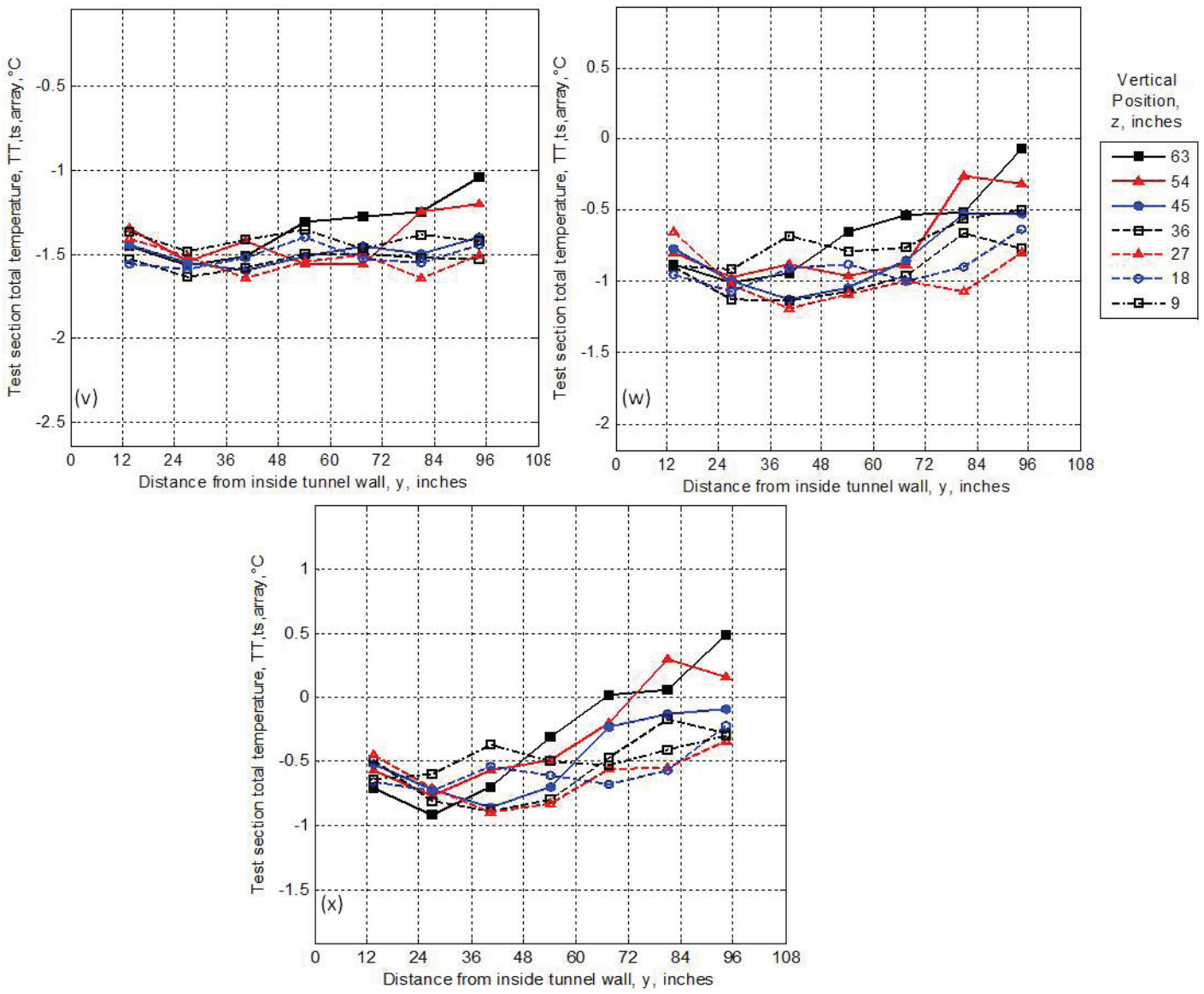

Continued Figure 23: (v) U_{ts} = 50 knots, $T_{T,davg}$ = -1.5°C, P_{air} = 0 psig (w) U_{ts} = 50 knots, $T_{T,davg}$ = -1.5°C, P_{air} = 30 psig (x) U_{ts} = 50 knots, $T_{T,davg}$ = -1.5°C, P_{air} = 60 psig

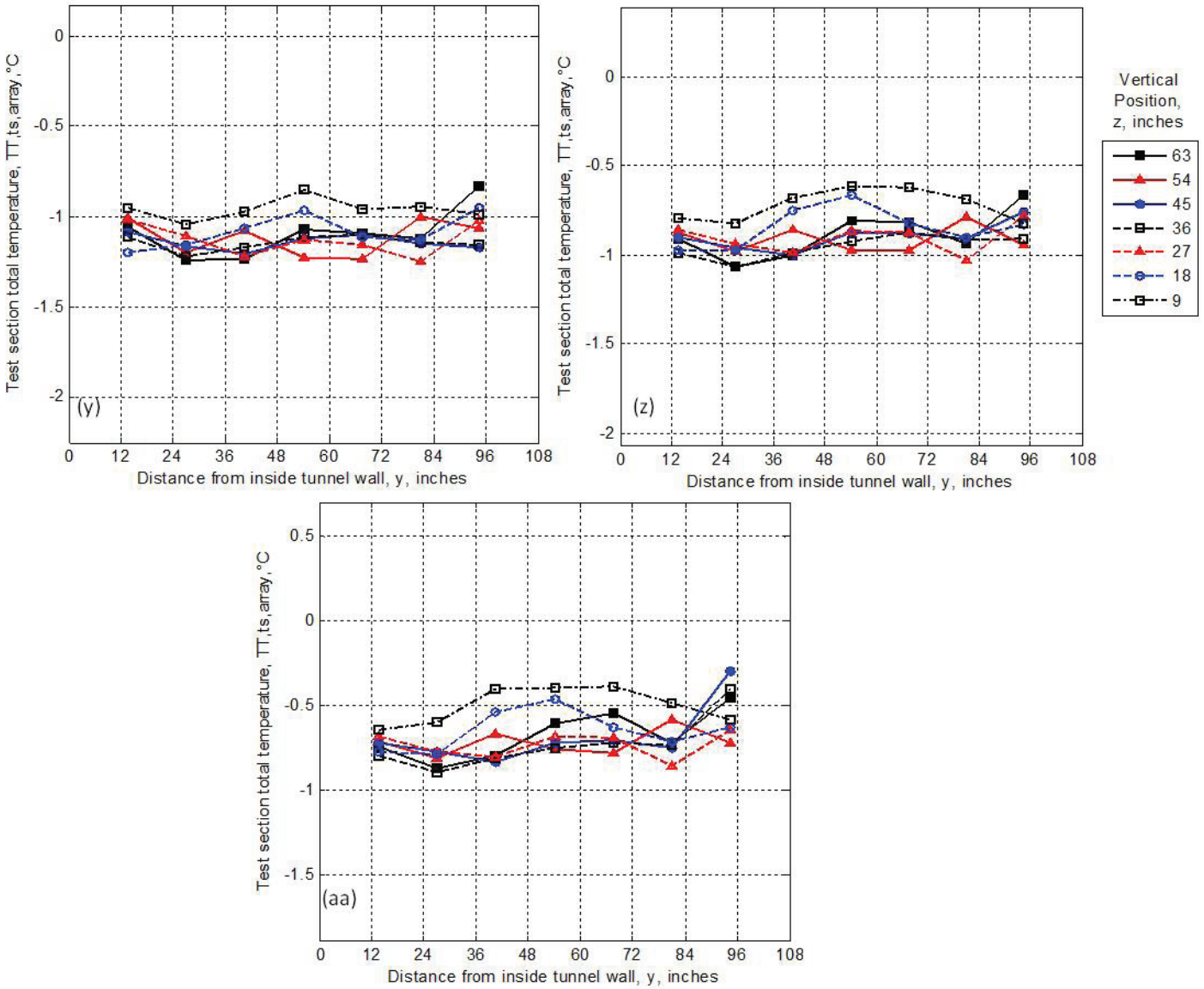

Continued Figure 23: (y) U_{ts} = 130 knots, $T_{T,davg}$ = -1.1°C, P_{air} = 0 psig (z) U_{ts} = 130 knots, $T_{T,davg}$ = -1.1°C, P_{air} = 30 psig (aa) U_{ts} = 130 knots, $T_{T,davg}$ = -1.1°C, P_{air} = 60 psig

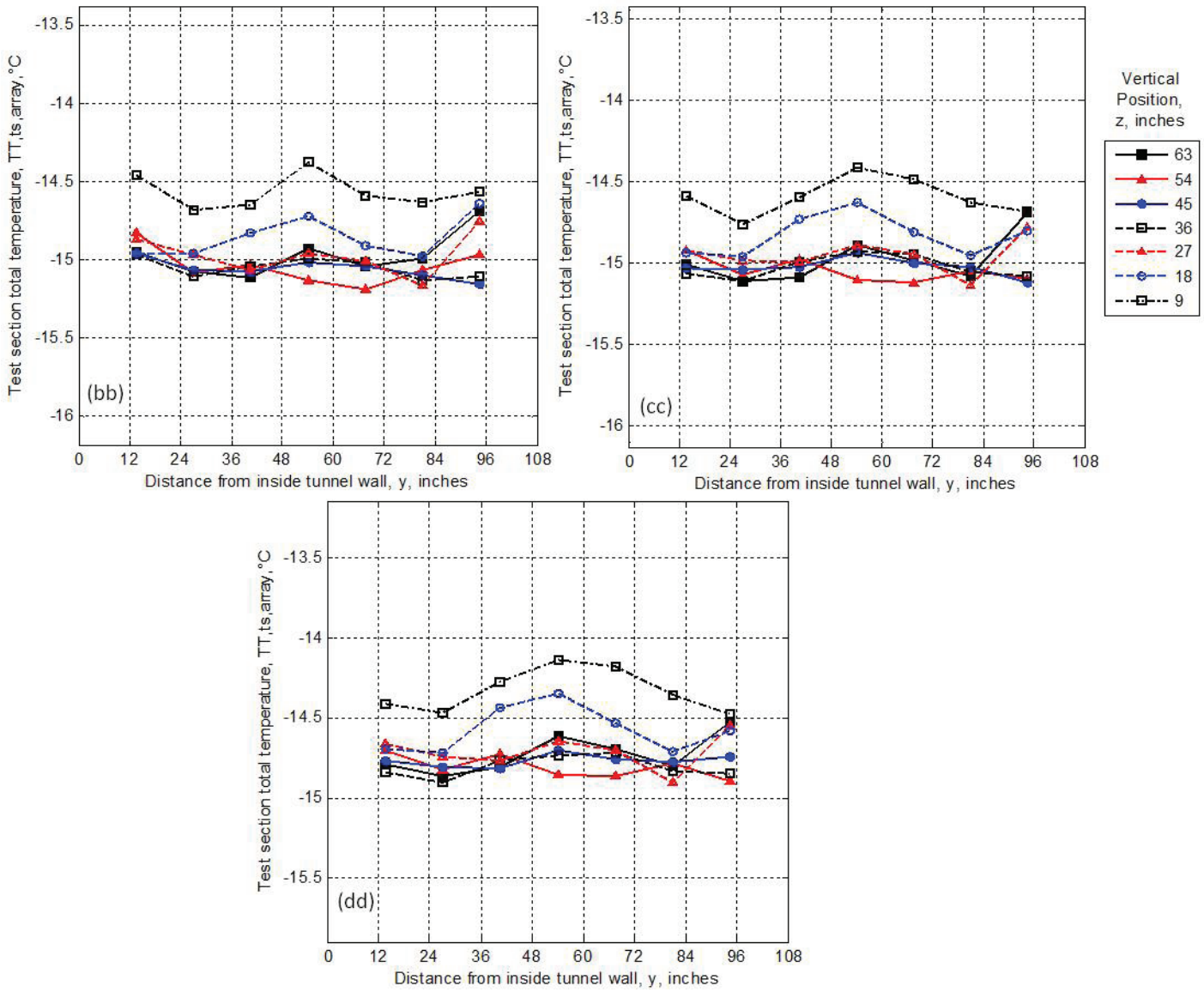

Continued Figure 23: (bb) U_{ts} = 220 knots, $T_{T,davg}$ = -15.1°C, P_{air} = 0 psig (cc) U_{ts} = 220 knots, $T_{T,davg}$ = -15.1°C, P_{air} = 30 psig (dd) U_{ts} = 220 knots, $T_{T,davg}$ = -15.1°C, P_{air} = 60 psig

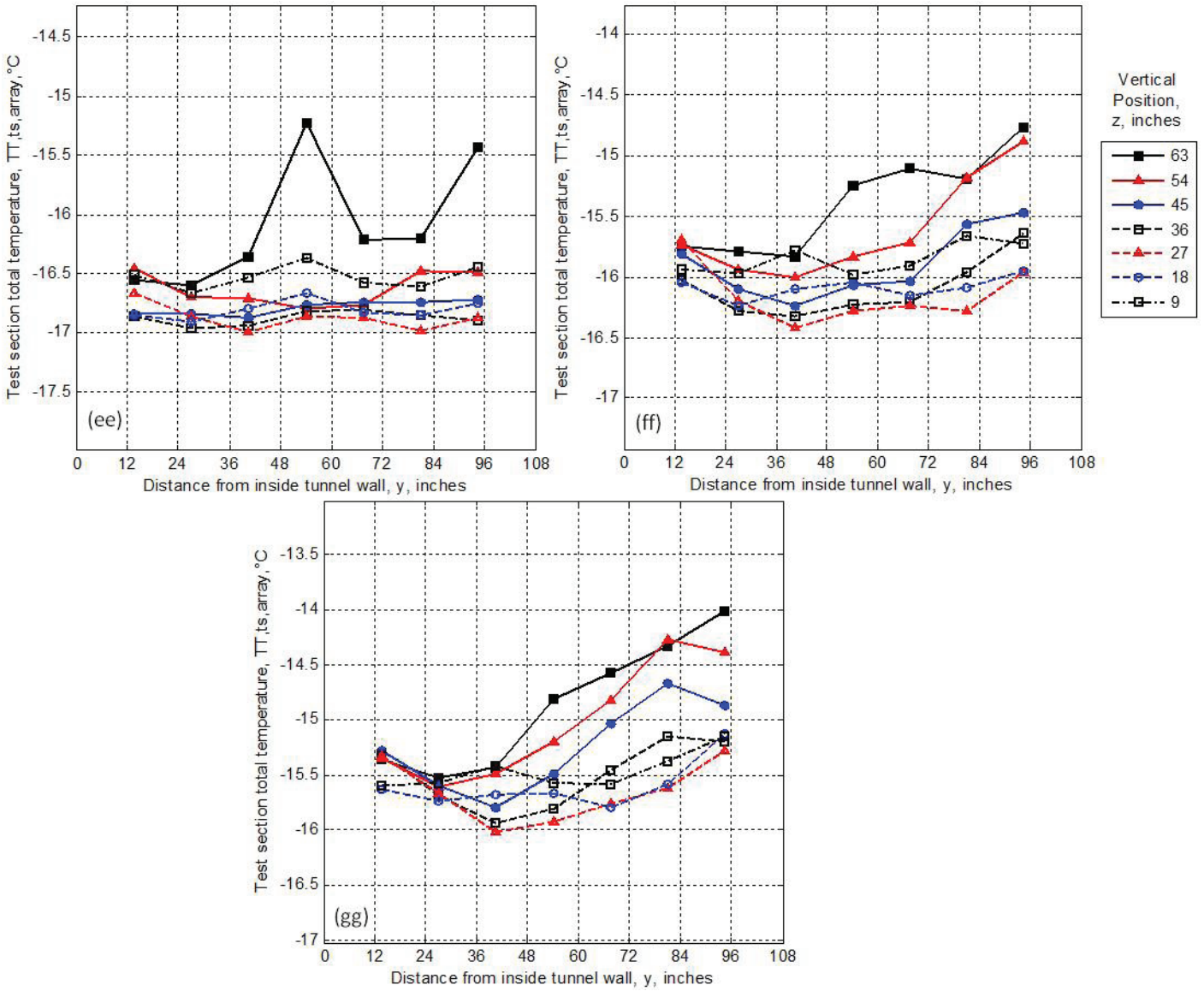

Continued Figure 23: (ee) U_{ts} = 50 knots, $T_{T,davg}$ = -16.9°C, P_{air} = 0 psig (ff) U_{ts} = 50 knots, $T_{T,davg}$ = -16.9°C, P_{air} = 30 psig (gg) U_{ts} = 50 knots, $T_{T,davg}$ = -16.9°C, P_{air} = 60 psig

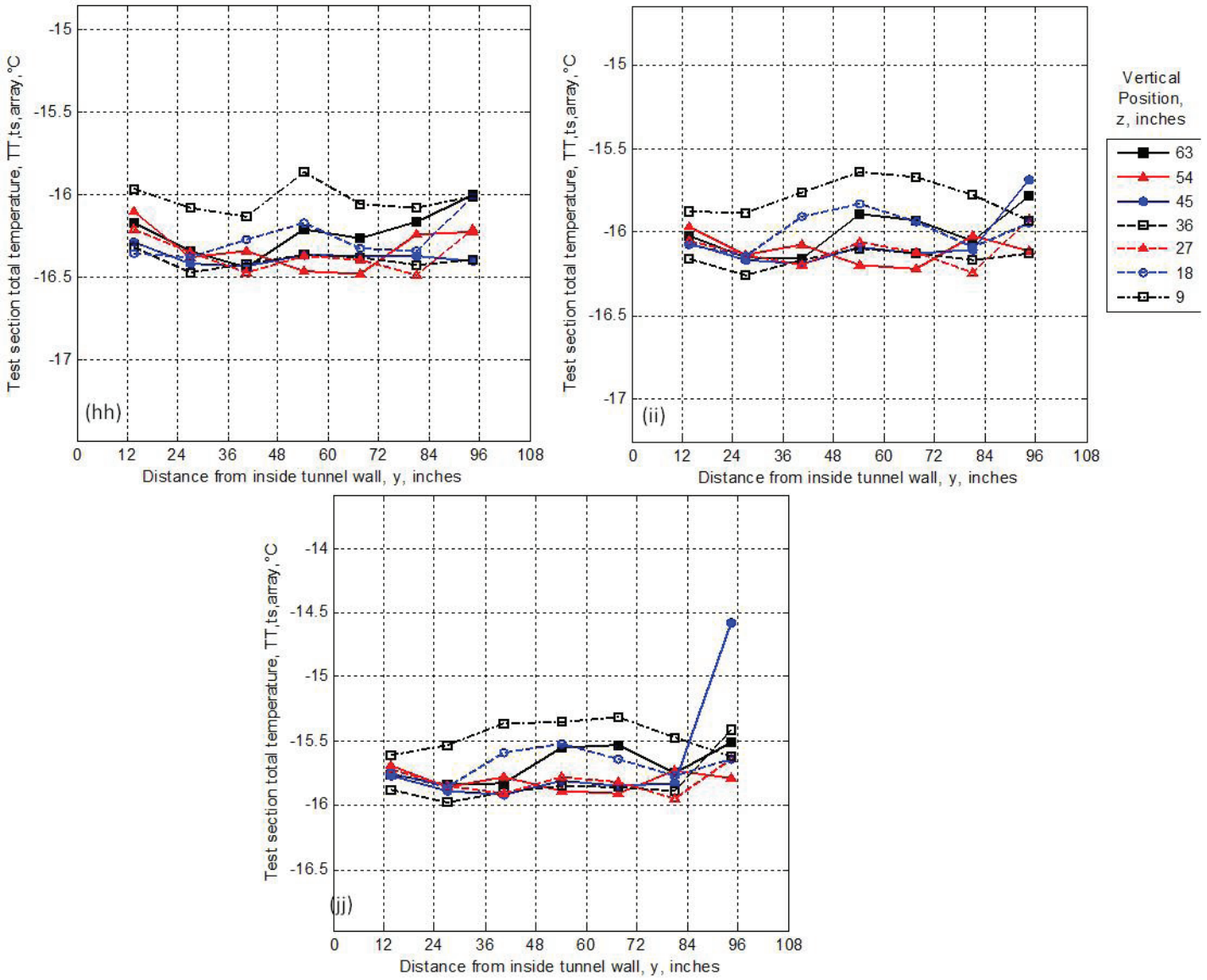

Continued Figure 23: (hh) U_{ts} = 130 knots, $T_{T,davg}$ = -16.4°C, P_{air} = 0 psig (ii) U_{ts} = 130 knots, $T_{T,davg}$ = -16.4°C, P_{air} = 30 psig (jj) U_{ts} = 130 knots, $T_{T,davg}$ = -16.4°C, P_{air} = 60 psig

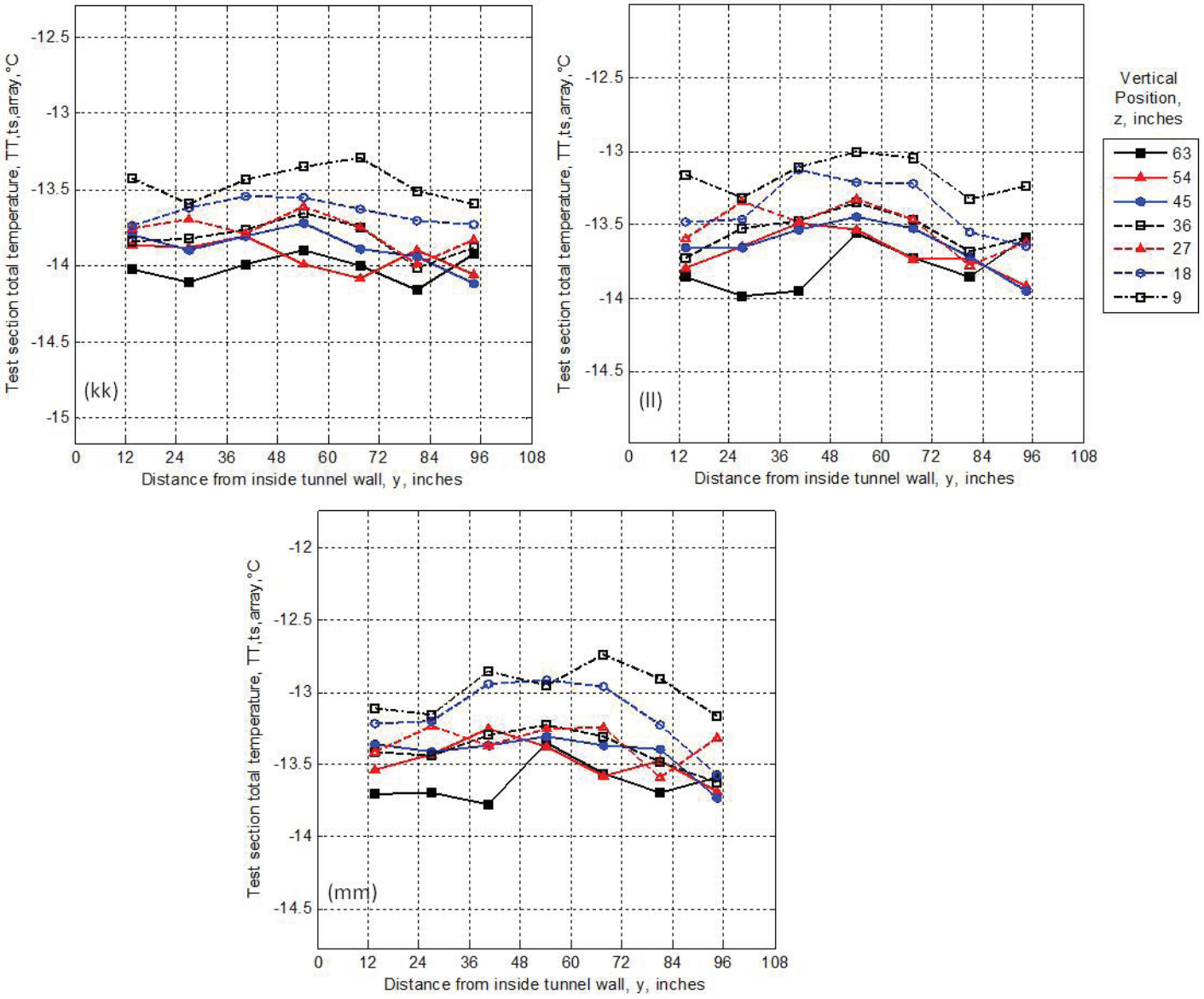

Continued Figure 23: (kk) U_{ts} = 300 knots, $T_{T,davg}$ = -13.6°C, P_{air} = 0 psig (ll) U_{ts} = 300 knots, $T_{T,davg}$ = -13.6°C, P_{air} = 30 psig (mm) U_{ts} = 300 knots, $T_{T,davg}$ = -13.6°C, P_{air} = 60 psig

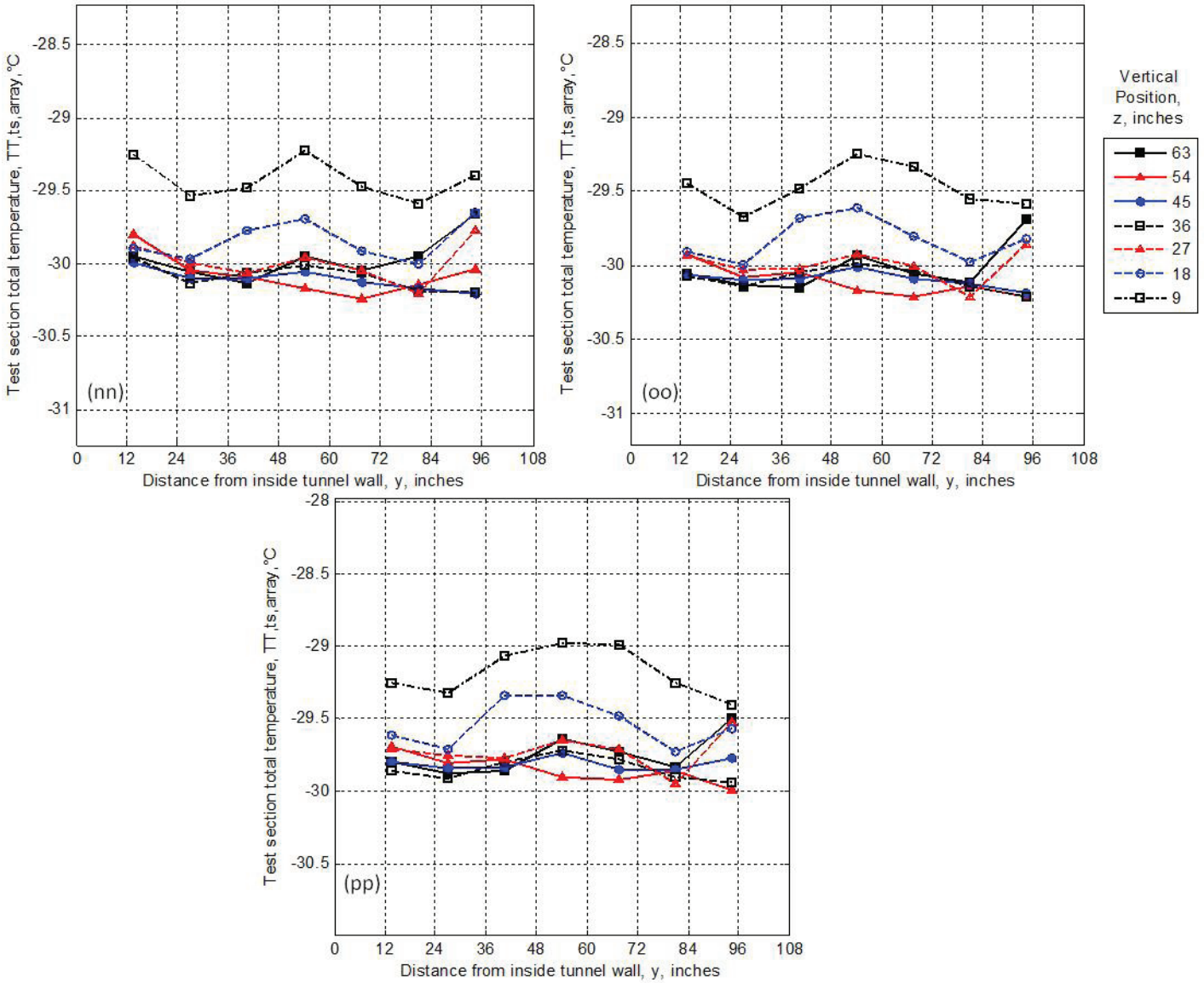

Continued Figure 23: (nn) U_{ts} = 220 knots, $T_{T,davg}$ = -30.0°C, P_{air} = 0 psig (oo) U_{ts} = 220 knots, $T_{T,davg}$ = -30.0°C, P_{air} = 30 psig (pp) U_{ts} = 220 knots, $T_{T,davg}$ = -30.0°C, P_{air} = 60 psig

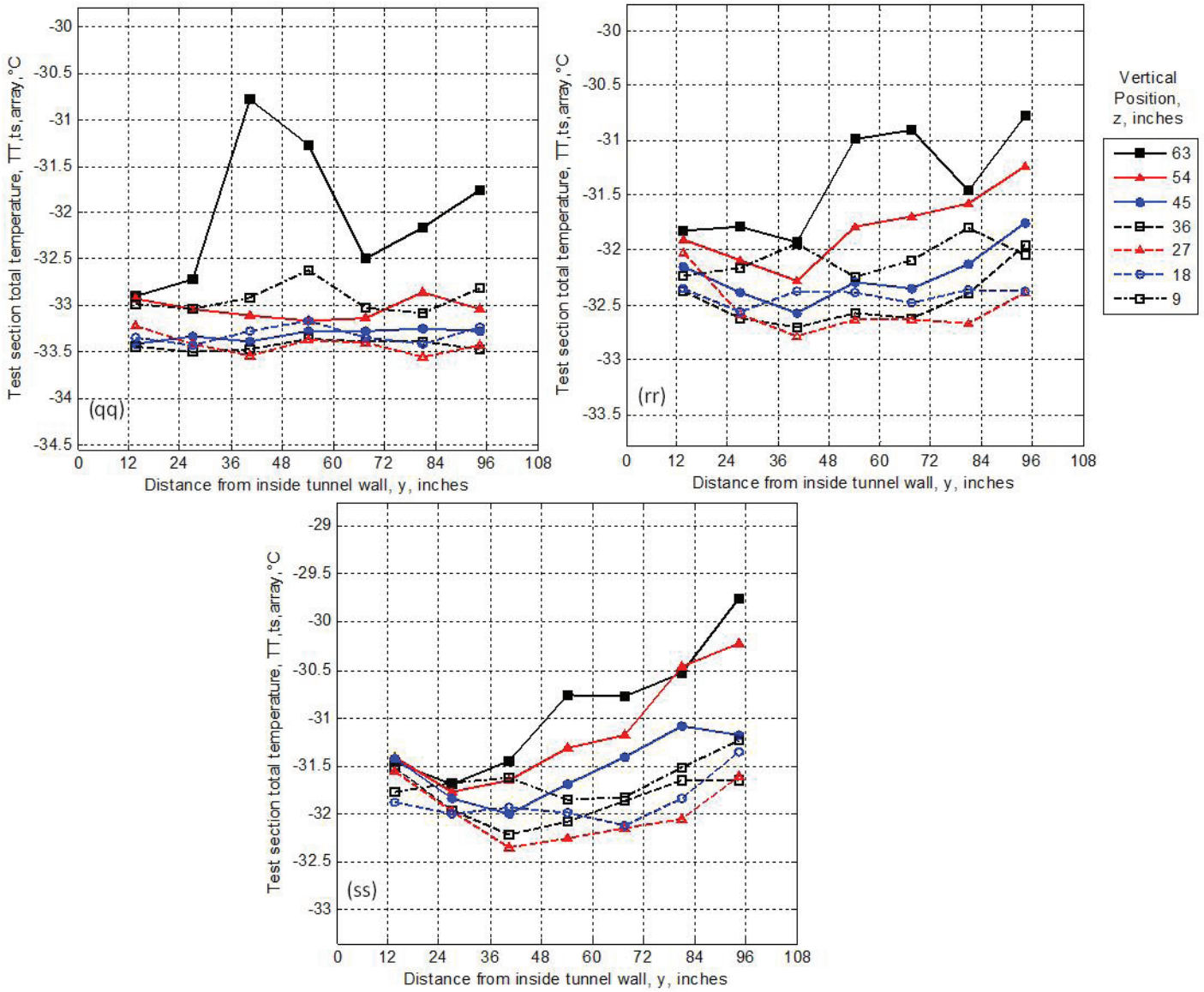

Continued Figure 23: (qq) U_{ts} = 50 knots, $T_{T,davg}$ = -33.3°C, P_{air} = 0 psig (rr) U_{ts} = 50 knots, $T_{T,davg}$ = -33.3°C, P_{air} = 30 psig (ss) U_{ts} = 50 knots, $T_{T,davg}$ = -33.3°C, P_{air} = 60 psig

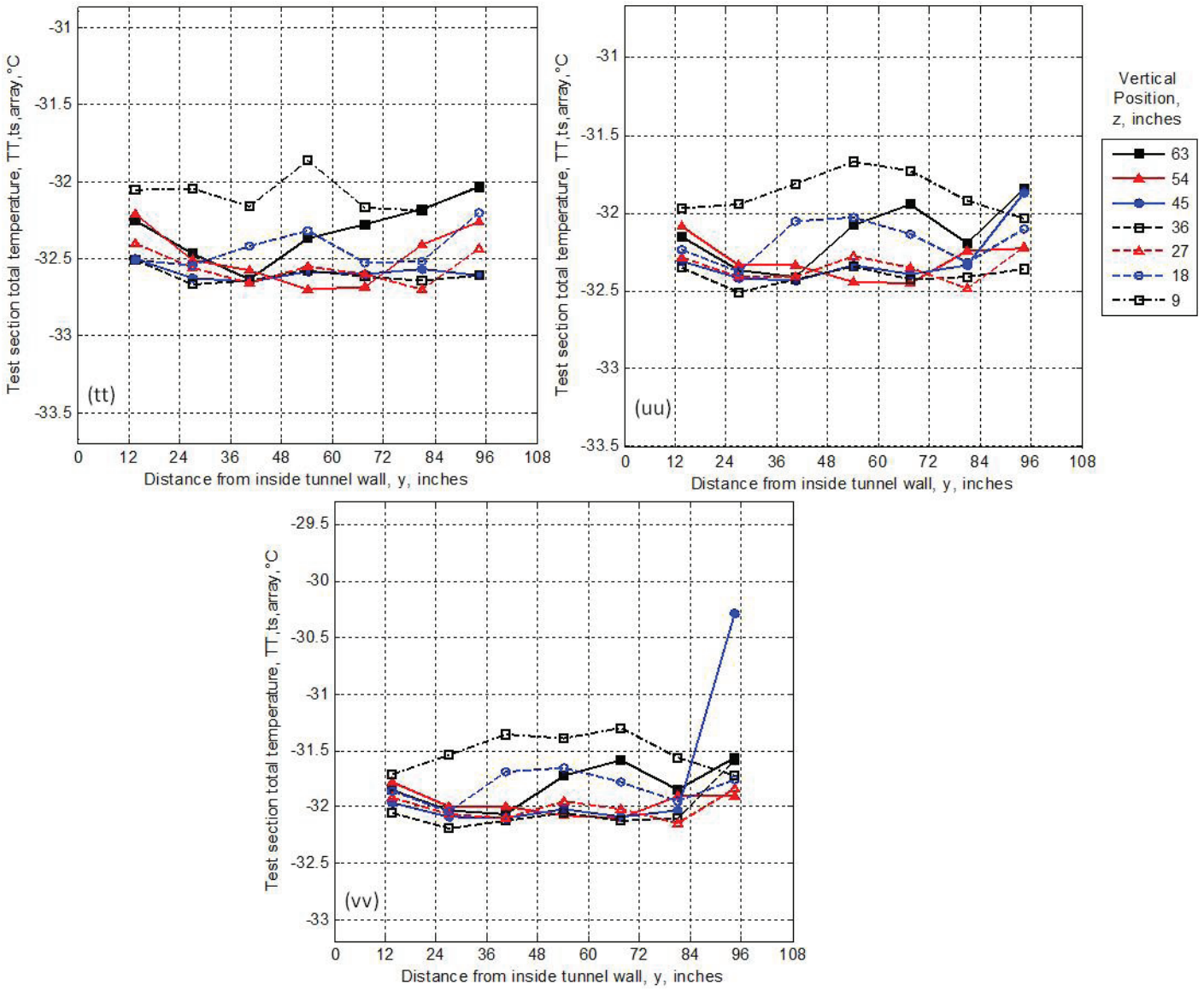

Continued Figure 23: (tt) U_{ts} = 130 knots, $T_{T,davg}$ = -32.6°C, P_{air} = 0 psig (uu) U_{ts} = 130 knots, $T_{T,davg}$ = -32.6°C, P_{air} = 30 psig (vv) U_{ts} = 130 knots, $T_{T,davg}$ = -32.6°C, P_{air} = 60 psig

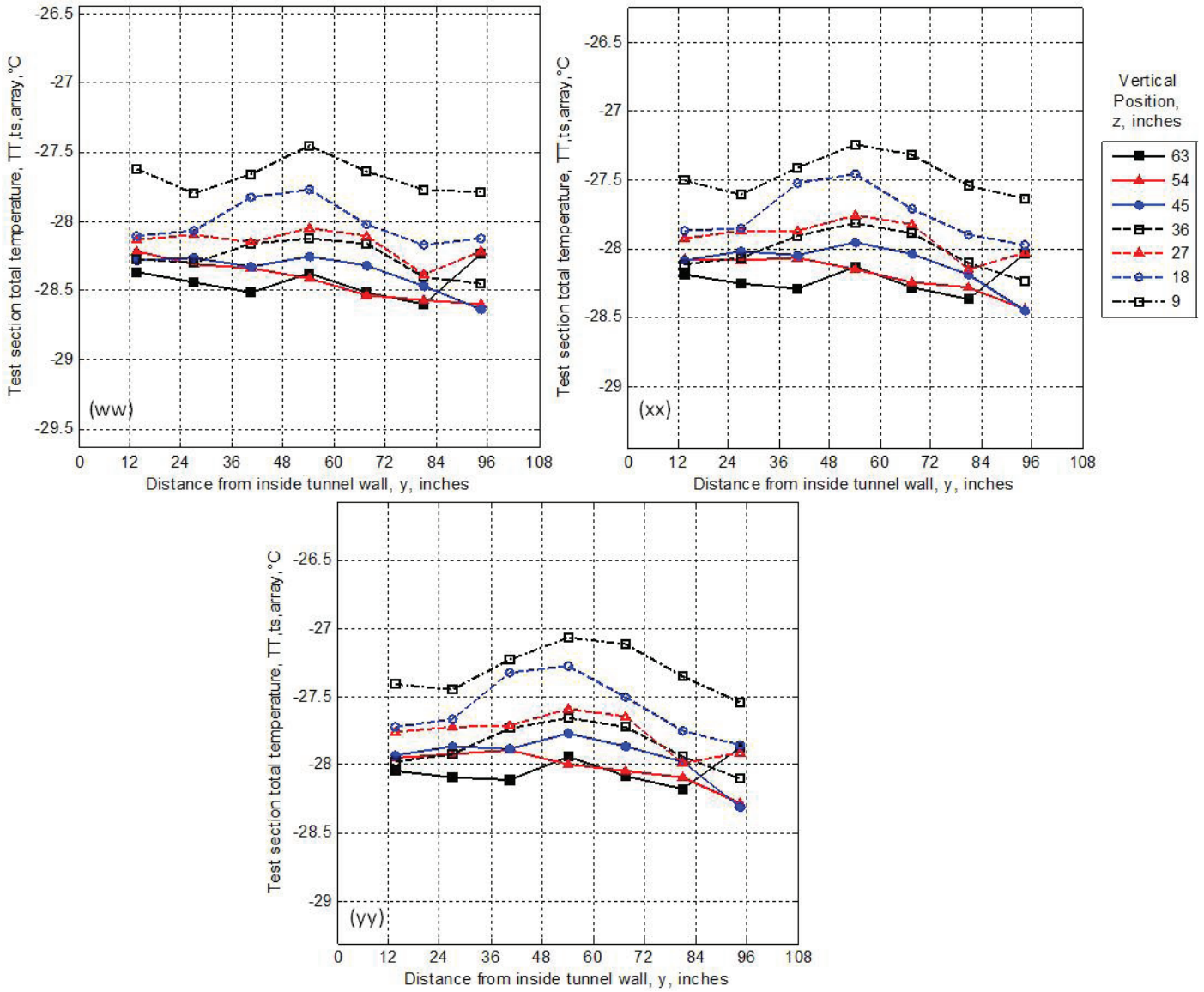

Continued Figure 23: (ww) U_{ts} = 300 knots, $T_{T,davg}$ = -28.2°C, P_{air} = 0 psig (xx) U_{ts} = 300 knots, $T_{T,davg}$ = -28.0°C, P_{air} = 30 psig (yy) U_{ts} = 300 knots, $T_{T,davg}$ = -28.0°C, P_{air} = 60 psig

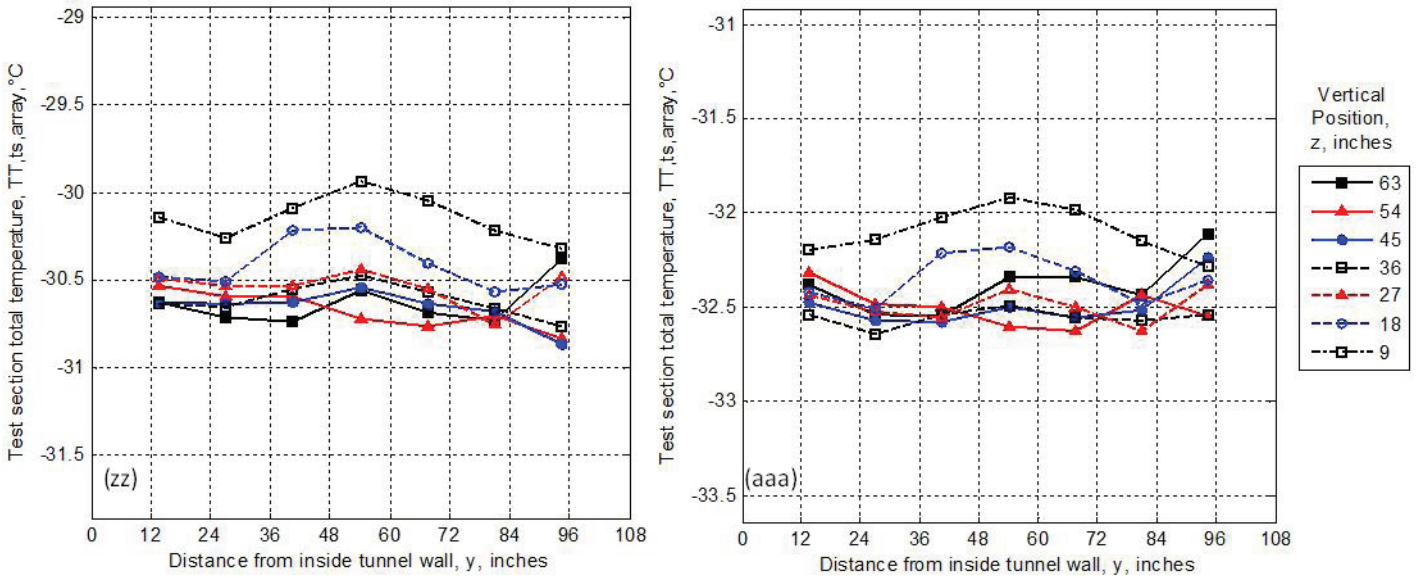

Continued Figure 23: (zz) U_{ts} = 220 knots, $T_{T,davg}$ = -30.7°C, P_{air} = 30 psi (aaa) U_{ts} = 130 knots, $T_{T,davg}$ = -32.7°C, P_{air} = 30 psig

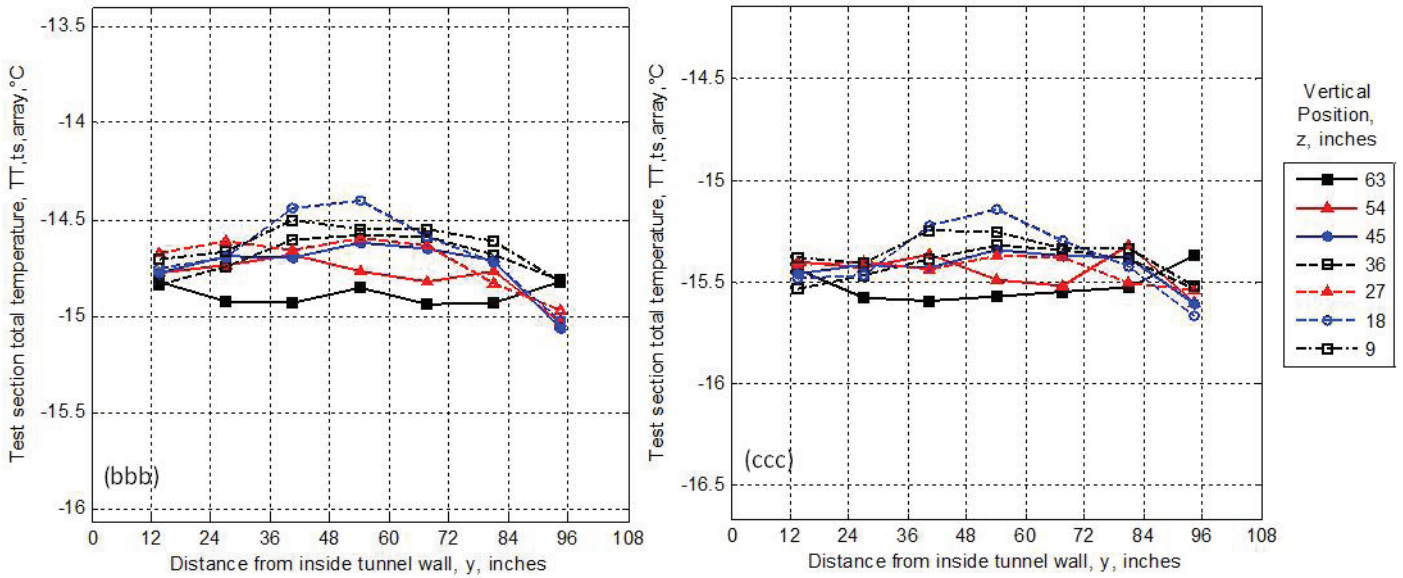

Continued Figure 23: (bbb) U_{ts} = 220 knots, $T_{T,davg}$ = -14.9°C, P_{air} = 30 psig (ccc) U_{ts} = 130 knots, $T_{T,davg}$ = -15.7°C, P_{air} = 30 psig

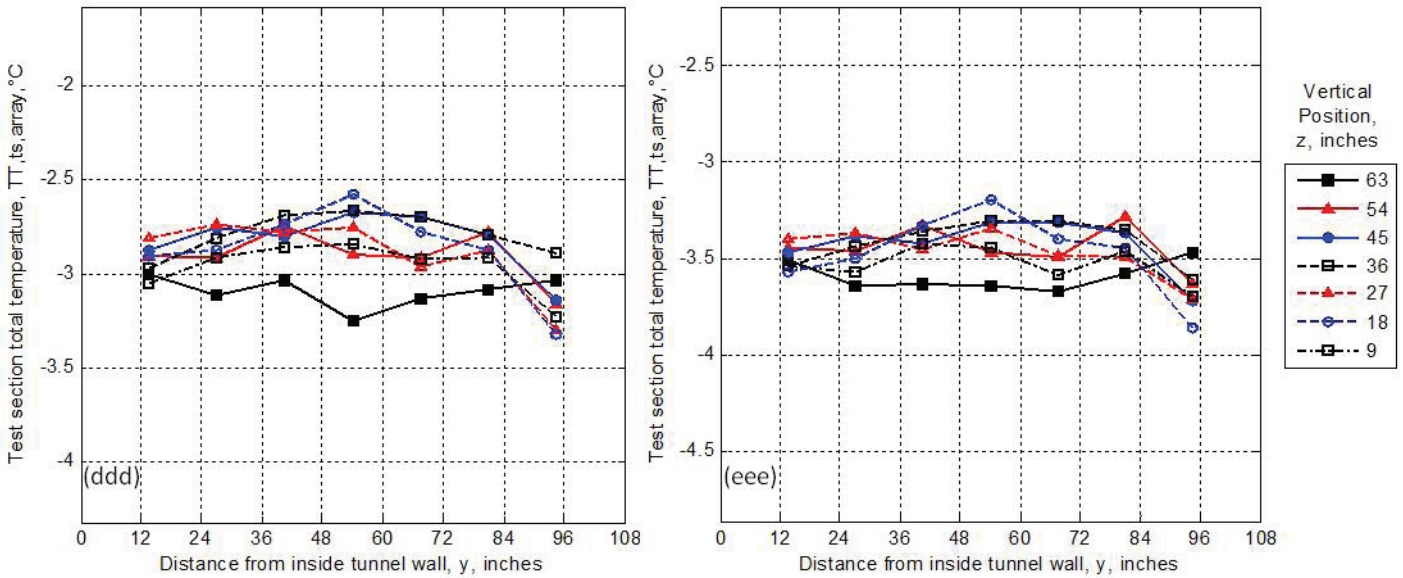

Continued Figure 23: (ddd) U_{ts} = 220 knots, $T_{T,davg}$ = -3.1°C, P_{air} = 30 psig (eee) U_{ts} = 130 knots, $T_{T,davg}$ = -3.7°C, P_{air} = 30 psig

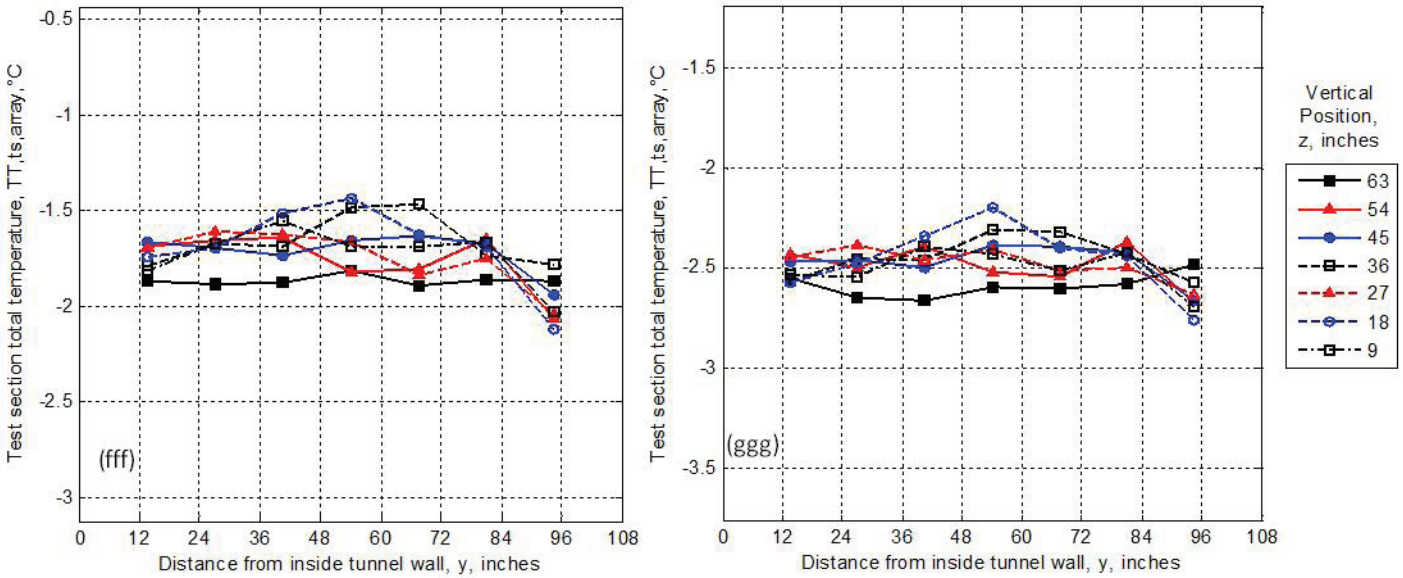

Continued Figure 23: (fff) U_{ts} = 220 knots, $T_{T,davg}$ = -1.8°C, P_{air} = 30 psig (ggg) U_{ts} = 130 knots, $T_{T,davg}$ = -2.7°C, P_{air} = 30 psig

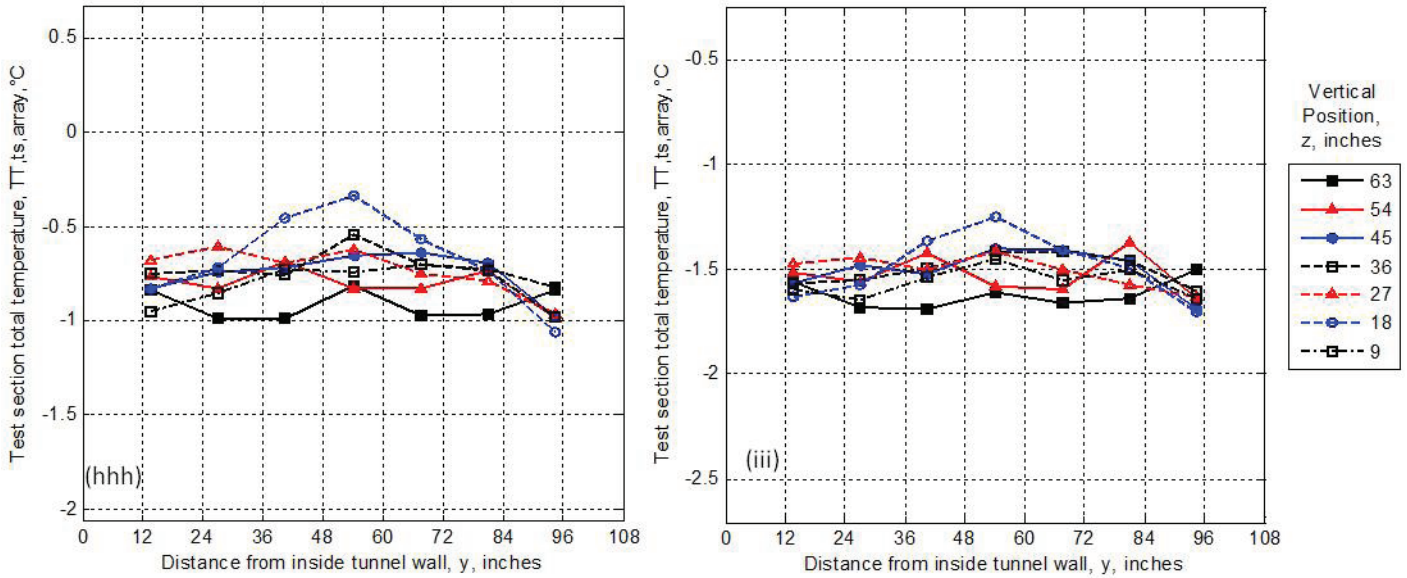

Continued Figure 23: (hhh) U_{ts} = 220 knots, $T_{T,davg}$ = -0.8°C, P_{air} = 30 psig (iii) U_{ts} = 130 knots, $T_{T,davg}$ = -1.7°C, P_{air} = 30 psig

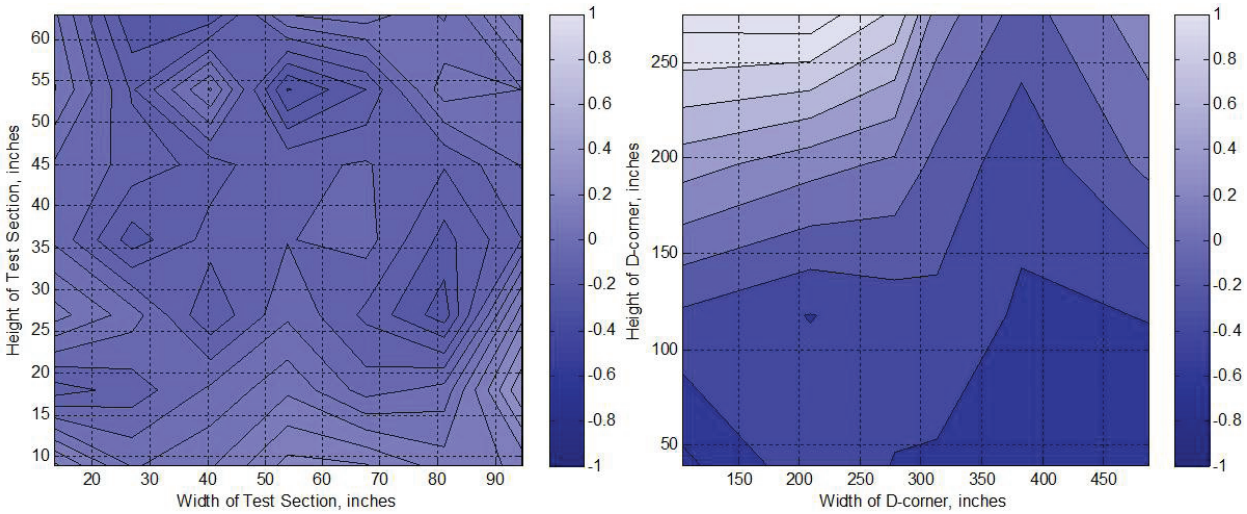

Figure 24: Test section versus D-corner surface plots (a) $V_{knots} = 200$ knots, $T_{T,davg} = 7°C$, $P_{air} = 0$ psig

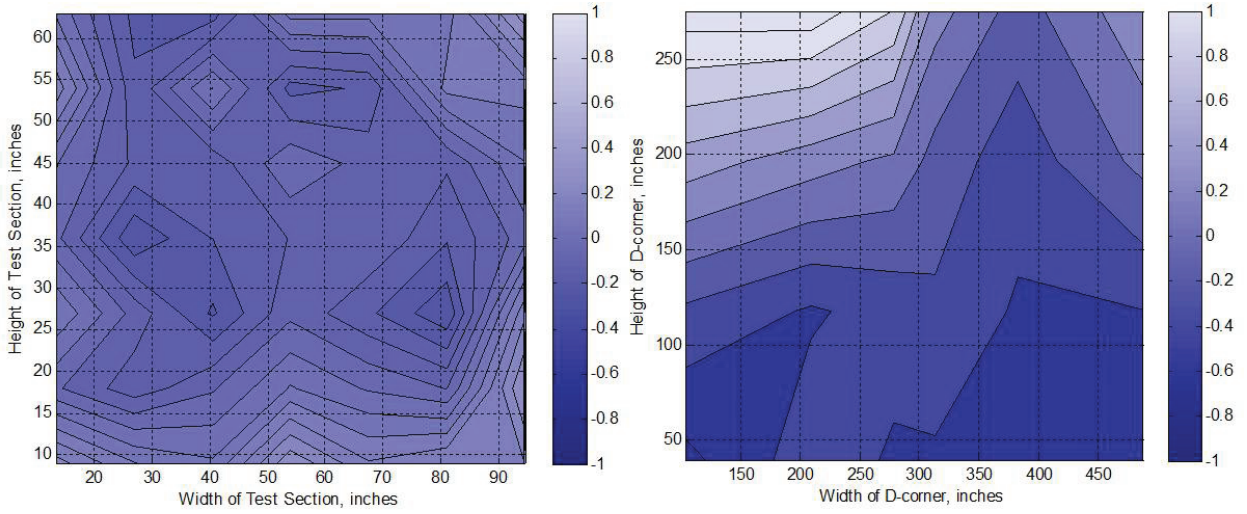

Continued Figure 24: (b) $V_{knots} = 150$ knots, $T_{T,davg} = 6°C$, $P_{air} = 0$ psig

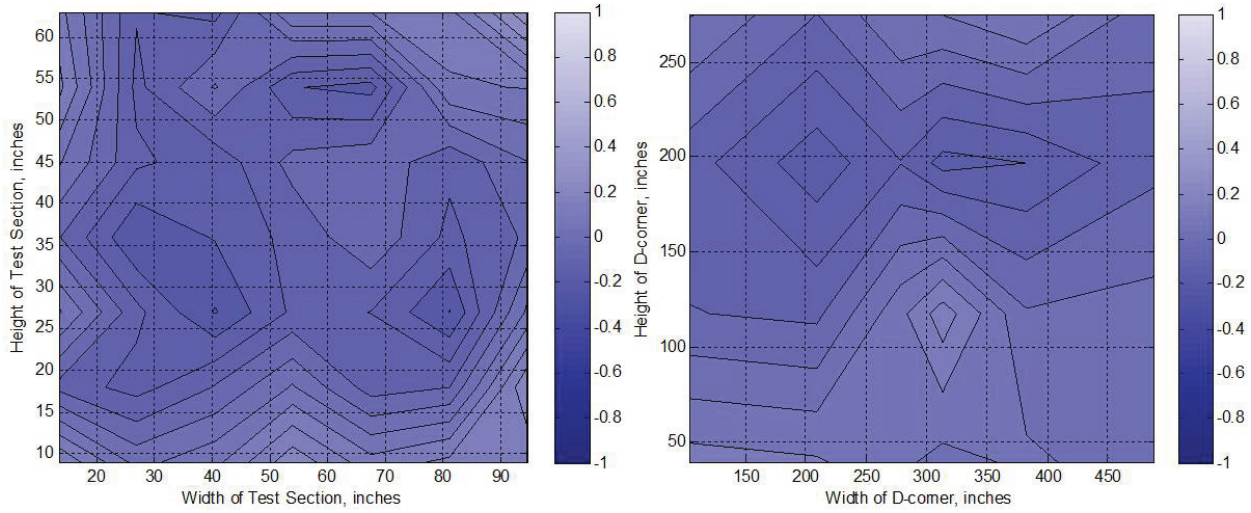

Continued Figure 24: (c) $V_{knots} = 100$ knots, $T_{T,davg} = 6°C$, $P_{air} = 0$ psig

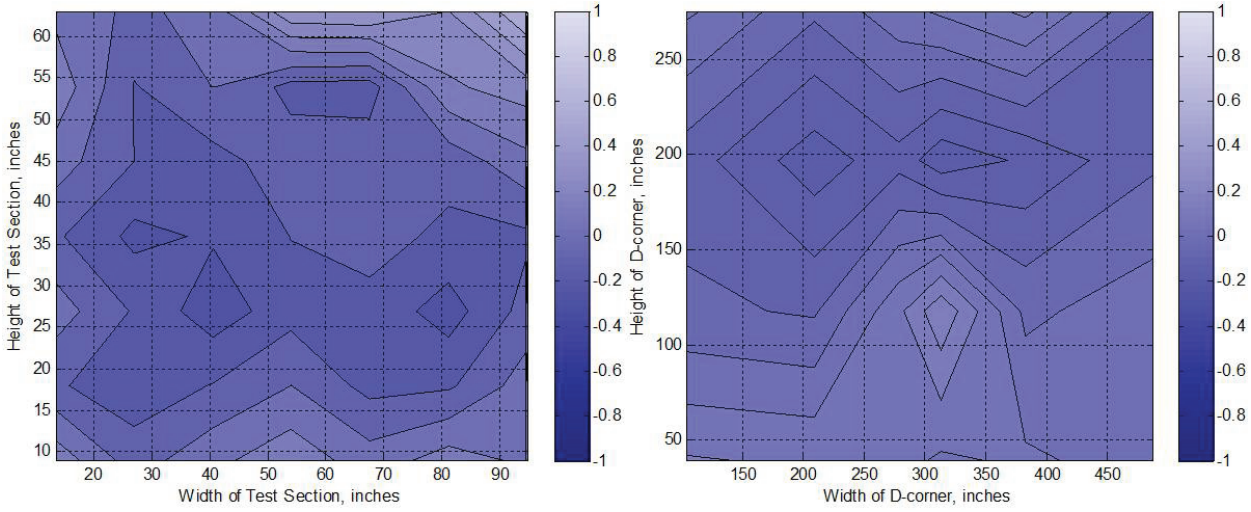

Continued Figure 24: (d) $V_{knots} = 50$ knots, $T_{T,davg} = 6°C$, $P_{air} = 0$ psig

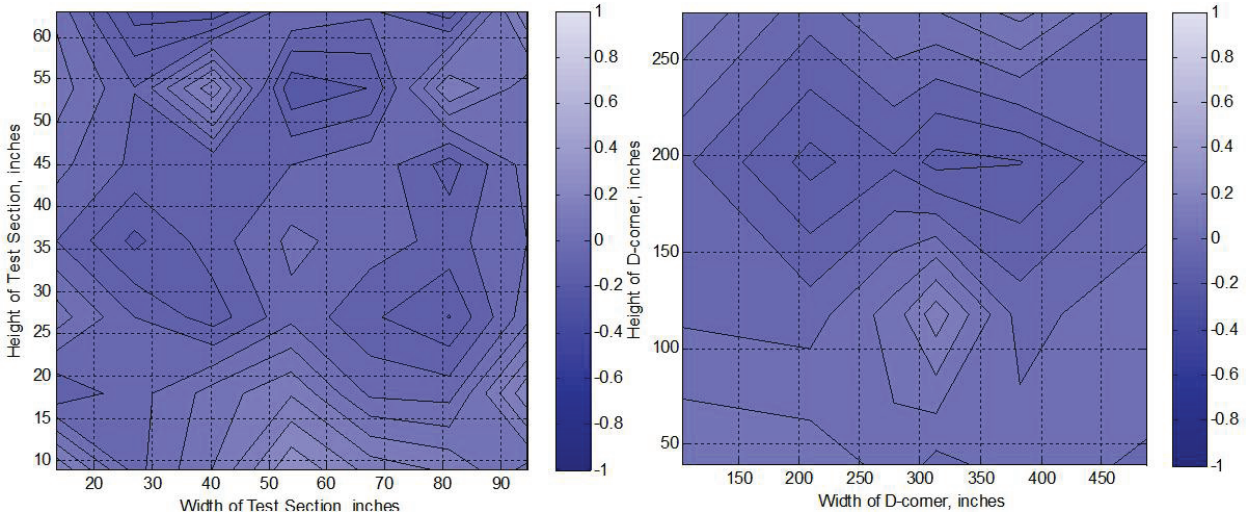

Continued Figure 24: (e) $V_{knots} = 220$ knots, $T_{T,davg} = 5°C$, $P_{air} = 0$ psig

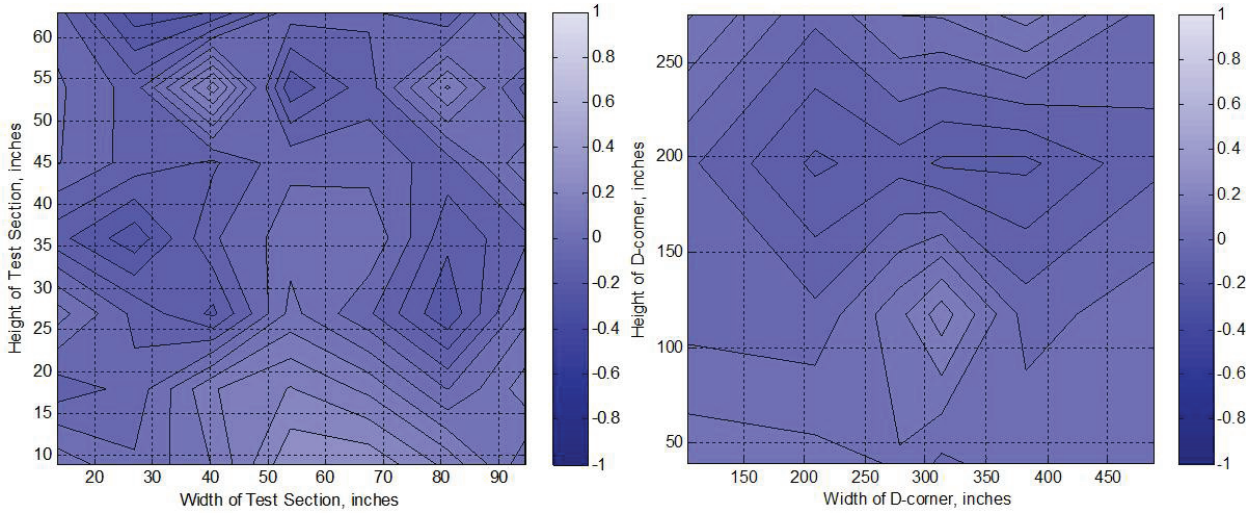

Continued Figure 24: (f) $V_{knots} = 220$ knots, $T_{T,davg} = 5°C$, $P_{air} = 60$ psig

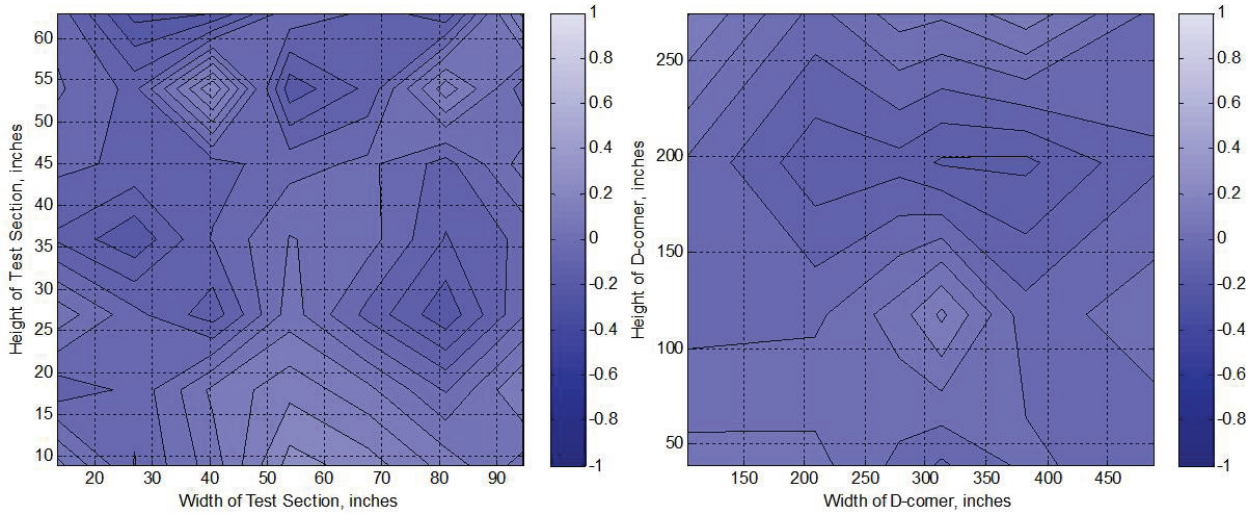

Continued Figure 24: (g) $V_{knots} = 220$ knots, $T_{T,davg} = 5°C$, $P_{air} = 30$ psig

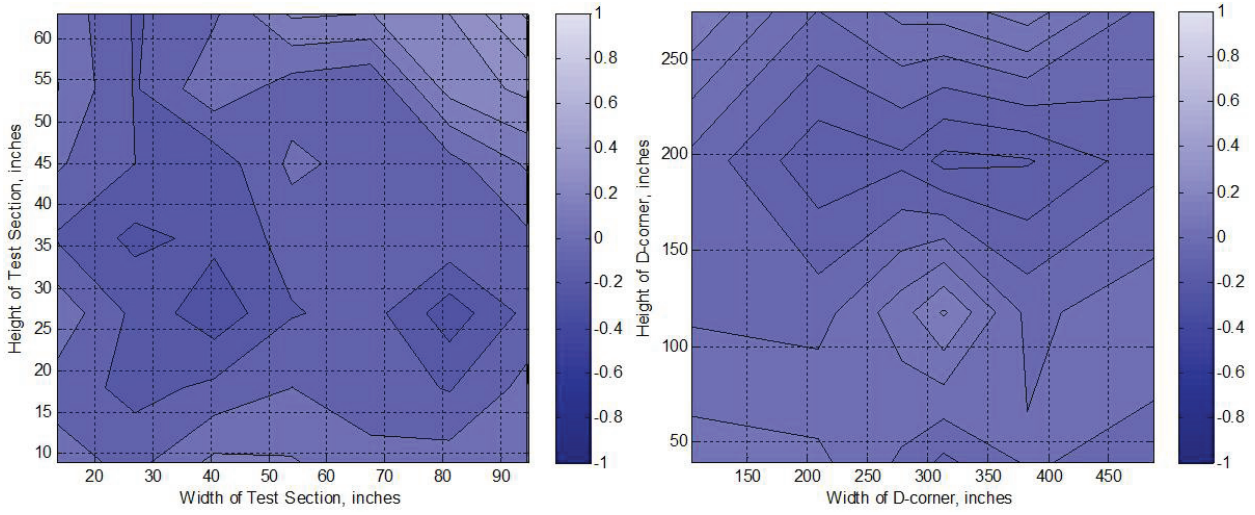

Continued Figure 24: (h) $V_{knots} = 50$ knots, $T_{T,davg} = 4°C$, $P_{air} = 0$ psig

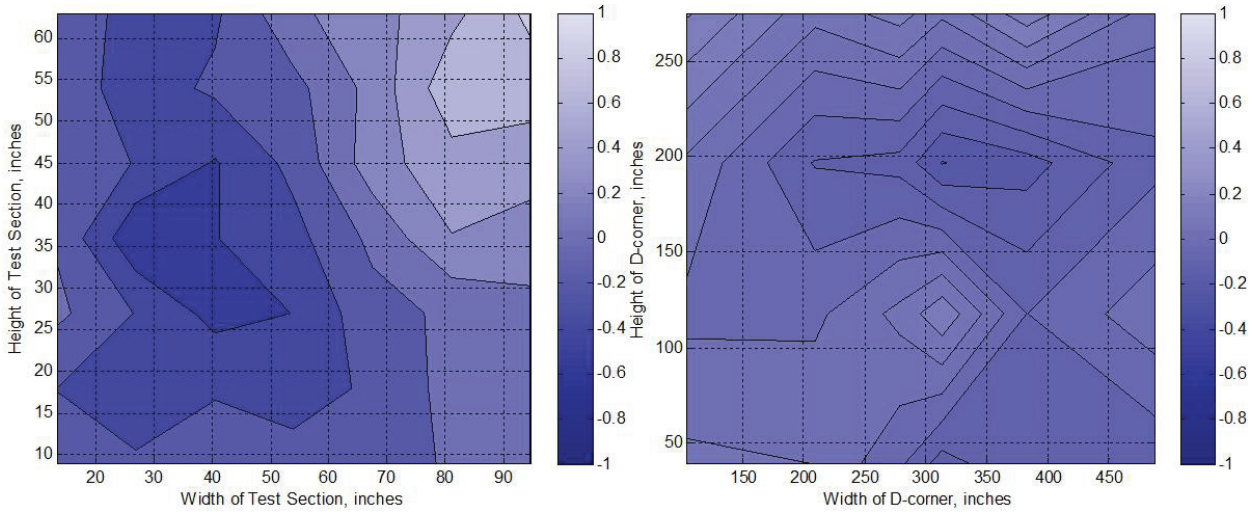

Continued Figure 24: (i) $V_{knots} = 50$ knots, $T_{T,davg} = 4°C$, $P_{air} = 60$ psig

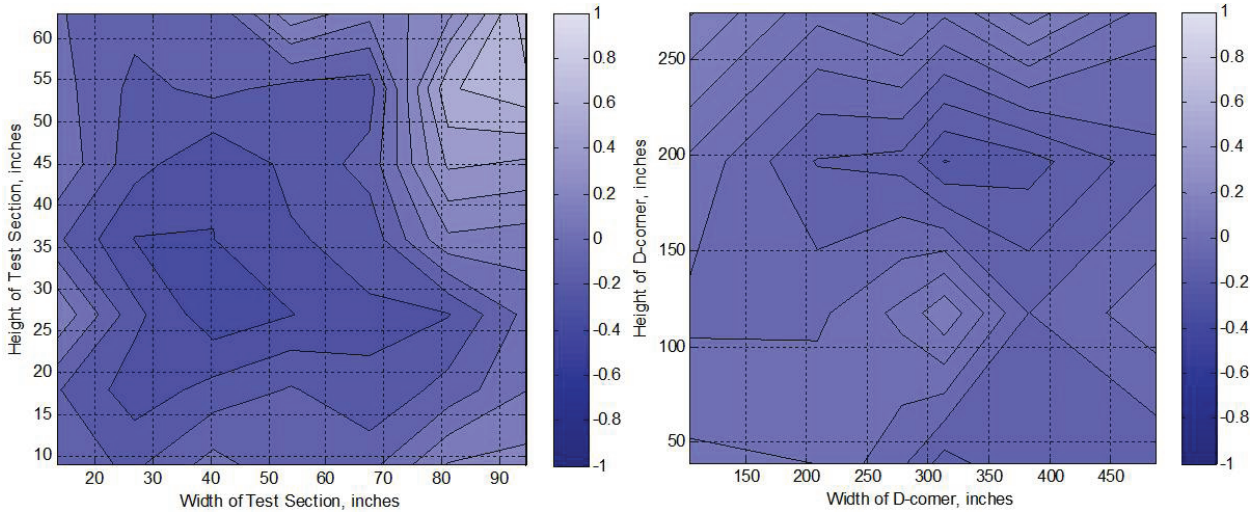

Continued Figure 24: (j) $V_{knots} = 50$ knots, $T_{T,davg} = 4°C$, $P_{air} = 30$ psig

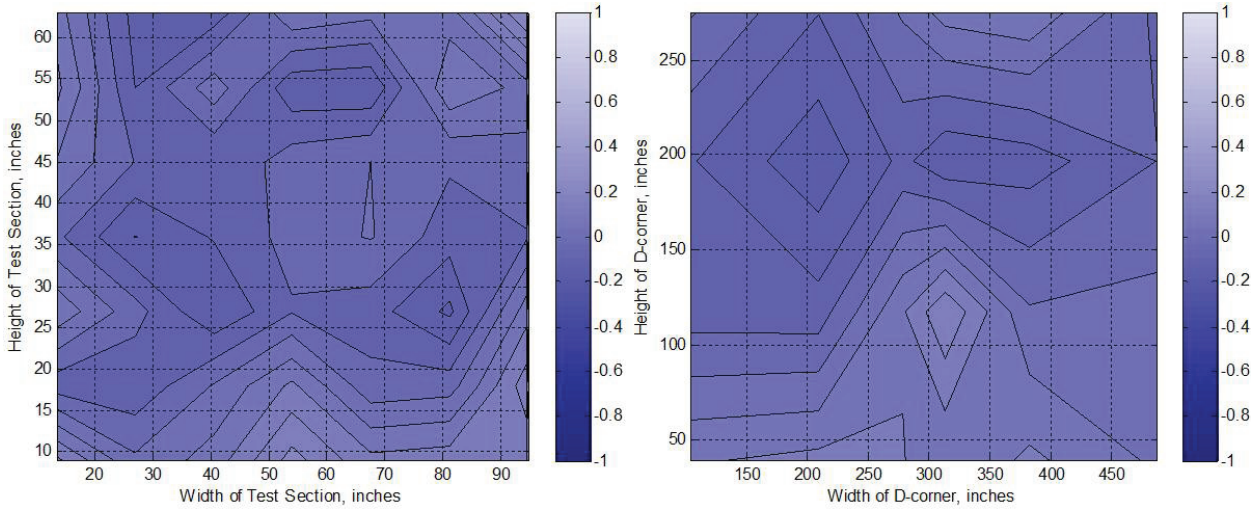

Continued Figure 24: (k) $V_{knots} = 130$ knots, $T_{T,davg} = 4°C$, $P_{air} = 0$ psig

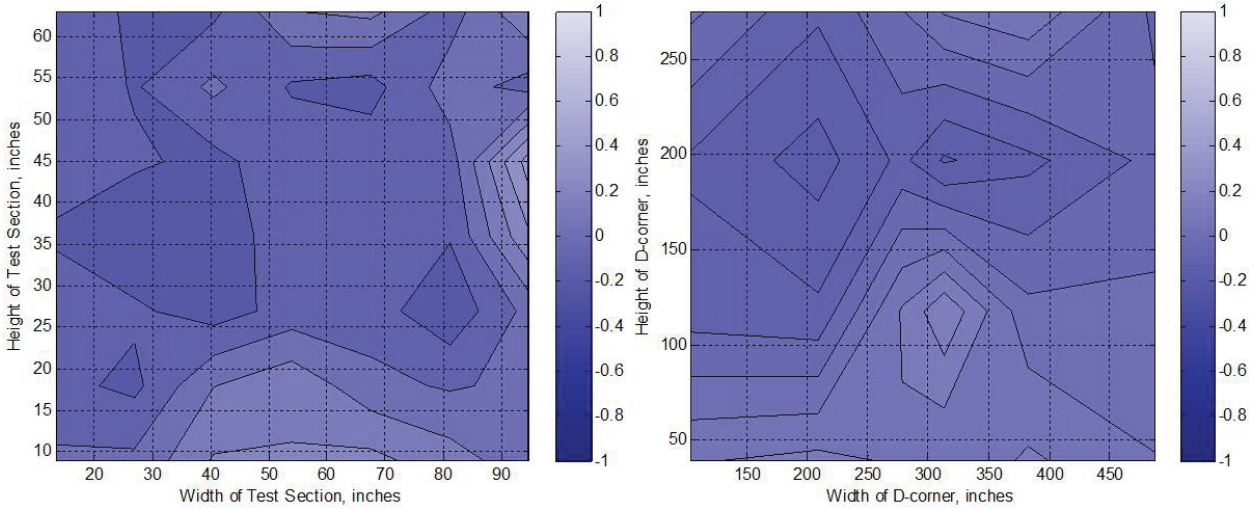

Continued Figure 24: (l) $V_{knots} = 130$ knots, $T_{T,davg} = 4°C$, $P_{air} = 60$ psig

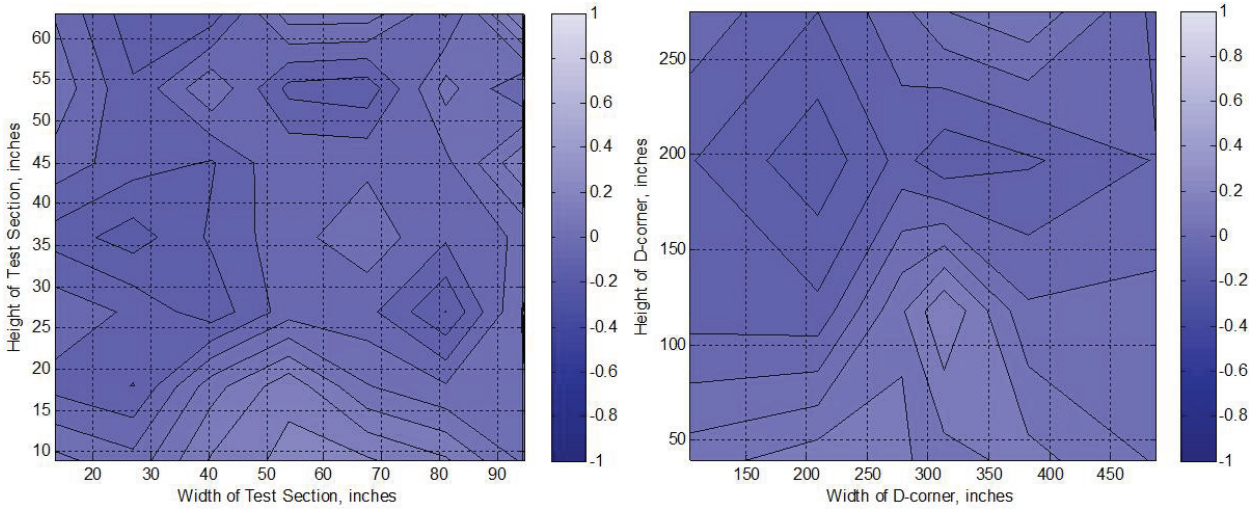

Continued Figure 24: (m) $V_{knots} = 130$ knots, $T_{T,davg} = 4°C$, $P_{air} = 30$ psig

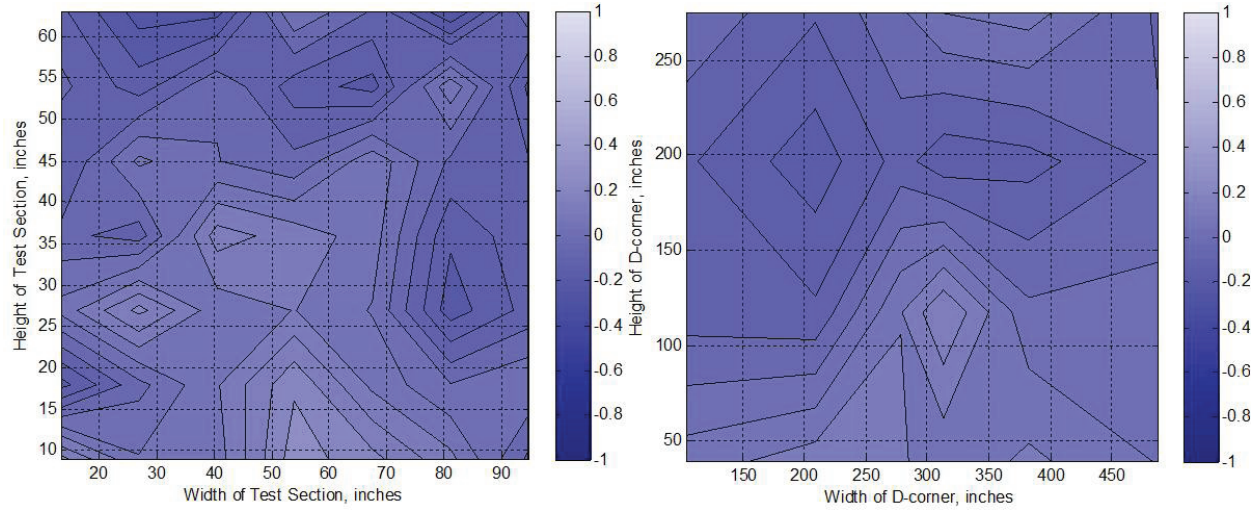

Continued Figure 24: (n) $V_{knots} = 300$ knots, $T_{T,davg} = 6°C$, $P_{air} = 0$ psig

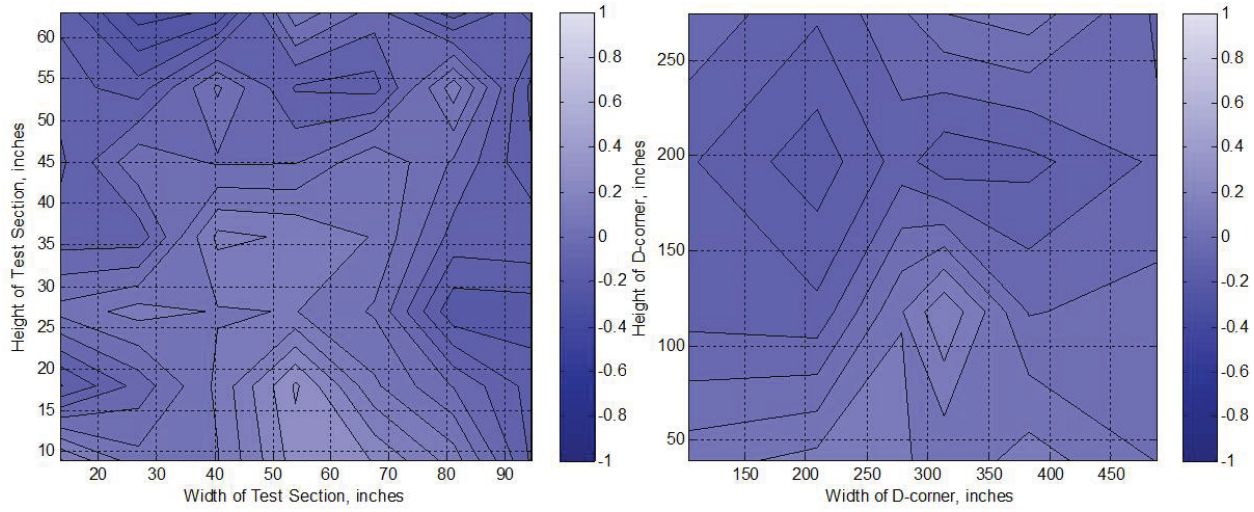

Continued Figure 24: (o) $V_{knots} = 300$ knots, $T_{T,davg} = 6°C$, $P_{air} = 60$ psig

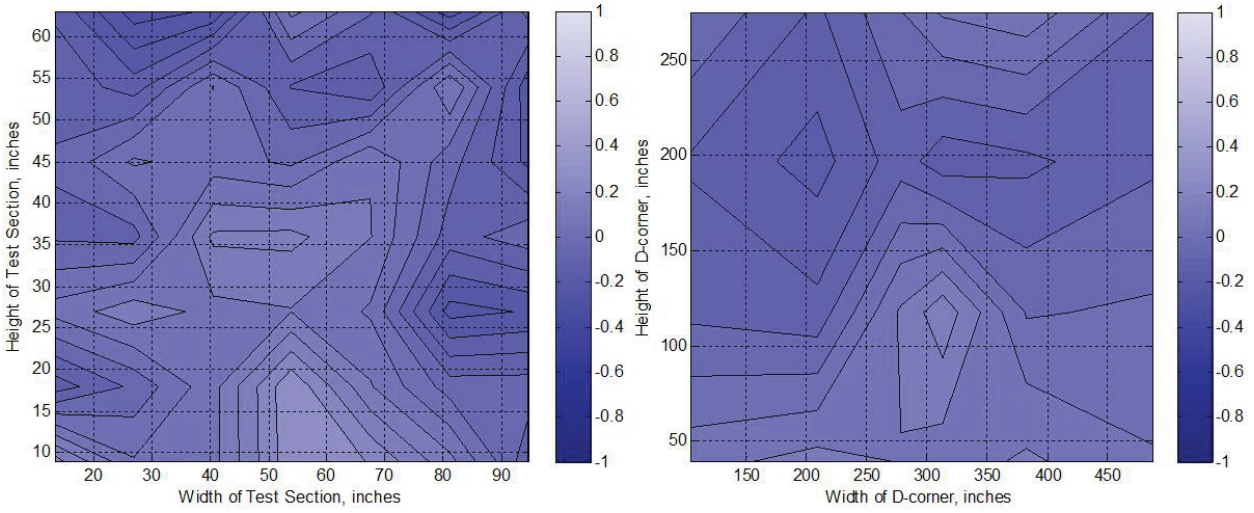

Continued Figure 24: (p) $V_{knots} = 300$ knots, $T_{T,davg} = 6°C$, $P_{air} = 30$ psig

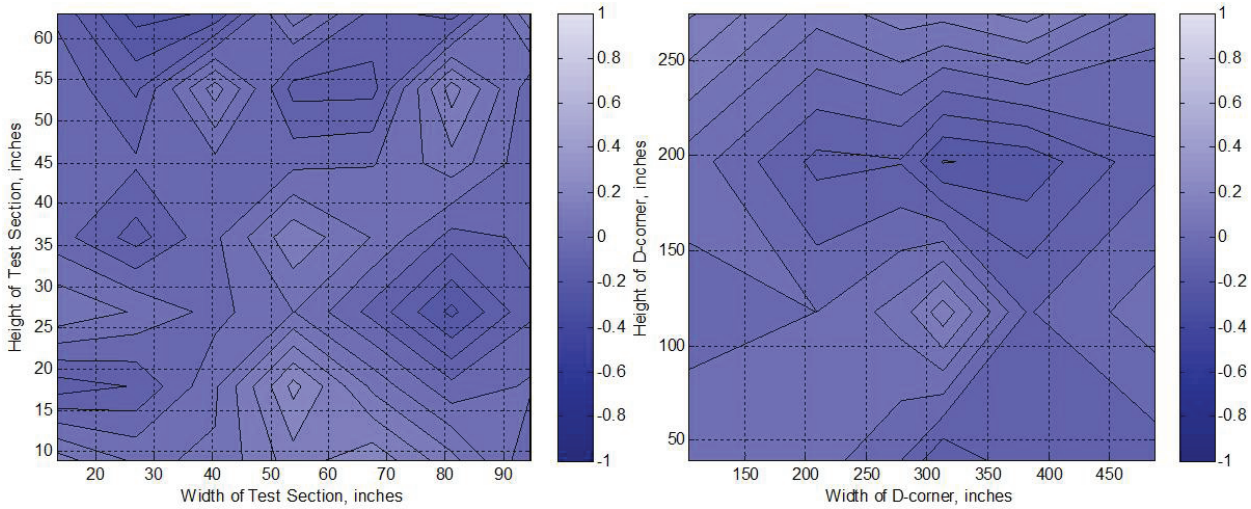

Continued Figure 24: (q) $V_{knots} = 220$ knots, $T_{T,davg} = 3°C$, $P_{air} = 30$ psig

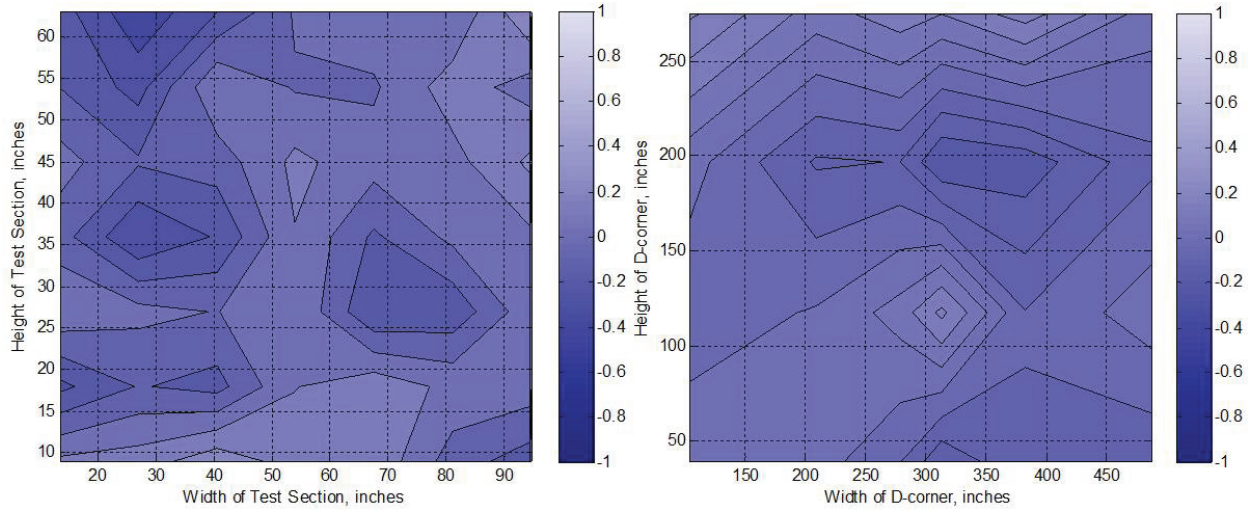

Continued Figure 24: (r) $V_{knots} = 130$ knots, $T_{T,davg} = 2°C$, $P_{air} = 30$ psig

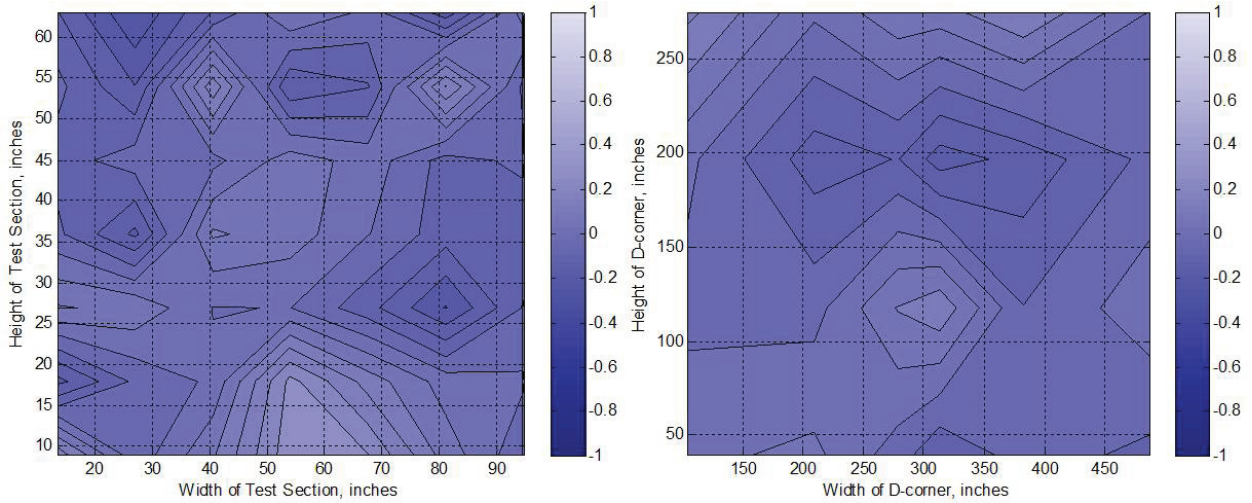

Continued Figure 24: (s) $V_{knots} = 220$ knots, $T_{T,davg} = 2°C$, $P_{air} = 30$ psig

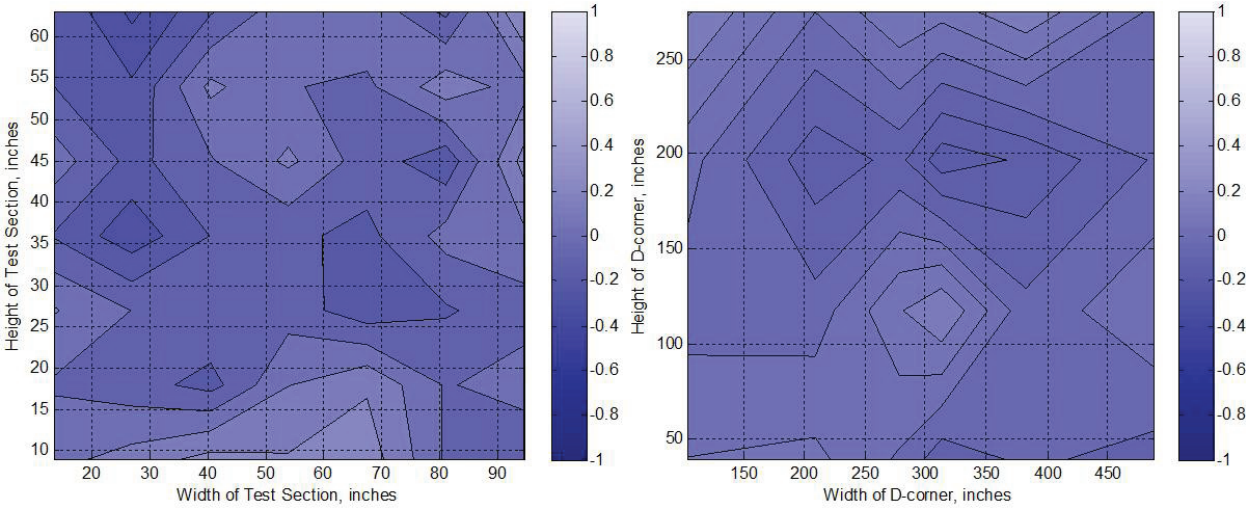

Continued Figure 24: (t) $V_{knots} = 130$ knots, $T_{T,davg} = 1°C$, $P_{air} = 30$ psig

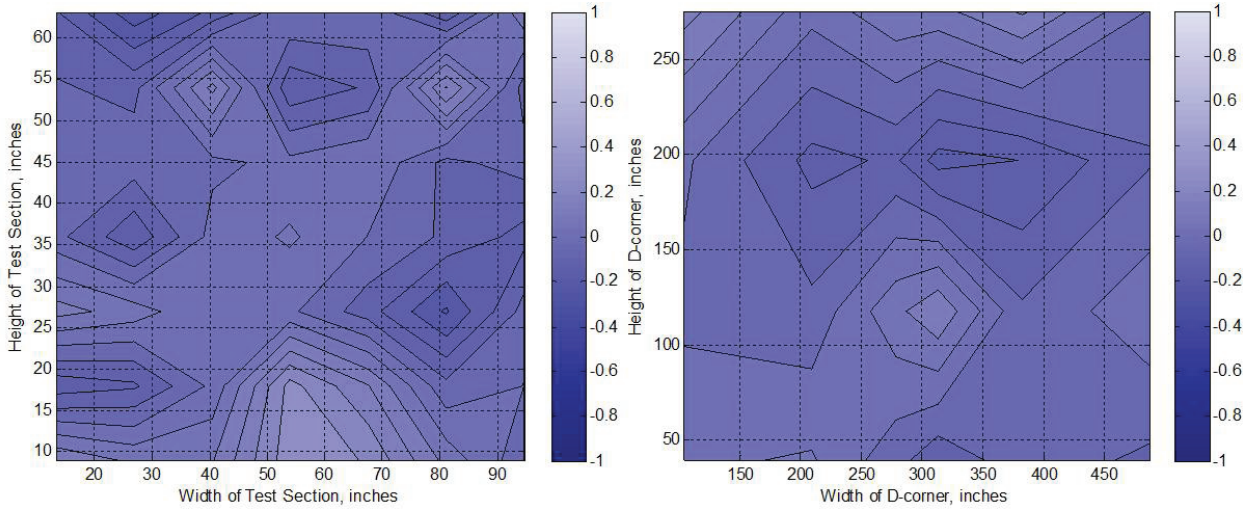

Continued Figure 24: (u) $V_{knots} = 220$ knots, $T_{T,davg} = 1°C$, $P_{air} = 30$ psig

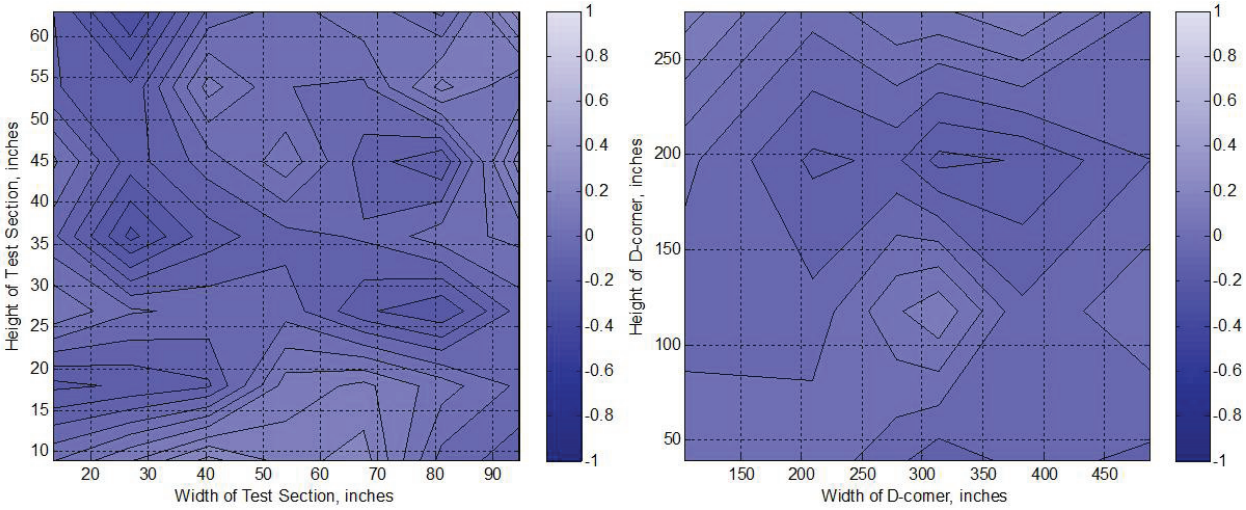

Continued Figure 24: (v) $V_{knots} = 130$ knots, $T_{T,davg} = 0°C$, $P_{air} = 30$ psig

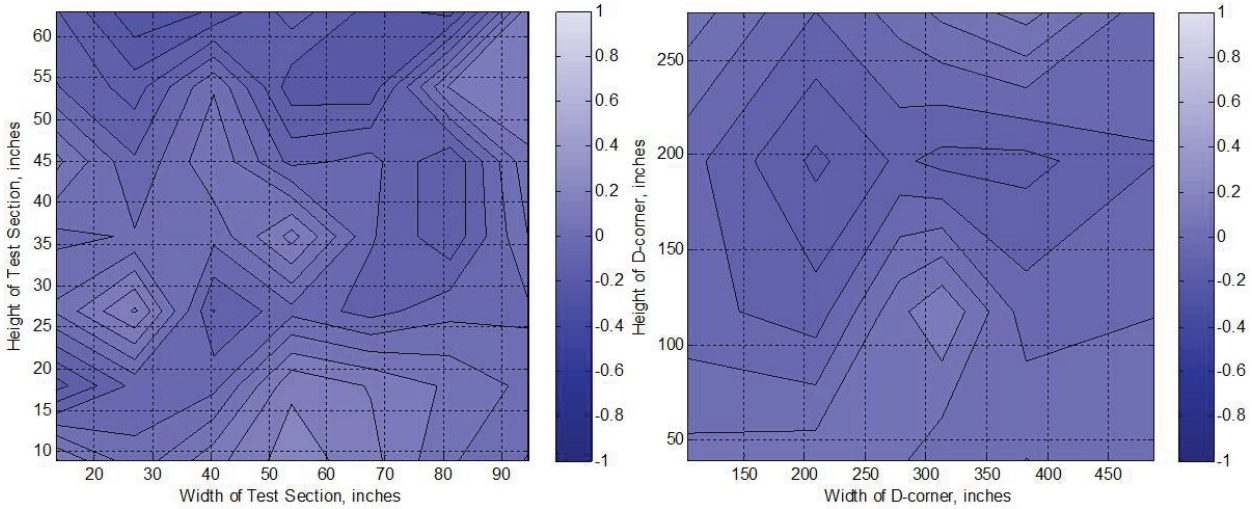

Continued Figure 24: (w) $V_{knots} = 220$ knots, $T_{T,davg} = 0°C$, $P_{air} = 0$ psig

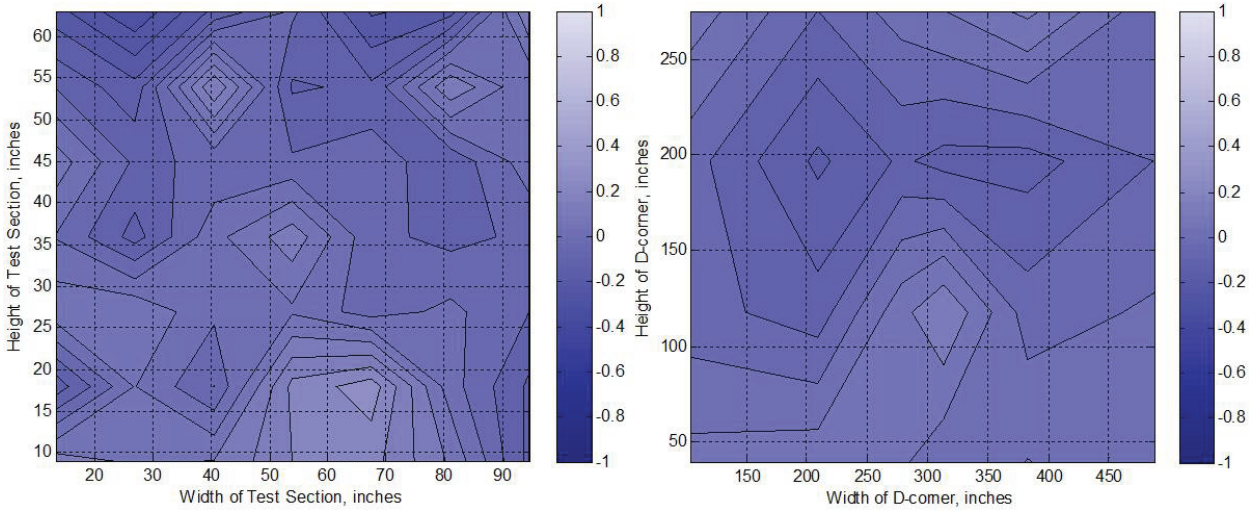

Continued Figure 24: (x) $V_{knots} = 220$ knots, $T_{T,davg} = 0°C$, $P_{air} = 60$ psig

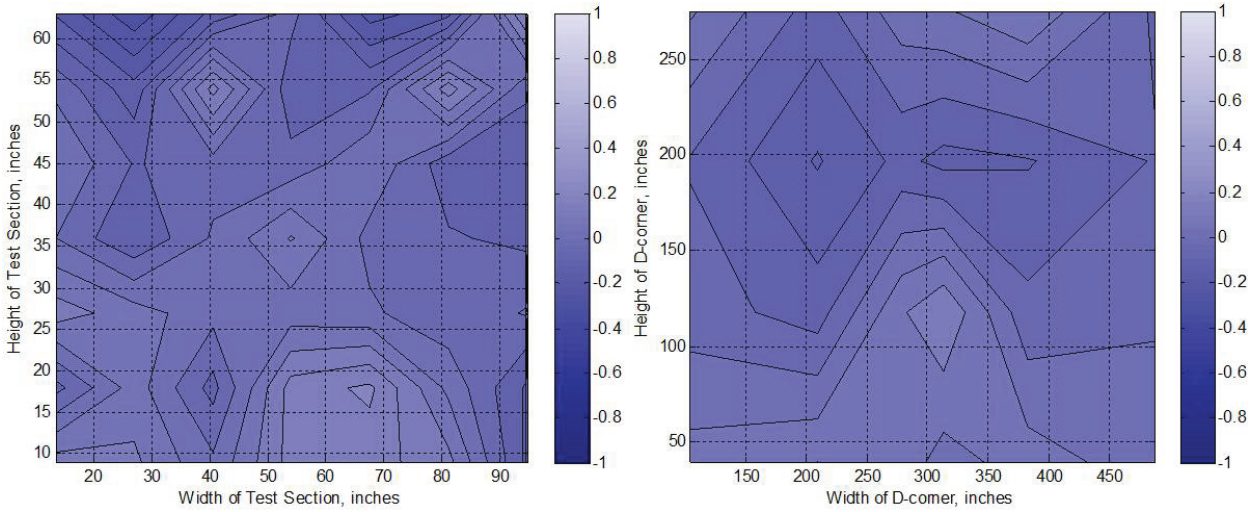

Continued Figure 24: (y) V_{knots} = 220 knots, $T_{T,davg}$ = 0°C, P_{air} = 30 psig

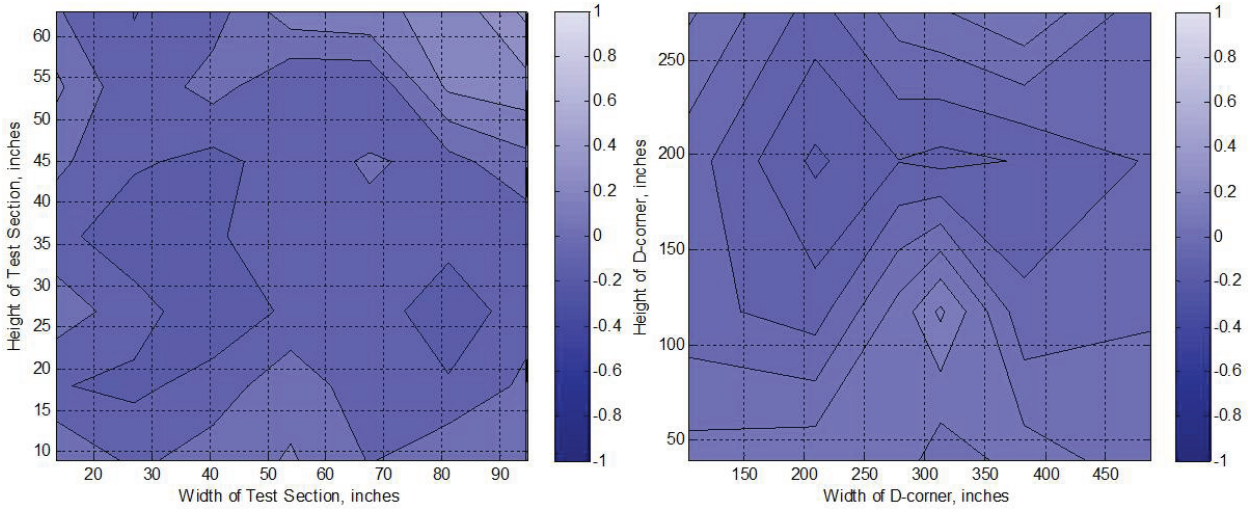

Continued Figure 24: (z) V_{knots} = 50 knots, $T_{T,davg}$ = -2°C, P_{air} = 0 psig

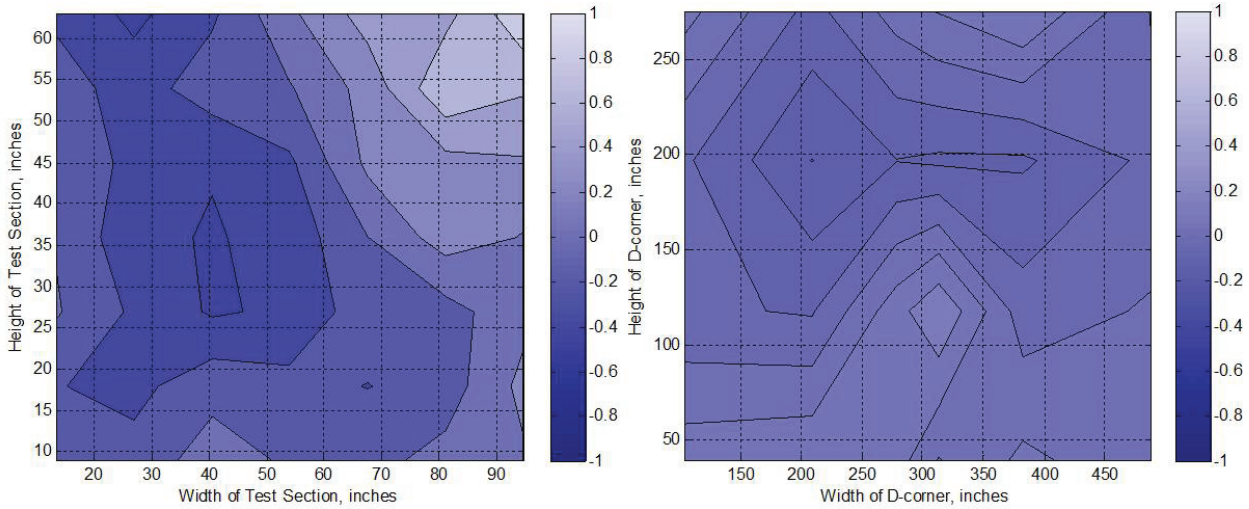

Continued Figure 24: (aa) V_{knots} = 50 knots, $T_{T,davg}$ = -2°C, P_{air} = 60 psig

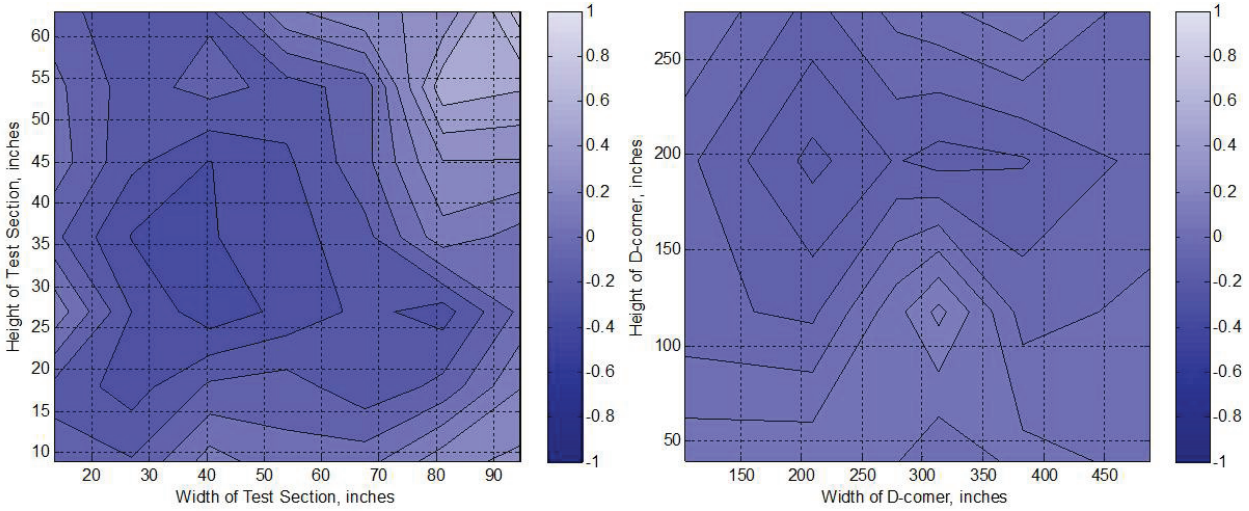

Continued Figure 24: (bb) V_{knots} = 50 knots, $T_{T,davg}$ = -2°C, P_{air} = 30 psig

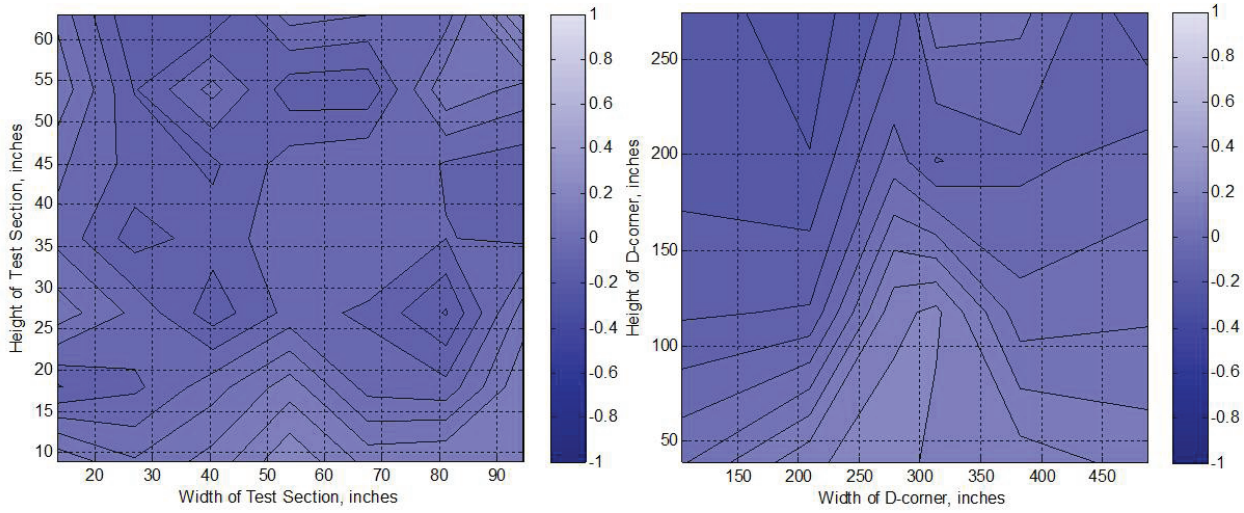

Continued Figure 24: (cc) V_{knots} = 130 knots, $T_{T,davg}$ = -1°C, P_{air} = 0 psig

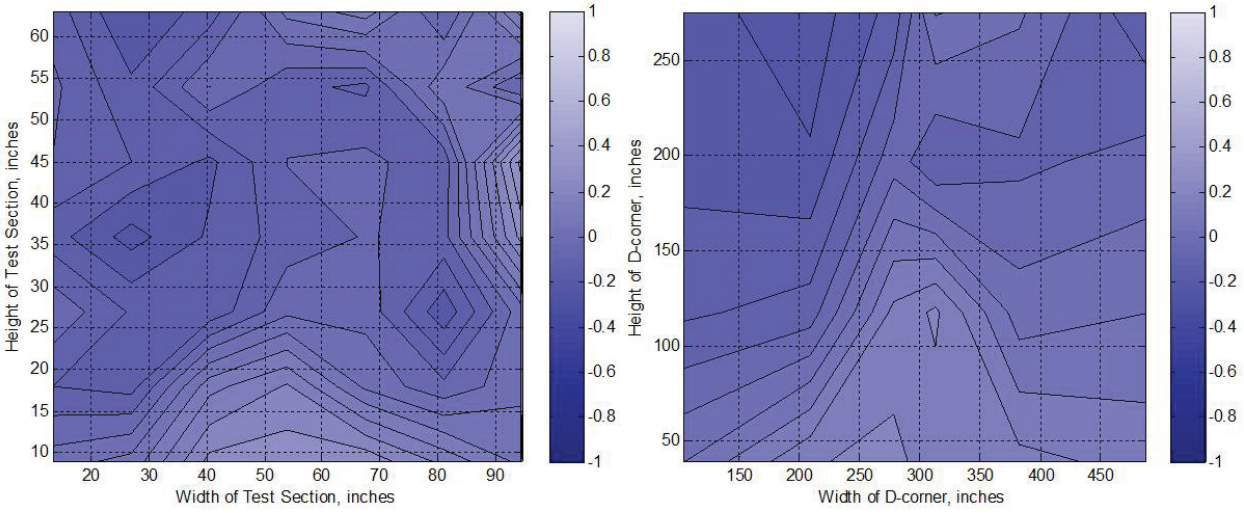

Continued Figure 24: (dd) V_{knots} = 130 knots, $T_{T,davg}$ = -1°C, P_{air} = 60 psig

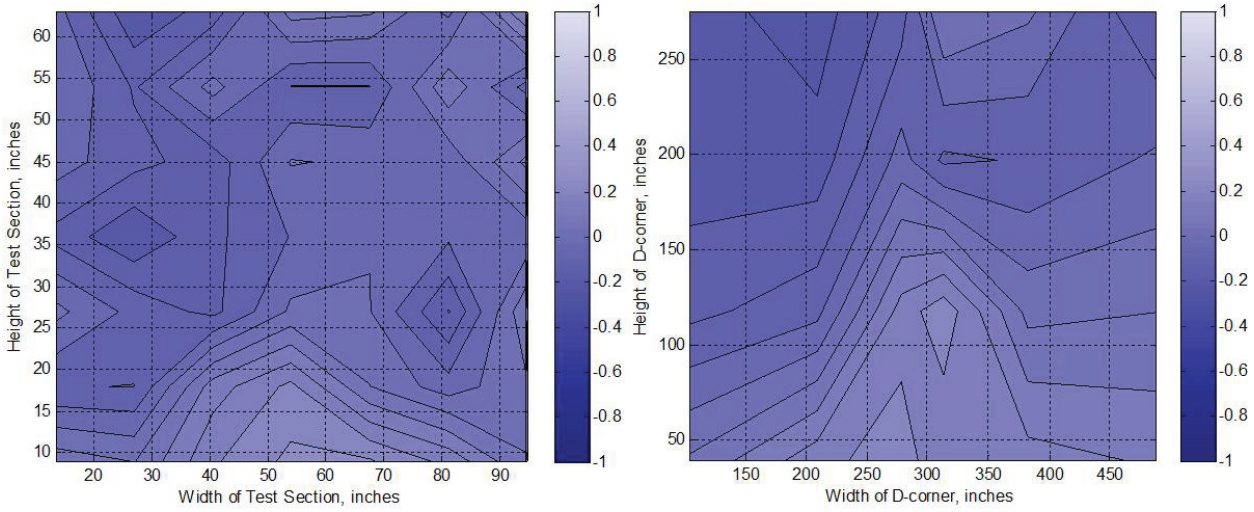

Continued Figure 24: (ee) V_{knots} = 130 knots, $T_{T,davg}$ = -1°C, P_{air} = 30 psig

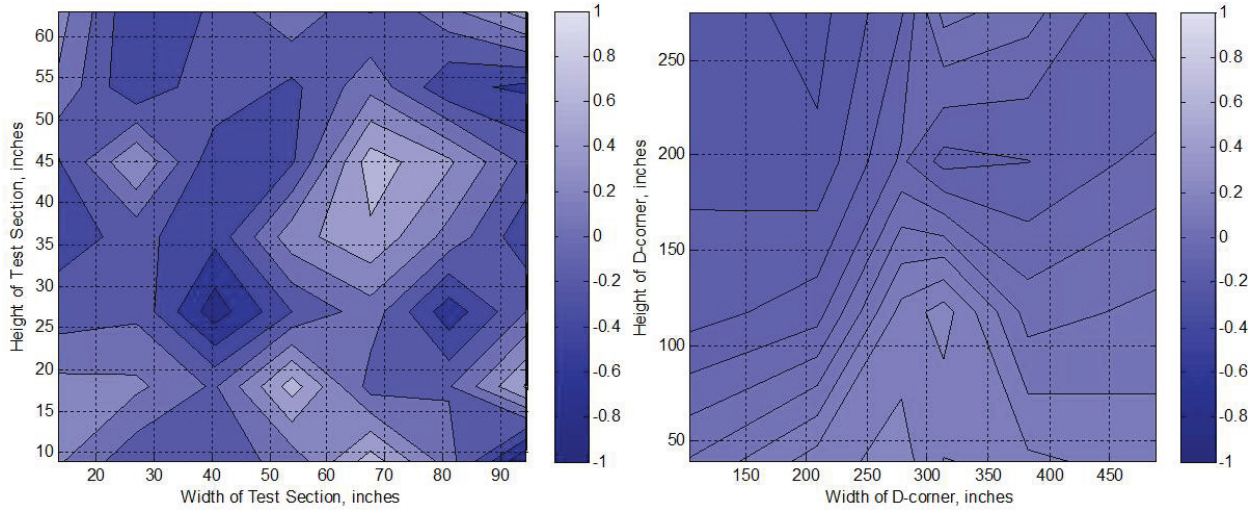

Continued Figure 24: (ff) V_{knots} = 300 knots, $T_{T,davg}$ = 1°C, P_{air} = 0 psig

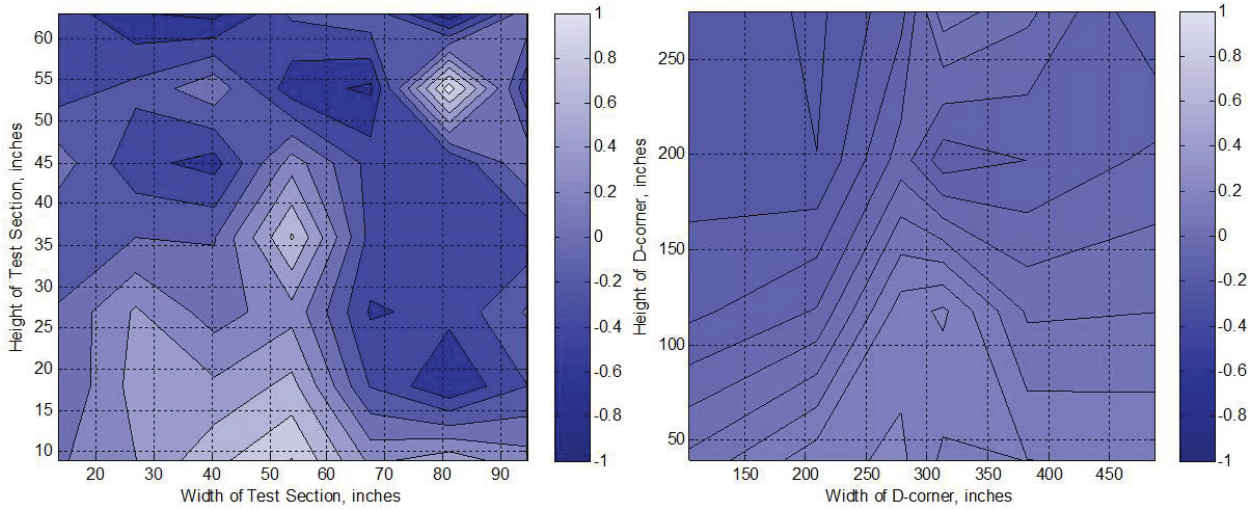

Continued Figure 24: (gg) $V_{knots} = 300$ knots, $T_{T,davg} = 1°C$, $P_{air} = 60$ psig

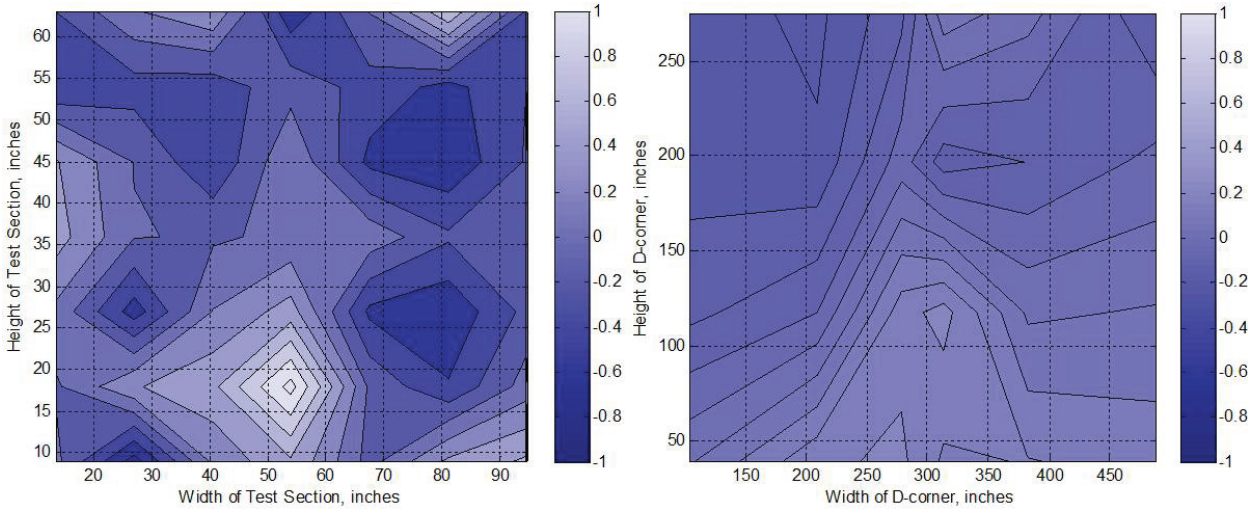

Continued Figure 24: (hh) $V_{knots} = 300$ knots, $T_{T,davg} = 1°C$, $P_{air} = 30$ psig

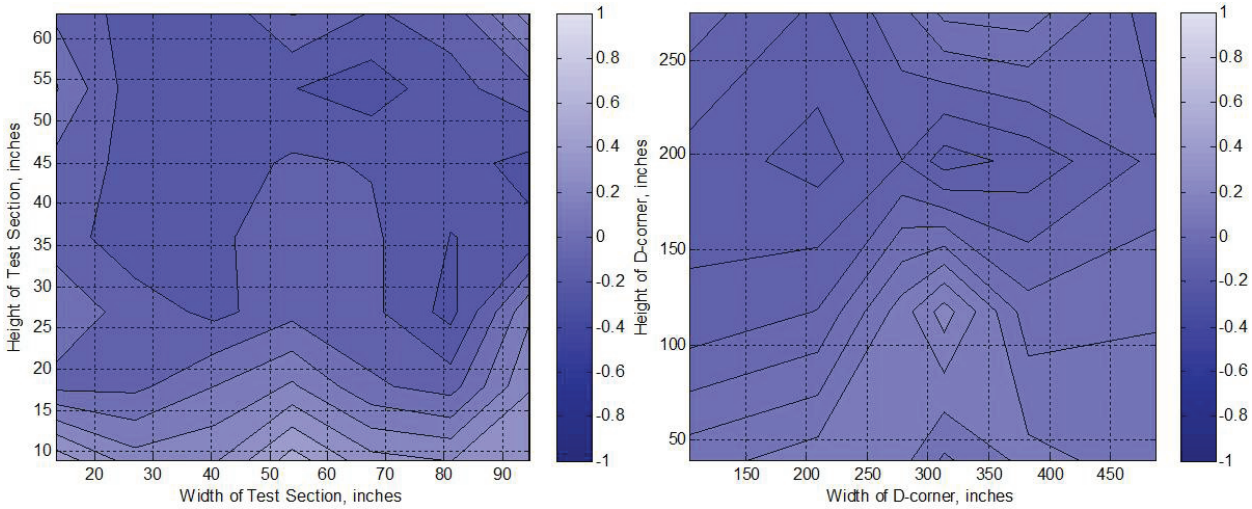

Continued Figure 24: (ii) V_{knots} = 220 knots, $T_{T,davg}$ = -15°C, P_{air} = 0 psig

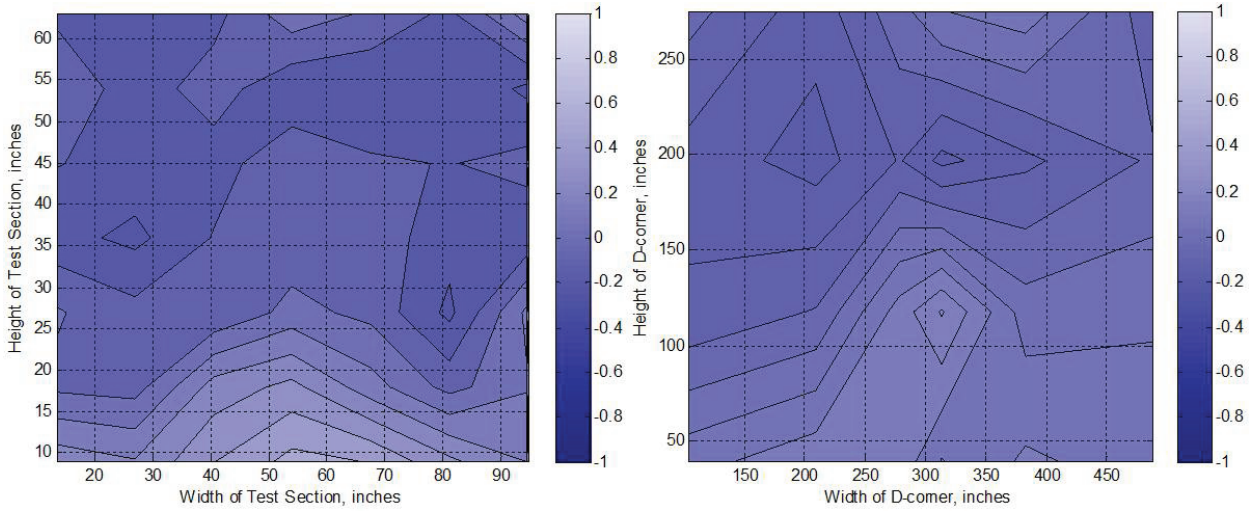

Continued Figure 24: (jj) V_{knots} = 220 knots, $T_{T,davg}$ = -15°C, P_{air} = 60 psig

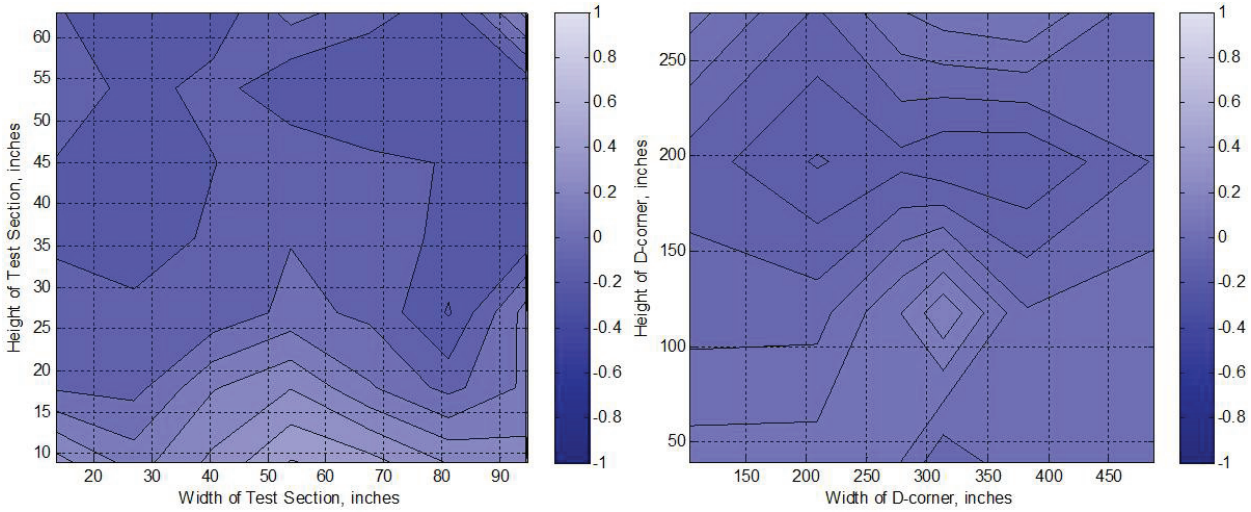

Continued Figure 24: (kk) V_{knots} = 220 knots, $T_{T,davg}$ = -15°C, P_{air} = 30 psig

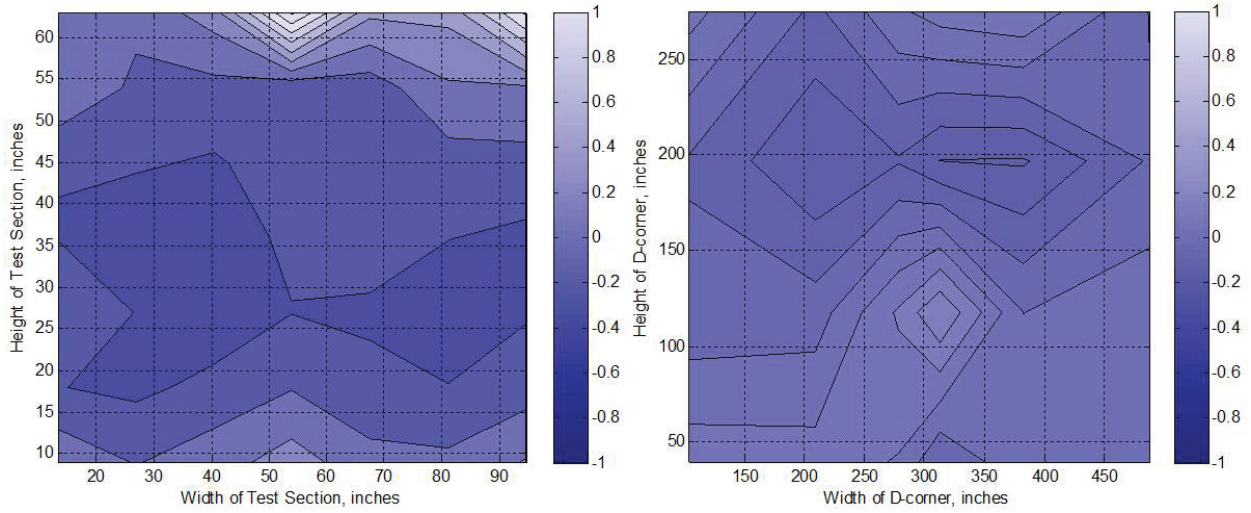

Continued Figure 24: (ll) V_{knots} = 50 knots, $T_{T,davg}$ = -17°C, P_{air} = 0 psig

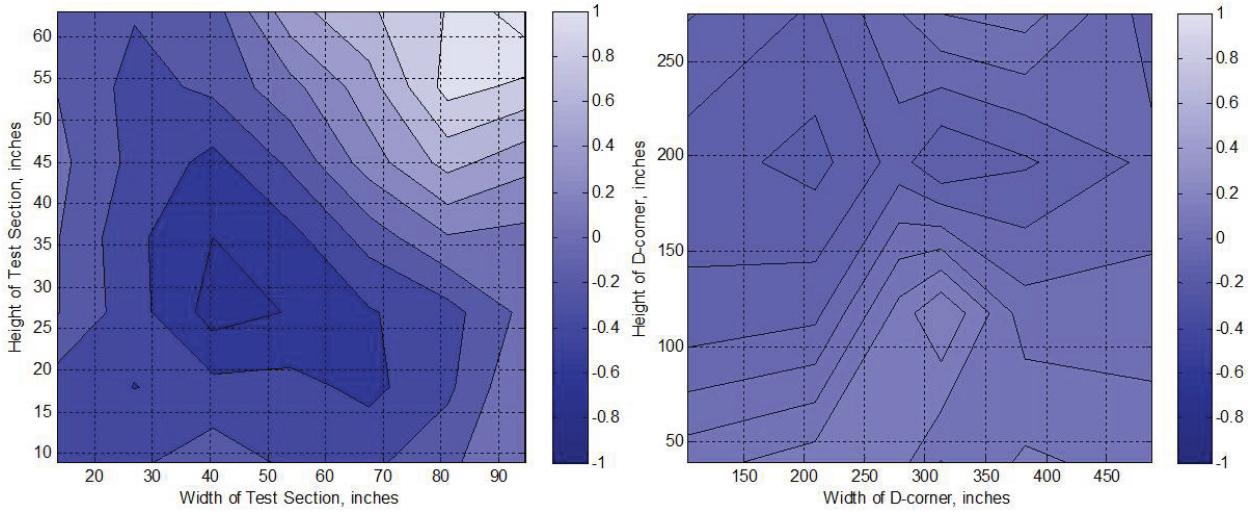

Continued Figure 24: (mm) V_{knots} = 50 knots, $T_{T,davg}$ = -17°C, P_{air} = 60 psig

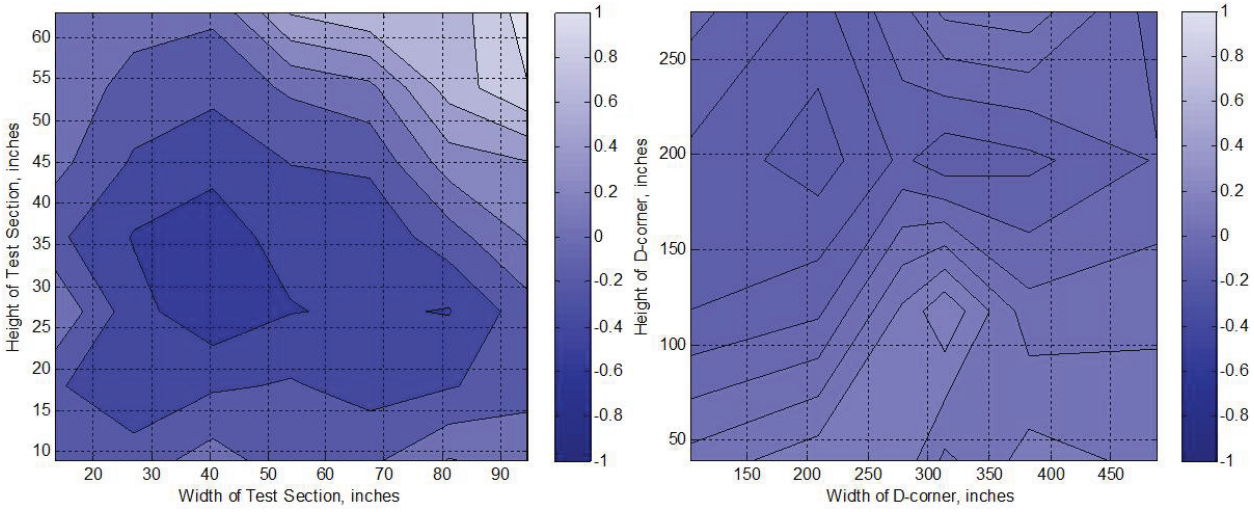

Continued Figure 24: (nn) V_{knots} = 50 knots, $T_{T,davg}$ = -17°C, P_{air} = 30 psig

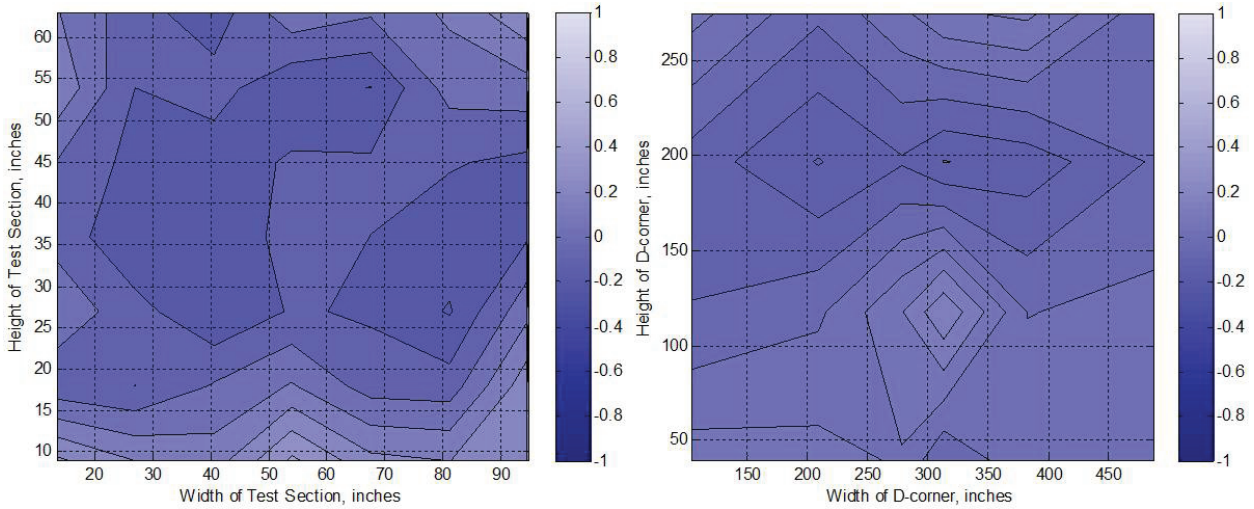

Continued Figure 24: (oo) V_{knots} = 130 knots, $T_{T,davg}$ = -16°C, P_{air} = 0 psig

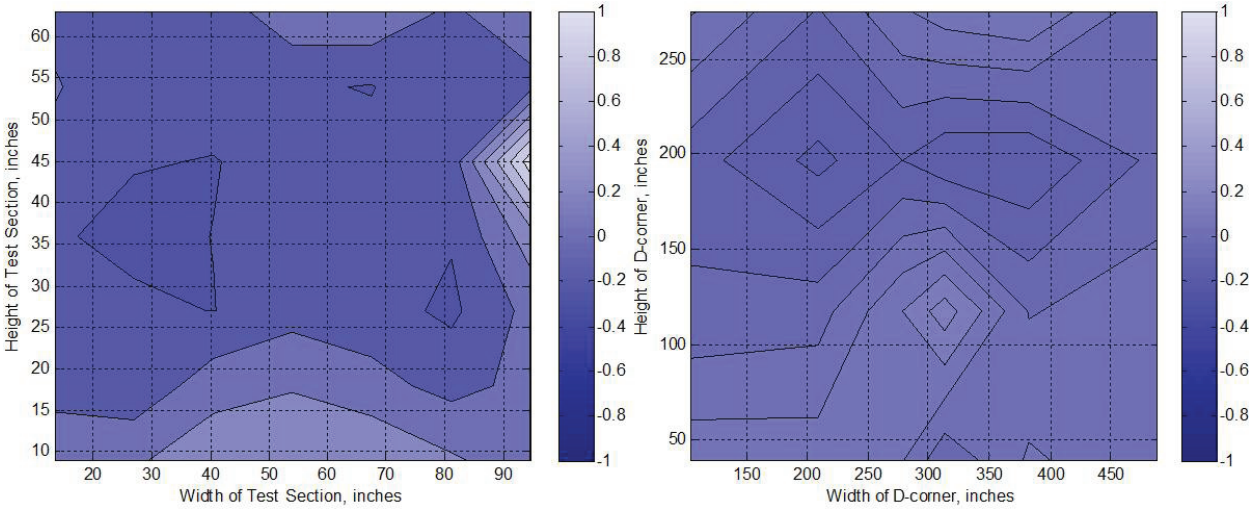

Continued Figure 24: (pp) V_{knots} = 130 knots, $T_{T,davg}$ = -16°C, P_{air} = 60 psig

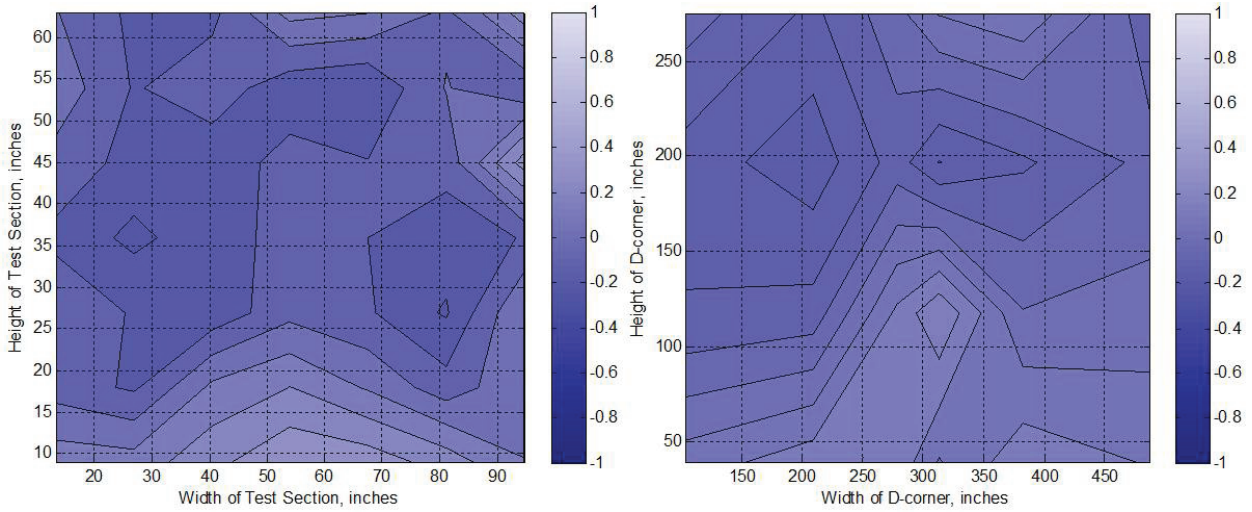

Continued Figure 24: (qq) V_{knots} = 130 knots, $T_{T,davg}$ = -16°C, P_{air} = 30 psig

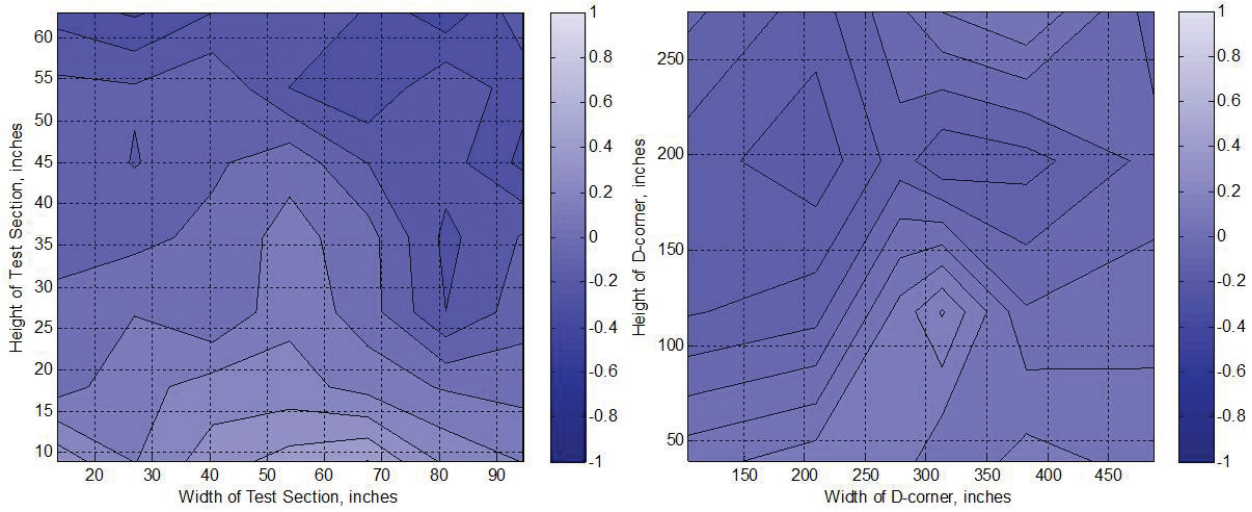

Continued Figure 24: (rr) V_{knots} = 300 knots, $T_{T,davg}$ = -14°C, P_{air} = 0 psig

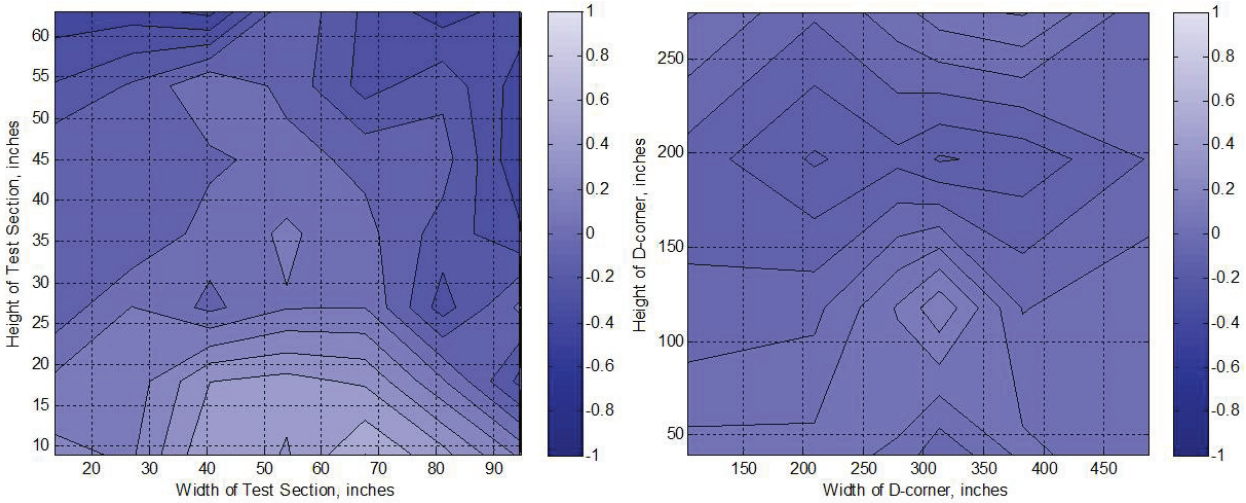

Continued Figure 24: (ss) V_{knots} = 300 knots, $T_{T,davg}$ = -14°C, P_{air} = 60 psig

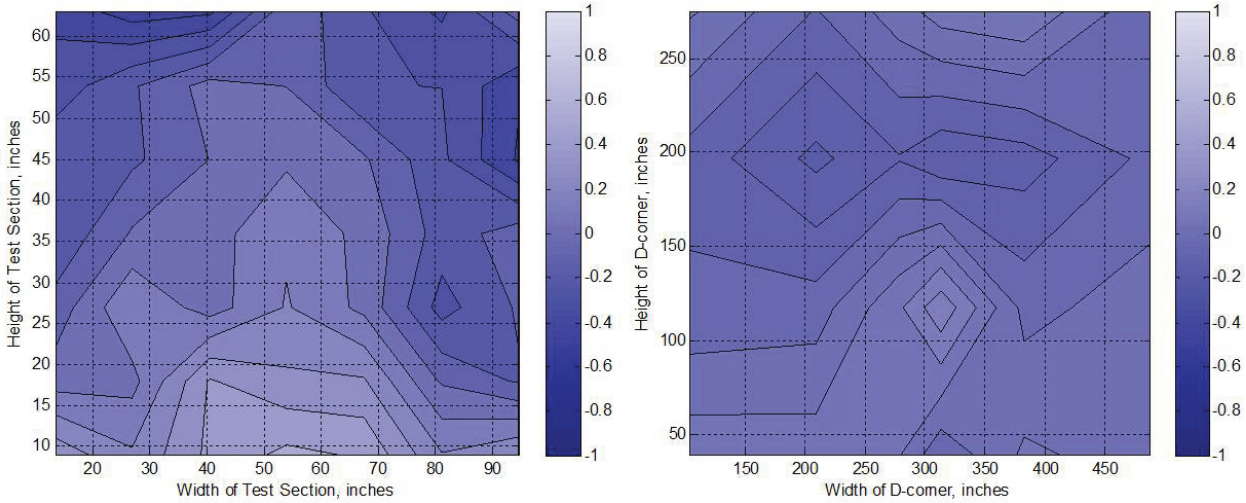

Continued Figure 24: (tt) V_{knots} = 300 knots, $T_{T,davg}$ = -14°C, P_{air} = 30 psig

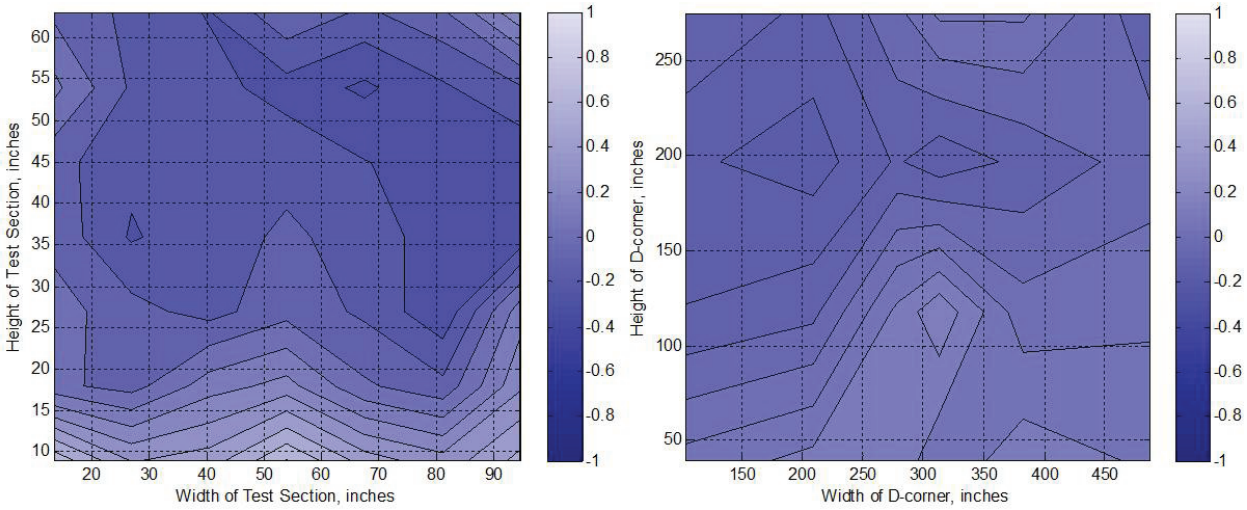

Continued Figure 24: (uu) V_{knots} = 220 knots, $T_{T,davg}$ = -30°C, P_{air} = 0 psig

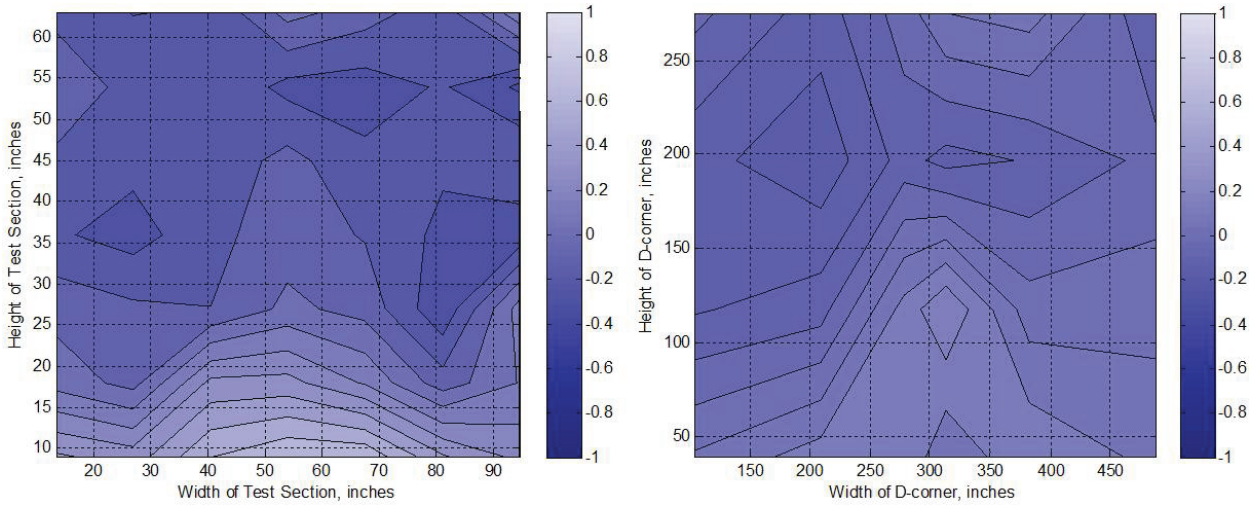

Continued Figure 24: (vv) V_{knots} = 220 knots, $T_{T,davg}$ = -30°C, P_{air} = 60 psig

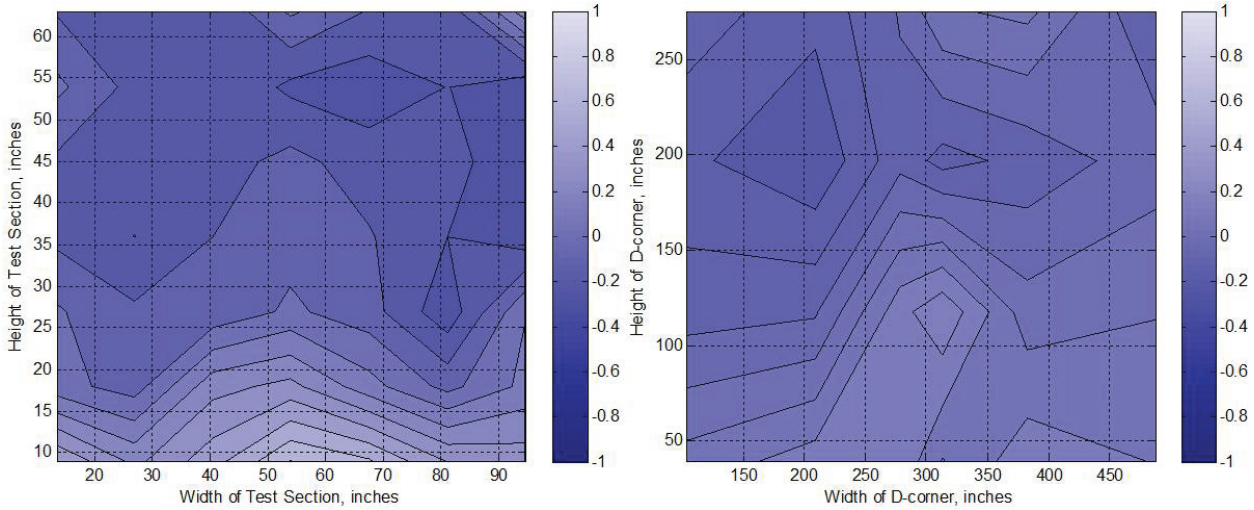

Continued Figure 24: (ww) V_{knots} = 220 knots, $T_{T,davg}$ = -30°C, P_{air} = 30 psig

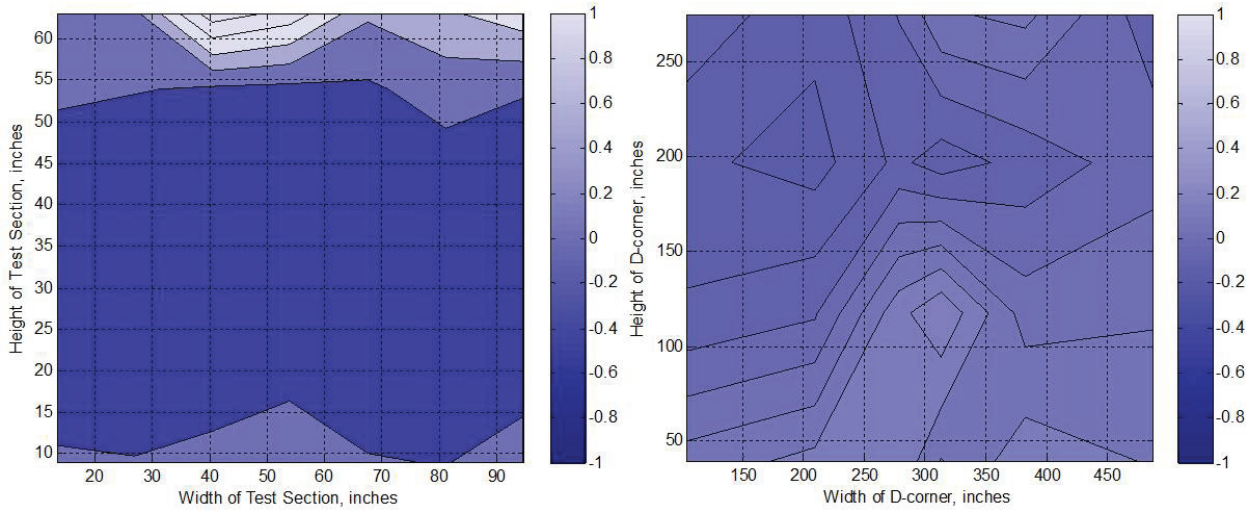

Continued Figure 24: (xx) V_{knots} = 50 knots, $T_{T,davg}$ = -33°C, P_{air} = 0 psig

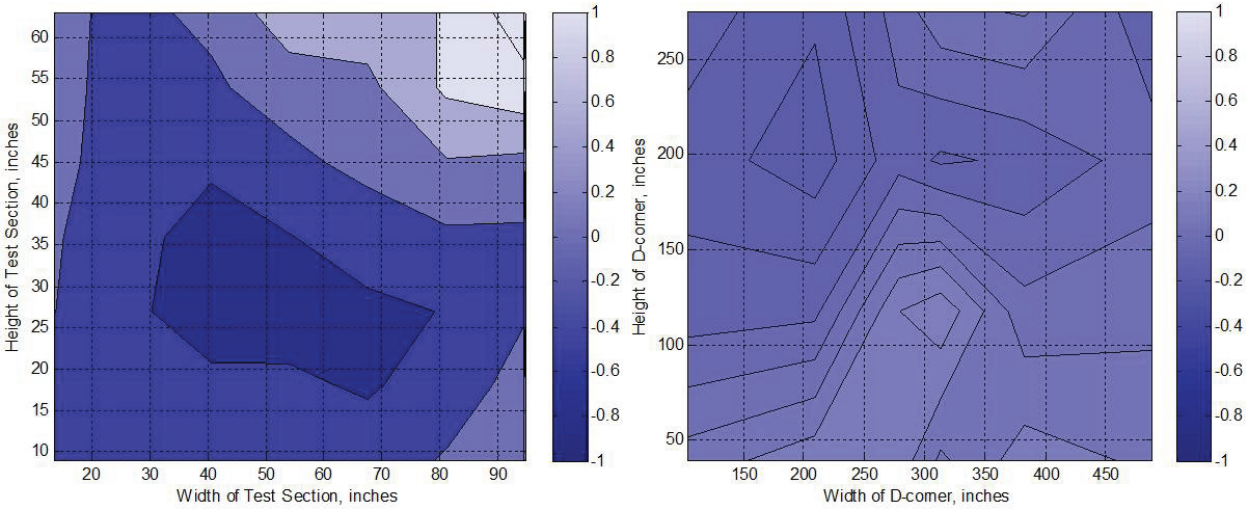

Continued Figure 24: (yy) V_{knots} = 50 knots, $T_{T,davg}$ = -33°C, P_{air} = 60 psig

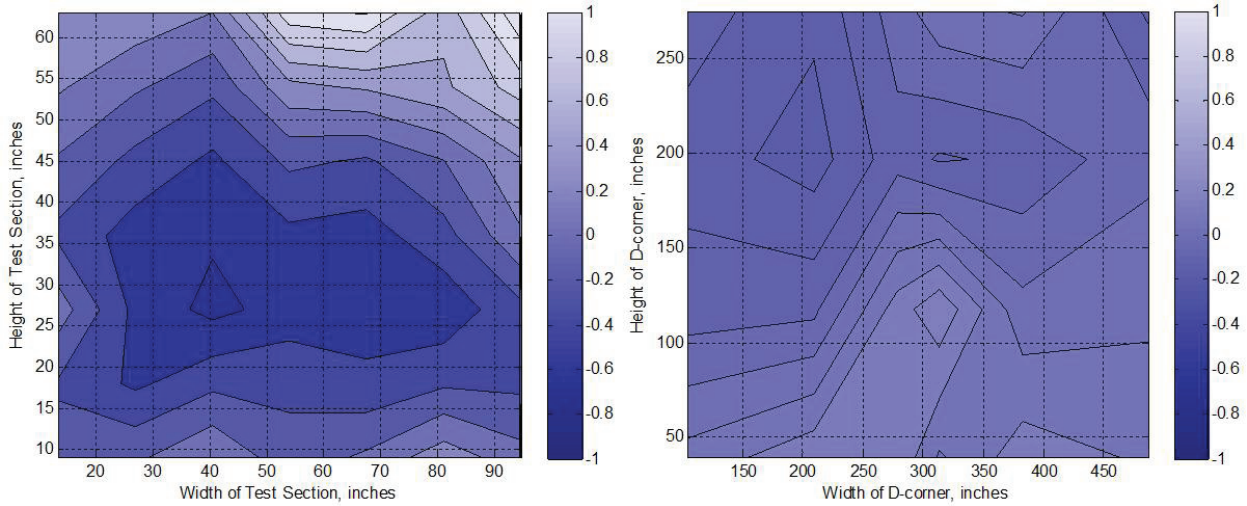

Continued Figure 24: (zz) V_{knots} = 50 knots, $T_{T,davg}$ = -33°C, P_{air} = 30 psig

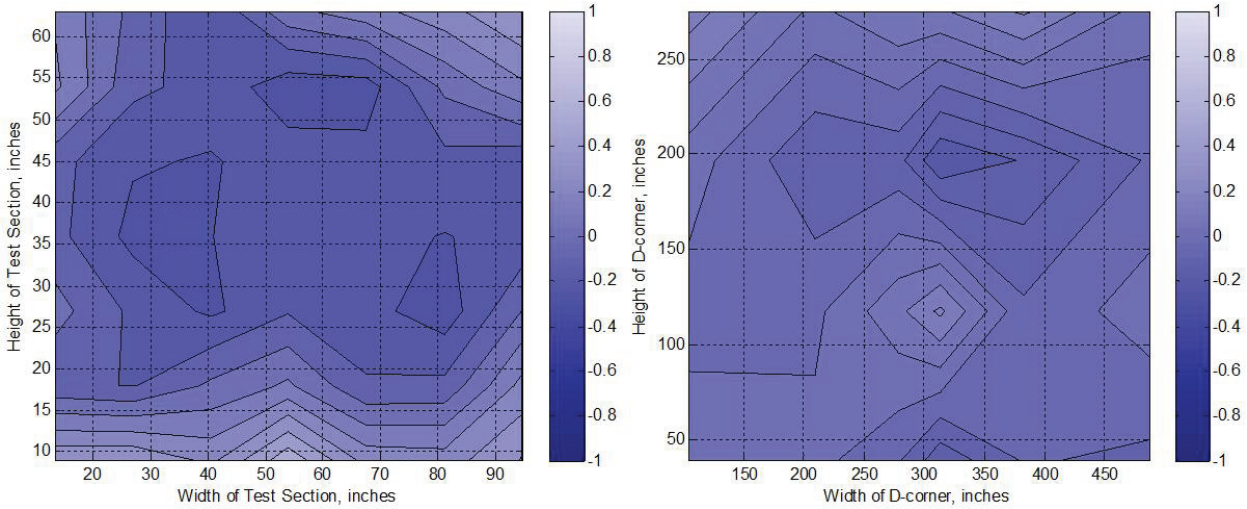

Continued Figure 24: (aaa) V_{knots} = 130 knots, $T_{T,davg}$ = -33°C, P_{air} = 0 psig

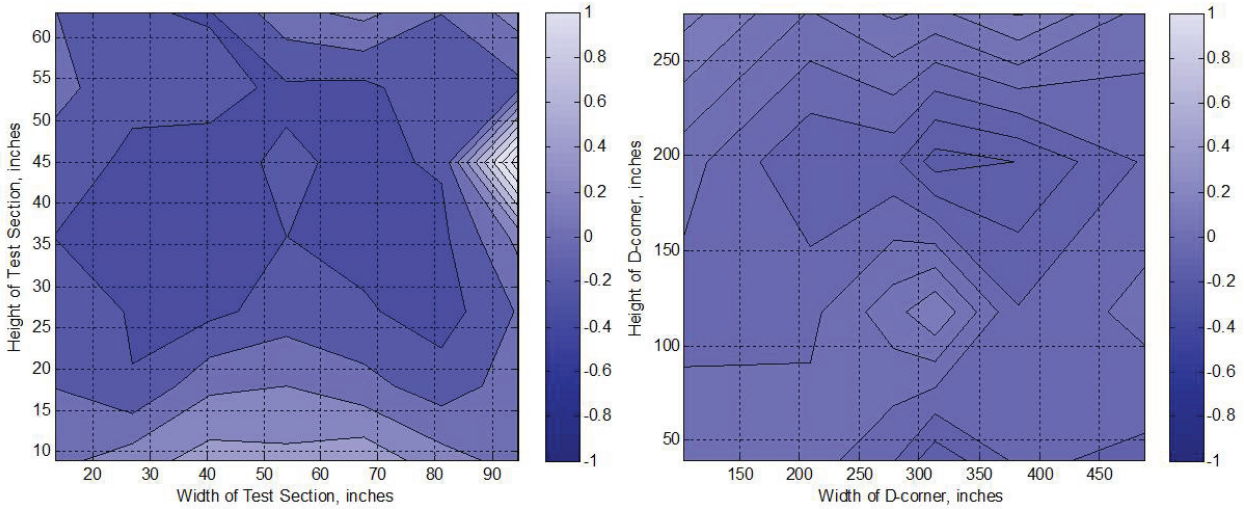

Continued Figure 24: (bbb) V_{knots} = 130 knots, $T_{T,davg}$ = -33°C, P_{air} = 60 psig

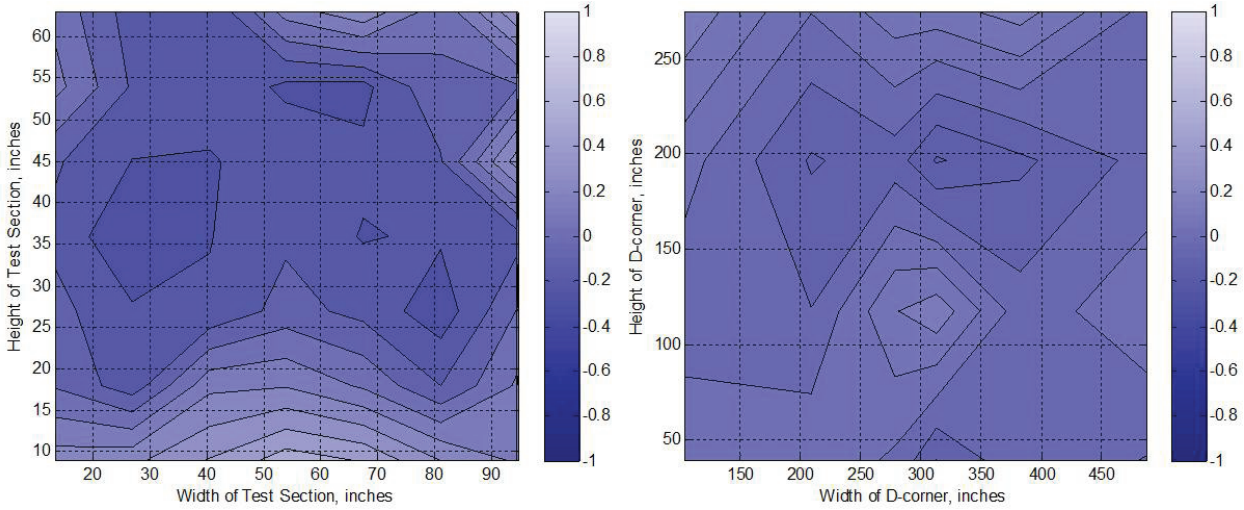

Continued Figure 24: (ccc) V_{knots} = 130 knots, $T_{T,davg}$ = -33°C, P_{air} = 30 psig

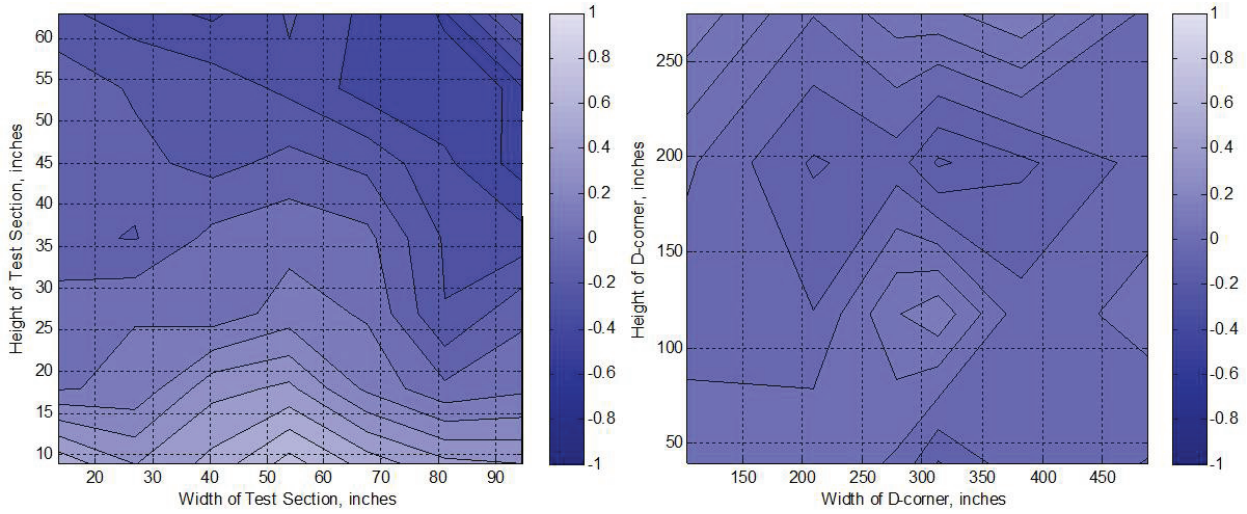

Continued Figure 24: (ddd) V_{knots} = 300 knots, $T_{T,davg}$ = -28°C, P_{air} = 0 psig

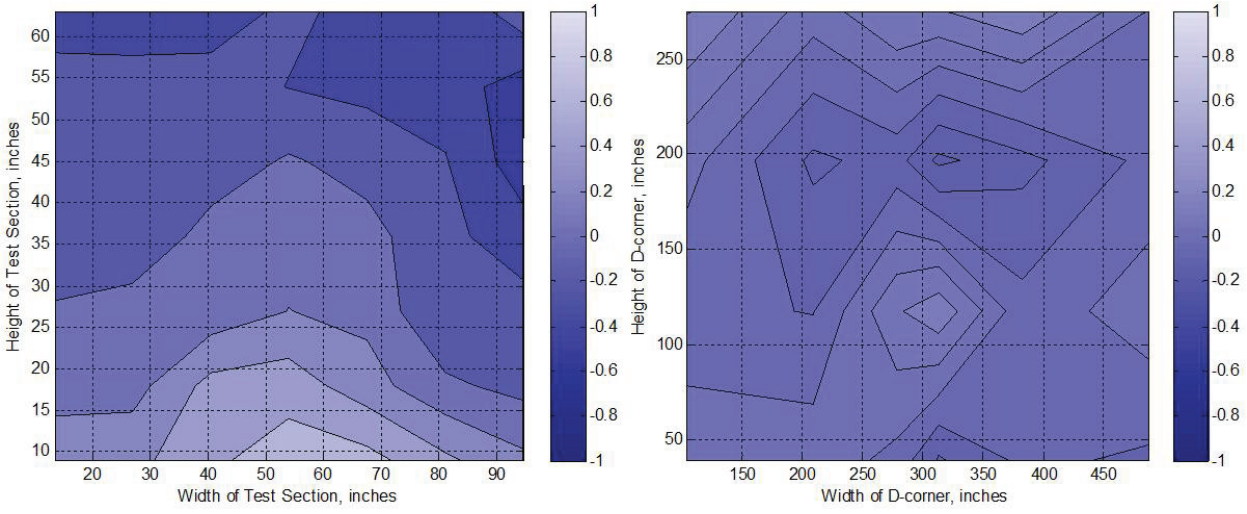

Continued Figure 24: (eee) V_{knots} = 300 knots, $T_{T,davg}$ = -28°C, P_{air} = 60 psig

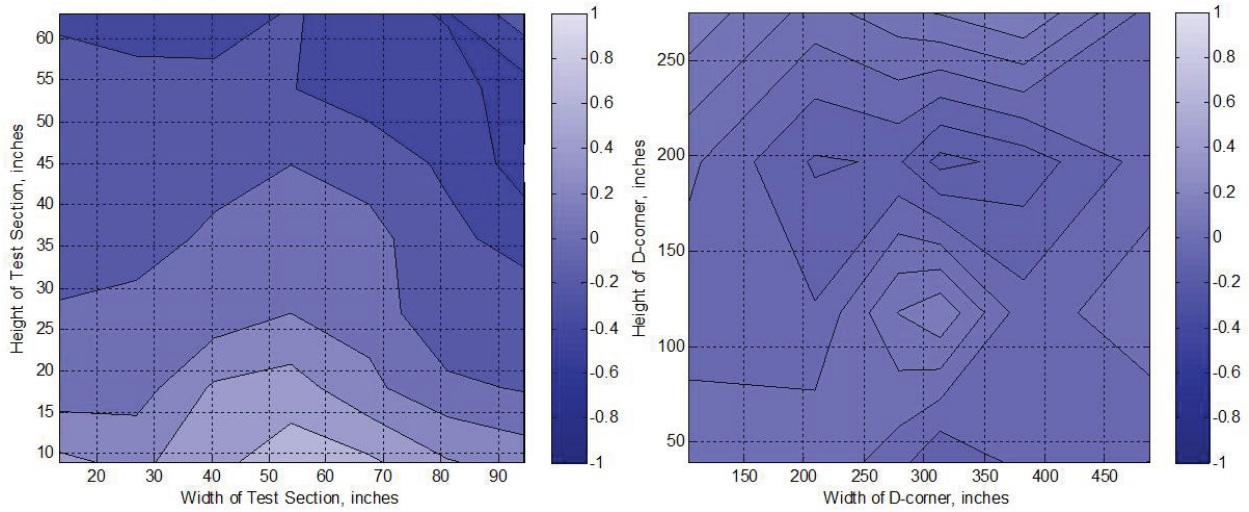

Continued Figure 24: (fff) V_{knots} = 300 knots, $T_{T,davg}$ = -28°C, P_{air} = 30 psig

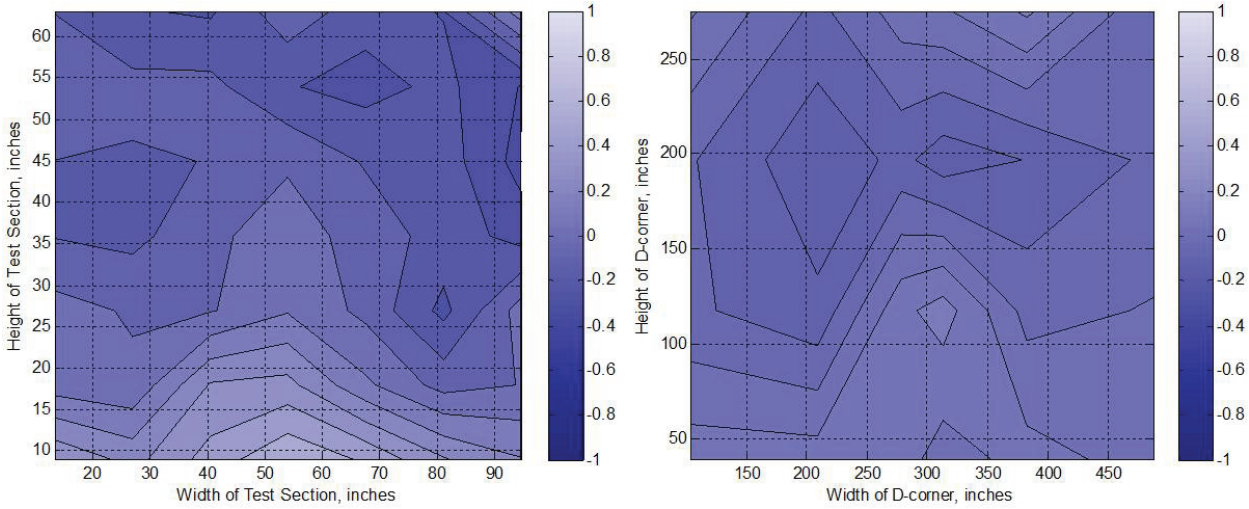

Continued Figure 24: (ggg) V_{knots} = 220 knots, $T_{T,davg}$ = -31°C, P_{air} = 30 psig

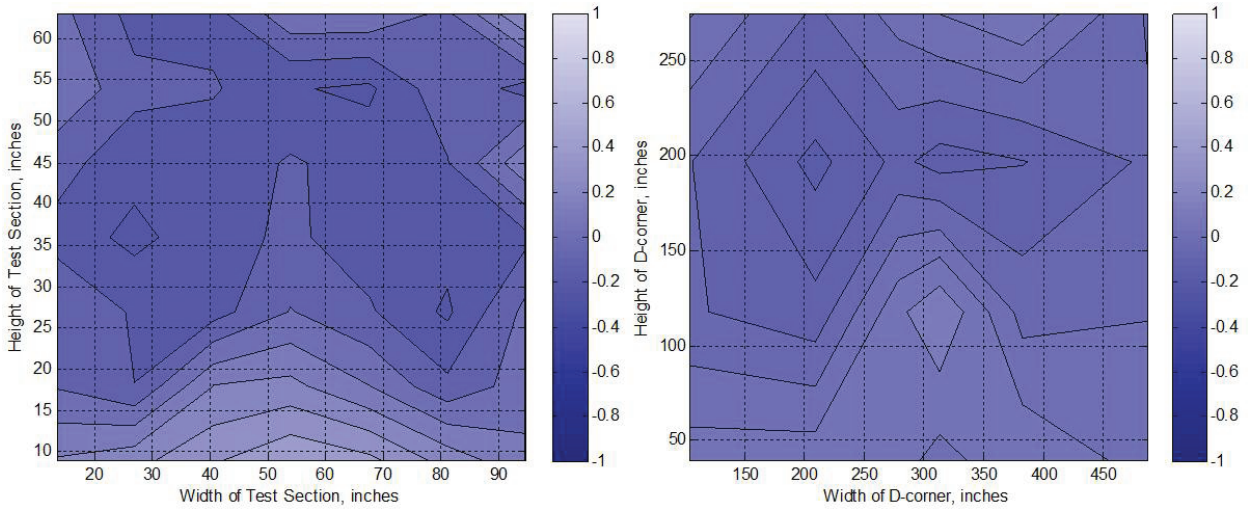

Continued Figure 24: (hhh) V_{knots} = 130 knots, $T_{T,davg}$ = -33°C, P_{air} = 30 psig

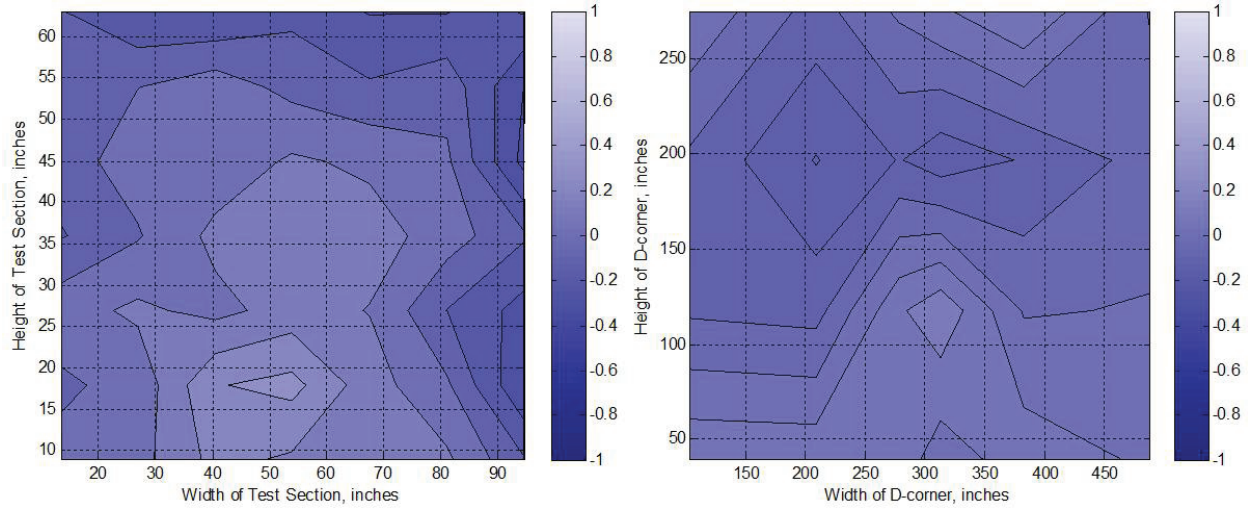

Continued Figure 24: (iii) V_{knots} = 220 knots, $T_{T,davg}$ = -15°C, P_{air} = 30 psig

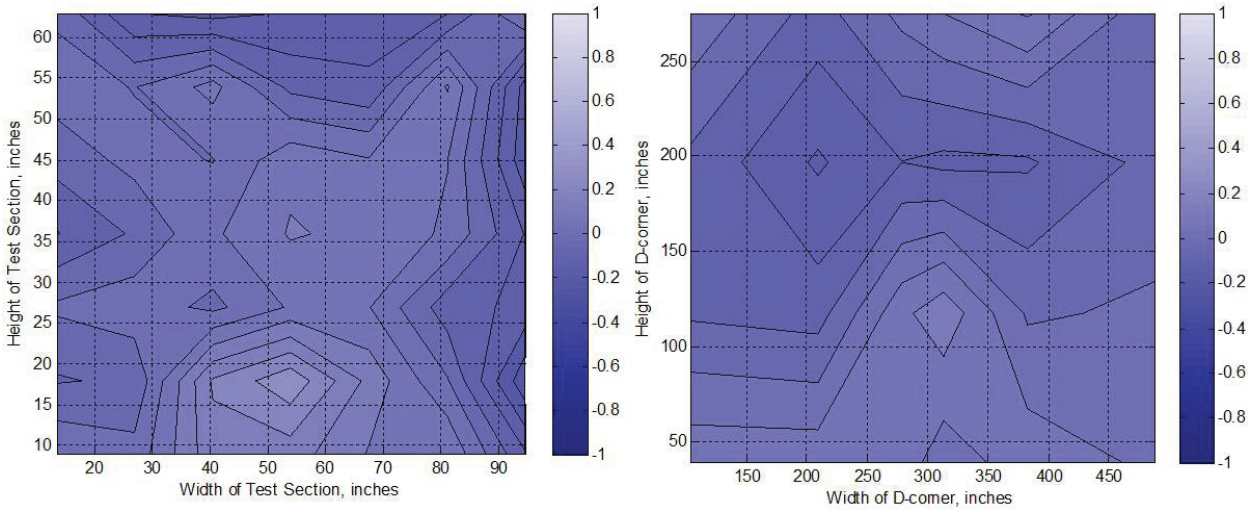

Continued Figure 24: (jjj) V_{knots} = 130 knots, $T_{T,davg}$ = -16°C, P_{air} = 30 psig

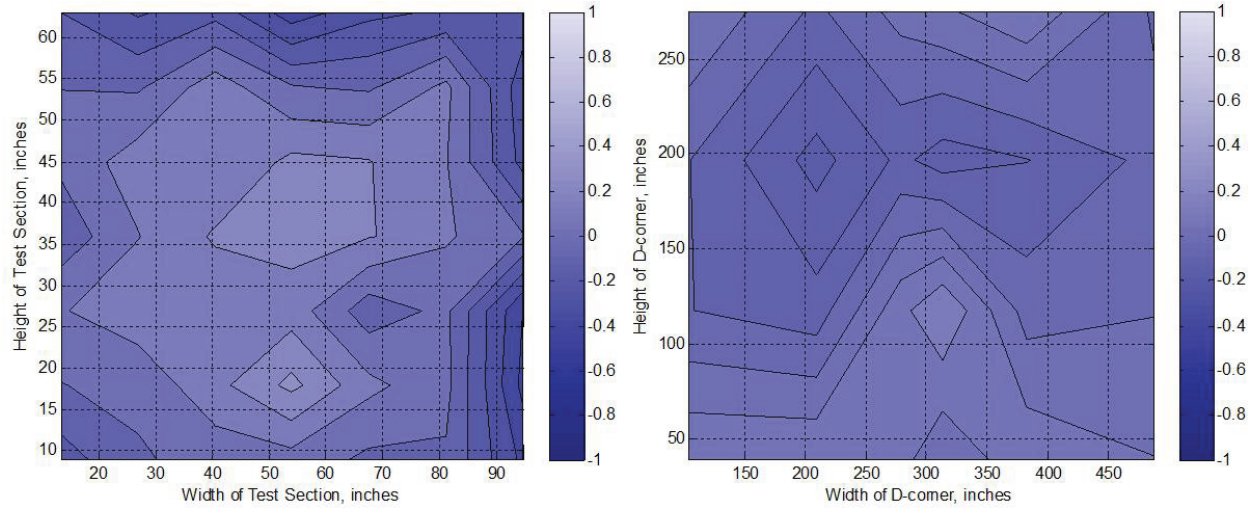

Continued Figure 24: (kkk) V_{knots} = 220 knots, $T_{T,davg}$ = -3°C, P_{air} = 30 psig

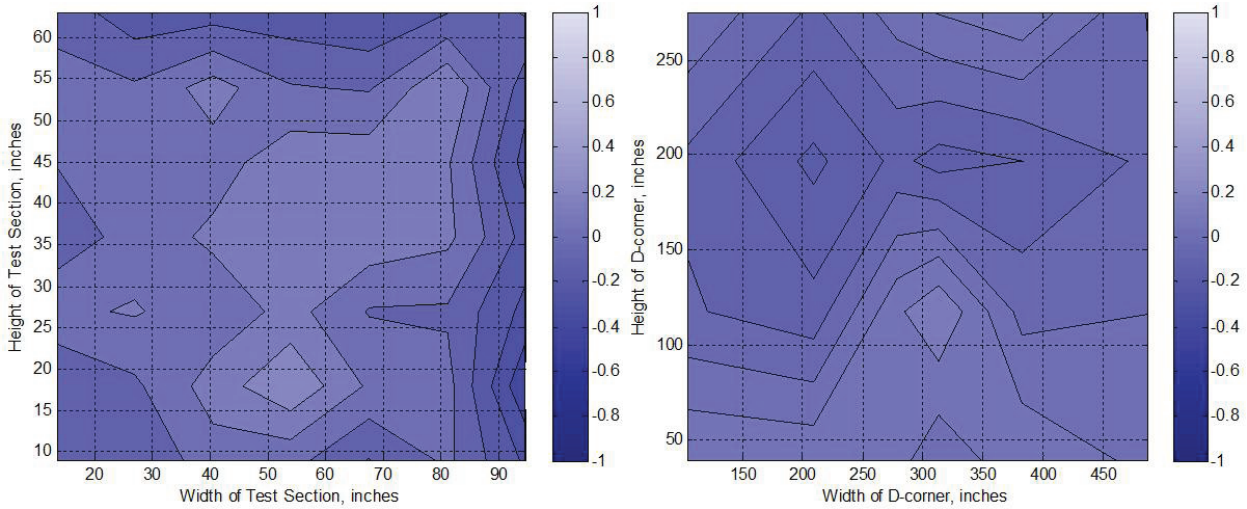

Continued Figure 24: (lll) V_{knots} = 130 knots, $T_{T,davg}$ = -4°C, P_{air} = 30 psig

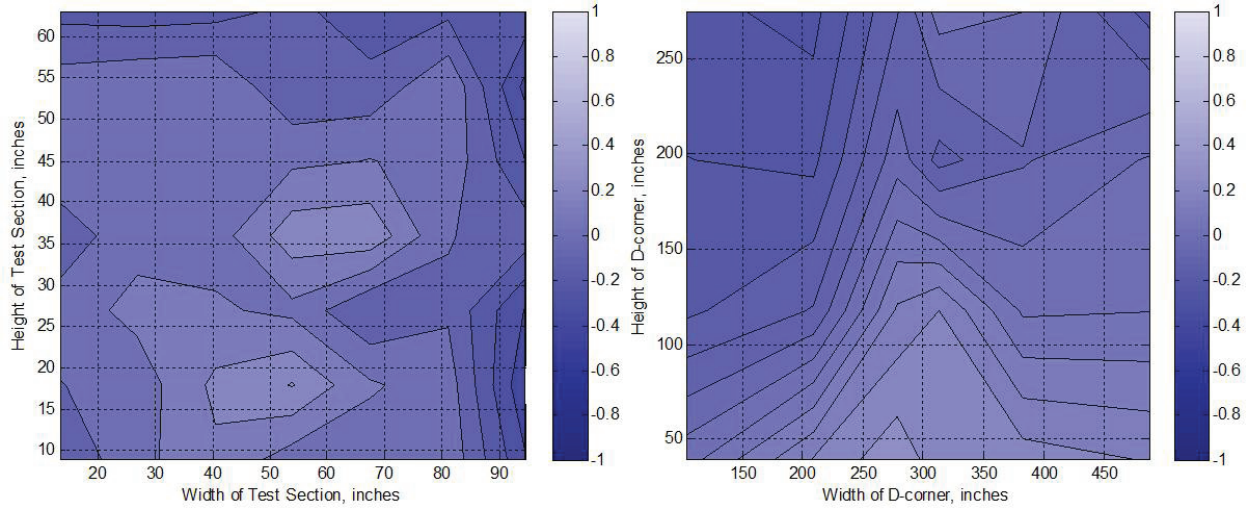

Continued Figure 24: (mmm) V_{knots} = 220 knots, $T_{T,davg}$ = -2°C, P_{air} = 30 psig

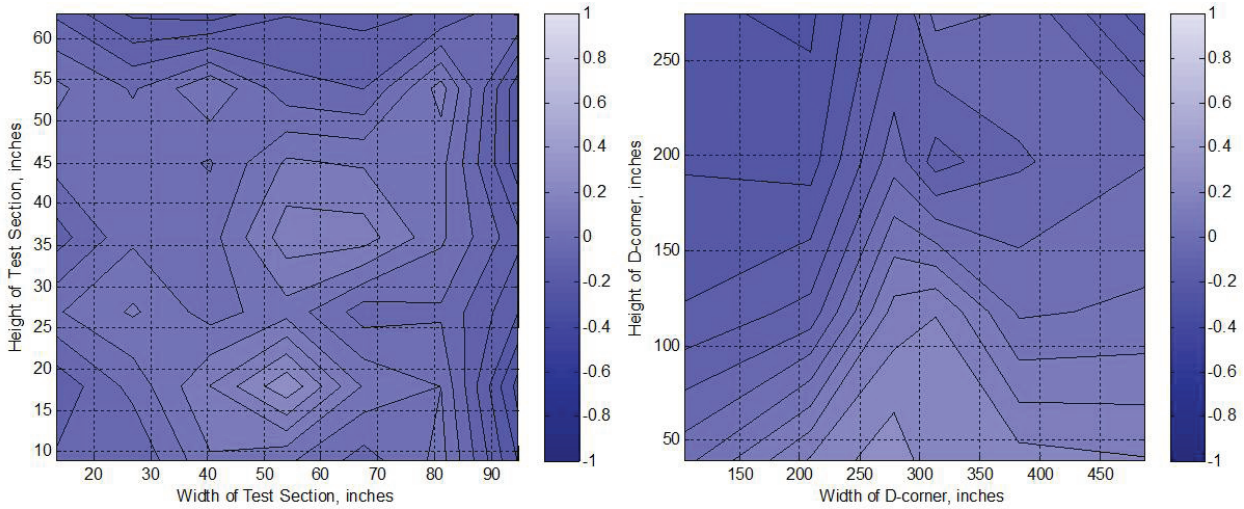

Continued Figure 24: (nnn) V_{knots} = 130 knots, $T_{T,davg}$ = -3°C, P_{air} = 30 psig

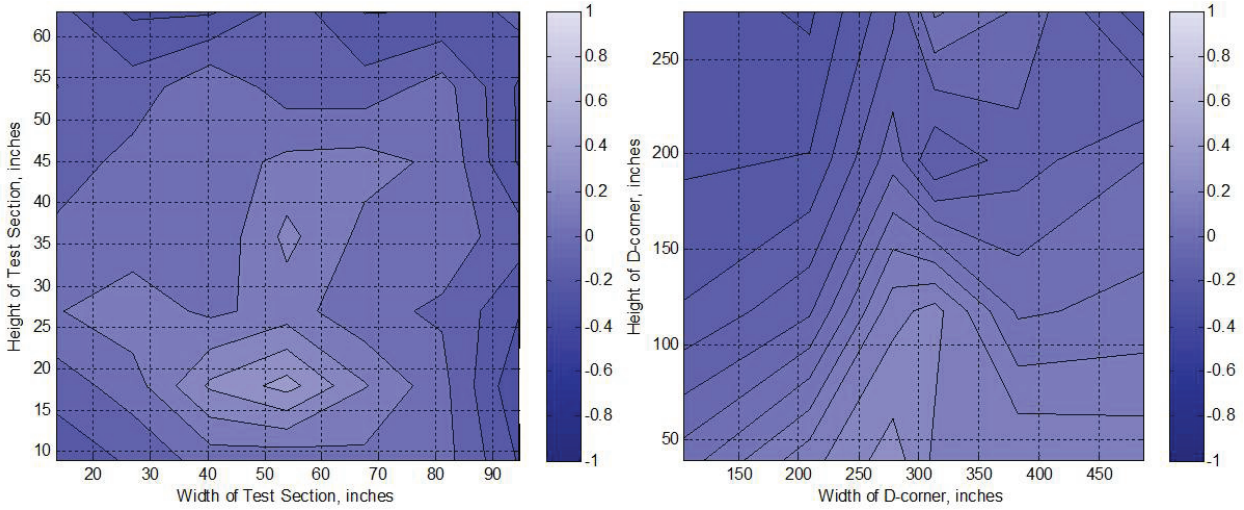

Continued Figure 24: (ooo) V_{knots} = 220 knots, $T_{T,davg}$ = -1°C, P_{air} = 30 psig

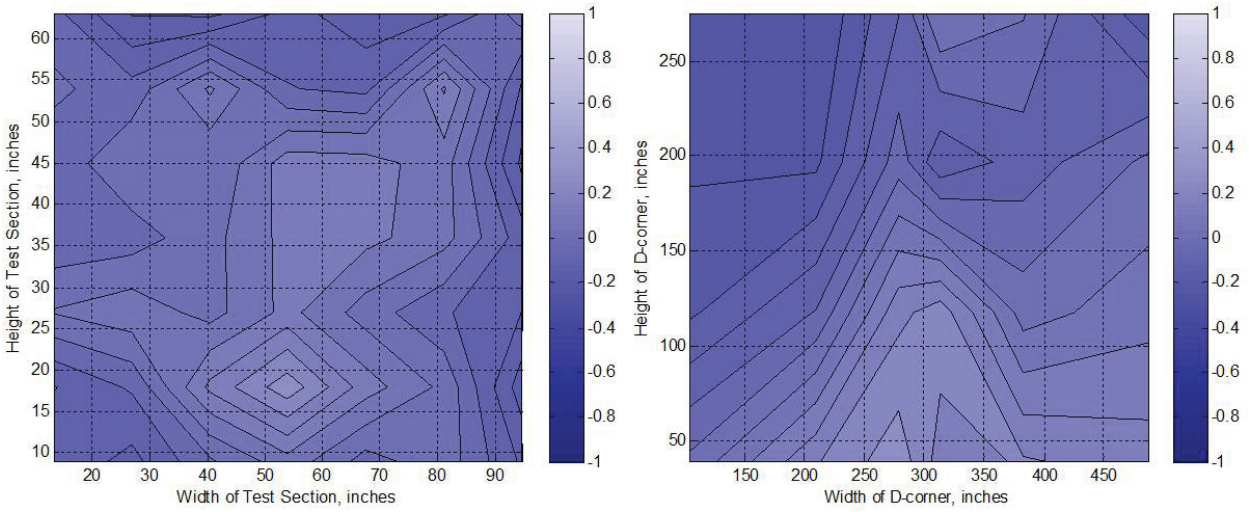

Continued Figure 24: (ppp) V_{knots} = 130 knots, $T_{T,davg}$ = -2°C, P_{air} = 30 psig

References

1. SAE Standards ARP(Aerospace Recommended Practice)5905, *Calibration and Acceptance of Icing Wind Tunnels*, 2003.

2. "Recommended Practice: Calibration of Subsonic and Transonic Wind Tunnels," 2003.

3. Soeder, R.H., S. D. I. R. S. D. and Andracchio, C., "NASA Glenn Icing Research Tunnel User Manual," Tech. Rep. NASA/TM-2003-212004, 2003.

4. Gonsalez, J. and Arrington, E., "Five-Hole Flow Angle Probe Calibration for the NASA Glenn Icing Research Tunnel," Tech. rep., 2001.

5. Gonsalez, J. and Arrington, E., "Improvements to the Total Temperature Calibration of the NASA Glenn Icing Research Tunnel," Tech. Rep. NASA/CR-2005-213875, AIAA-2005-4276, 2005.

6. Staff, A. R., "Equations, Tables, and Charts for Compressible Flow," Tech. Rep. Report 1135, 1953, National Advisory Committee for Aeronautics.

7. *Springer Handbook of Experimental Fluid Mechanics*, Springer, 2007.

REPORT DOCUMENTATION PAGE	Form Approved OMB No. 0704-0188

1. REPORT DATE *(DD-MM-YYYY)*	2. REPORT TYPE	3. DATES COVERED *(From - To)*
01-03-2013	Final Contractor Report	

4. TITLE AND SUBTITLE
Aero-Thermal Calibration of the NASA Glenn Icing Research Tunnel (2012 Tests)

5a. CONTRACT NUMBER
NNC05CA95C

5b. GRANT NUMBER

5c. PROGRAM ELEMENT NUMBER

6. AUTHOR(S)
Pastor-Barsi, Christine; Arrington, E., Allen

5d. PROJECT NUMBER

5e. TASK NUMBER

5f. WORK UNIT NUMBER
WBS 122711.03.07.03.02

7. PERFORMING ORGANIZATION NAME(S) AND ADDRESS(ES)
Sierra-Lobo, Inc.

8. PERFORMING ORGANIZATION REPORT NUMBER
E-18548

9. SPONSORING/MONITORING AGENCY NAME(S) AND ADDRESS(ES)
National Aeronautics and Space Administration
Washington, DC 20546-0001

10. SPONSORING/MONITOR'S ACRONYM(S)
NASA

11. SPONSORING/MONITORING REPORT NUMBER
NASA/CR-2013-217812

12. DISTRIBUTION/AVAILABILITY STATEMENT
Unclassified-Unlimited
Subject Category: 09
Available electronically at http://www.sti.nasa.gov
This publication is available from the NASA Center for AeroSpace Information, 443-757-5802

13. SUPPLEMENTARY NOTES

14. ABSTRACT
A full aero-thermal calibration of the NASA Glenn Icing Research Tunnel (IRT) was completed in 2012 following the major modifications to the facility that included replacement of the refrigeration plant and heat exchanger. The calibration test provided data used to fully document the aero-thermal flow quality in the IRT test section and to construct calibration curves for the operation of the IRT.

15. SUBJECT TERMS
Wind tunnel calibration

16. SECURITY CLASSIFICATION OF:			17. LIMITATION OF ABSTRACT	18. NUMBER OF PAGES	19a. NAME OF RESPONSIBLE PERSON
a. REPORT	b. ABSTRACT	c. THIS PAGE			STI Help Desk (email:help@sti.nasa.gov)
U	U	U	UU	126	19b. TELEPHONE NUMBER *(include area code)* 443-757-5802